Elucidating the Role of the Fes Tyrosine Kinase in Breast Cancer

by

Connie Shengnan Zhang

A thesis submitted to the Department of Pathology and

Molecular Medicine in conformity with the requirements

for the degree of Doctor of Philosophy

Queen's University

Kingston, Ontario, Canada

December, 2013

Abstract

Fes was first discovered as a protein-tyrosine kinase-encoded by the v-*fes* retroviral oncogene. Retrovirally encoded Fes oncoproteins induced tumors in chickens and cats and cause tumors in transgenic mice; however, a role for Fes in human cancer has not been established. This thesis identifies tumor promoting roles of Fes through effects on stromal cells using genetic mouse models. First, in an orthotopic mouse mammary gland engraftment model, I found that loss of Fes in the host correlated with reductions in engrafted tumor growth rates, metastasis and circulating tumor cells, which may be partly due to reduced vascularity and fewer tumor-associated macrophages. We also showed Fes-deficient macrophages were less capable of promoting tumor cell invasion in co-culture experiments. Next, I observed delayed tumor onset in the absence of Fes in a transgenic mouse model of breast cancer driven by an activated HER2/Neu allele. This longer tumor latency correlated with hyperinflammatory status of Fes-deficient normal mammary glands. Taken together, these observations argue that Fes inhibition might provide therapeutic benefits in breast cancer, by attenuating tumor-associated angiogenesis and the metastasis-promoting functions of tumor-associated macrophages, or by delaying breast tumor onset in women with HER2 overexpression.

Finally, we showed that mice engrafted with IL-4 producing tumor cells developed tumors with significantly reduced growth rates and a complete attenuation of lung metastasis, which correlated with increased numbers of macrophages and enhanced phagocytic capability of macrophages in the tumor microenvironment. These observations suggest that IL-4 could be a good candidate for immunotherapy.

Co-Authorship

The co-authors of this thesis are Hyeyeon Kim, Violeta Chitu, David Lebrun, Bruce Elliott, Richard Stanley, and Peter Greer.

Chapter 2: This chapter has been published in the Cancer Research Journal, in February 2011 (Zhang *et al.* Cancer Res, 2011. 71 (4): p. 1465-73). The authors are Connie Zhang, Violeta Chitu, Richard Stanley, Bruce Elliott, and Peter Greer. Dr. Violeta Chitu, a collaborator at the Albert Einstein College of Medicine, performed the collagen invasion assay (Figure 2.11). The rest of data figures were generated by me. I wrote the initial draft of the manuscript, and participated in subsequent editing. The bulk of the editing of this manuscript was done by Dr. Peter Greer. Dr. Richard Stanley and Dr. Bruce Elliott contributed to the discussion of this manuscript.

Chapter 3: This chapter will be modified as a manuscript to be sent out for peer review. Dr. David LeBrun performed all histopathological assessment of H&E sections and contributed to interpretation of that data in Figure 3.3 and Figure 3.6. All the data and figures were generated by me.

Chapter 4: This chapter will be modified as a manuscript to be sent out for peer review. Hyeyeon Kim, a fourth year undergraduate student, initiated the project under my supervision. ELISA analysis of IL-4 and data in Figures 4.5 and 4.6 were generated by Hyeyeon Kim. All other experiments were performed by me.

Acknowledgements

First, I would like to sincerely thank my supervisor, Dr. Peter Greer, for providing me with the opportunity to carry out graduate studies, and for providing me guidance, advice and support along the way. Without his encouragement and trust, I could not have finished this project.

I would like to thank my committee members, Dr. Bruce Elliott and Dr. Lois Mulligan, for their excellent advice and thoughtful discussions as well as great recommendation letters that helped me get the postdoctoral training opportunity.

I would like to thank all past and present members of the Greer lab. They have been extremely helpful, and it has been a great experience to work with them all.

I would also like to thank the following people for their technical support. Without their help, this project would not be possible. Dr Yan Gao engineered AC2M2 cells with GFP expression and provided assistance throughout this project. Chris Hall managed mouse breeding, genotyping and organized all the animals used for the entire project. Jalna Meens and Changnian Shi provided technical assistance with engraftment experiments. Jeff Mewburn and Matt Gordon provided technical assistance for imaging and flow cytometry experiments. John Dacosta, Oliver Jones and Xiaohu Yan provided technical assistance for tissue paraffin embedding, Lee Boudreau performed tissue staining using the Ventana automated staining system, and Shakeel Virk scanned stained tissue sections.

I would like to thank my parents for their constant support financially and emotionally. Without their support, I could not succeed at this stage in my academic career.

Finally, I would like to thank my husband, Kun, for sharing his experience of graduate studies and for making my graduate study more enjoyable. A special thank to my lovely daughter, Chloe, who was a surprising gift during my graduate study.

Funding for this study has been generously provided by the Canadian Cancer Society and the Canadian Institutes of Health Research. I received PhD fellowship from the Canadian Breast Cancer Foundation and the Terry Fox Foundation training program in Transdisciplinary Cancer Research in Partnership with CIHR.

Table of Contents

Abstract……...i

Co-Authorship……ii

Acknowledgements……iii

Table of Contents……..iv

Lists of Figures……..x

List of Abbreviations……..xii

Chapter 1: General Introduction……1

1.1 Breast cancer……1

1.1.1 Introduction……1

1.1.2 Types of breast cancer……1

1.1.3 Risk factors……2

1.1.4 Molecular subtypes of breast cancer……...4

1.1.5 Breast cancer treatment……...5

1.1.6 Metastasis……...7

1.1.7 Tumor microenvironment……...9

1.1.8 Models to study breast cancer……...13

1.1.8.1 Cell culture system……..13

1.1.8.2 Xenograft model……..14

1.1.8.3 Transgenic mouse model……16

1.2 Fes kinase……...18

1.2.1 Introduction……..18

1.2.2 Discovery of *fes/fps* as transforming retroviral oncogenes……..19

1.2.3 Structural features of Fes and Fer proteins……..20

1.2.4 Expression patterns and subcellular localization of Fes and Fer…….23

1.2.5 Studies using transgenic and gene targeted mouse models of Fes kinase……24
1.2.6 An identity crisis for Fes: Oncogene or Tumor suppressor……27
1.2.6.1 Evidence for oncogenic functions of Fes……27
1.2.6.2 Evidence for tumor suppressor functions of Fes……28
1.3 Interleukin-4……...29
1.3.1 Introduction……..29
1.3.2 Biological functions of IL-4……30
1.3.3 IL-4 receptor complex……..32
1.3.4 IL-4 signaling pathways……...36
1.3.4.1 JAK-STAT pathway……36
1.3.4.2 PI3K-AKT pathway……37
1.3.4.3 RAS-MAPK pathway……..39
1.3.5 IL-4 and disease……40
1.3.5.1 Asthma……40
1.3.5.2 Rheumatoid arthritis……..41
1.3.5.3 Cancer……..42
1.4 Goals of this work……..43

Chapter 2: Fes tyrosine kinase expression in the tumor niche correlates with enhanced tumor growth, angiogenesis, circulating tumor cells, metastasis, and infiltrating macrophages……45
2.1 Abstract……..45
2.2 Introduction……46
2.3 Materials and methods……48
2.3.1 Cell culture……48
2.3.2 Mice……..49
2.3.3 Orthotopic mammary gland engraftment model……..49

2.3.4 *In vivo* macrophage imaging……50
2.3.5 Flow cytometry measurement of macrophages and endothelial cells..50
2.3.6 Immunoblotting……51
2.3.7 Immunofluorescence analysis of tumors and stroma……52
2.3.8 Peritoneal lavage……...53
2.3.9 *In vitro* macrophage phagocytosis of dextran beads……54
2.3.10 Tail vein injection lung metastasis model……54
2.3.11 Detection of circulating tumor cells……55
2.3.12 Collagen invasion assay……...55
2.3.13 Statistics……...55
2.4 Results
2.4.1 Fes does not affect tumorigenesis in a tumor cell autonomous fashion...
……..56
2.4.2 Fes plays a tumor promoting role in the niche……60
2.4.3 Reduced vascularity in the *fes-null* tumor niche……..60
2.4.4 Reduced involvement of tumor-associated macrophages in *fes-null* mice……...67
2.4.5 *Fes-null* macrophages are deficient in promoting tumor cell migration and invasion……..71
2.4.6 Fes deficiency in the lung niche does not compromise tumor cell invasion and initial growth rates at the metastatic site……74
2.4.7 Fes deficiency in the niche compromises the escape of tumor cells from the primary tumor site……..74
2.5 Discussions……76

Chapter 3: Deficiency of Fes kinase expression correlates with delayed mammary tumor onset in a MMTV-Neu transgenic mouse model……..83
3.1 Abstract……..83

3.2 Introduction……84
3.3 Materials and methods……86
3.3.1 Mice……..86
3.3.2 Spontaneous mammary tumor model……..87
3.3.3 Immunoblotting……88
3.3.4 Histopathological assessment of H&E sections……...88
3.3.5 Immunohistochemical staining……89
3.3.6 Statistics……89
3.4 Results……90
3.4.1 Fes deficiency correlates with delayed tumor onset in *Neu*$^{NT/o}$ transgenic mice……90
3.4.2 Fes deficiency does not affect tumor growth rates in *Neu*$^{NT/o}$ transgenic mice……...90
3.4.3 Decreased levels of epithelial dysplasia and increased numbers of lymphocytes and granulocytes in Fes-deficient normal mammary glands……92
3.4.4 Elevated levels of NFκB in *fes*-deficient normal mammary glands at the pre-malignant stage……94
3.4.5 Higher stromal grading in *fes*-deficient malignant tumor-bearing mammary glands……..99
3.5 Discussions……102

Chapter 4: Tumor cell-derived IL-4 suppresses tumorigenesis in mouse orthotopic mammary engraftment models of breast cancer……106
4.1 Abstract……106
4.2 Introduction……..107
4.3 Materials and methods……..110
4.3.1 Cell lines……110

4.3.2 ELISA……111
4.3.3 Cell proliferation assay……..111
4.3.4 Dose-response stimulation experiment……..112
4.3.5 Immunoblotting analysis……112
4.3.6 Mice……113
4.3.7 Orthotopic mouse engraftment model……114
4.3.8 Peritoneal lavage……115
4.3.9 Immunofluorescent microscopy……115
4.3.10 Overnight video time-lapse……116
4.3.11 Flow cytometry analysis……116
4.3.12 Immunohistochemical staining……..117
4.3.13 Statistics……..117
4.4 Results……...117
4.4.1 Tumor cell-derived IL-4 has biological effects on macrophages *in vitro* ……117
4.4.2 IL-4-expressing tumor cells do not develop tumors in immune competent mice……..120
4.4.3 IL-4 suppresses tumor growth and eliminates lung metastasis in nude mice……122
4.4.4 Tumor derived IL-4 significantly inhibits primary tumor growth and completely abolishes lung metastasis in $Rag2^{-/-}$; $IL2R\gamma c^{-/-}$ mice…..127
4.4.5 Increased numbers of tumor-associated macrophages and macrophage phagocytosis of tumor cells in IL4-expressing tumor stroma……136
4.4.6 More prominent macrophage phagocytosis of tumor cells in IL-4 expressing co-culture……..139
4.5 Discussions……...144

Chapter 5: General Discussion……150

5.1 Summary of finds and significance of results……..150

5.1.1 Stromal tumor promoting roles for Fes in regulating tumorigenesis….

……151

5.1.2 Possible tumor cell intrinsic roles of Fes in tumorigenesis……152

5.1.3 Possible roles of Fes on different phenotypes of macrophages…….154

5.1.4 Possible role of IL-4 on macrophages in tumorigenesis……159

5.2 Future directions……160

5.2.1 Inhibition of Fes in human breast cancer……160

5.2.2 IL-4 as a good candidate for tumor vaccines……..161

5.2.3 Molecular mechanisms related to Fes…….163

References……..165

Appendix 1 Quantitative RT-PCR primers…….192

Appendix 2 Inhibition of Fes phosphorylation by Fes kinase inhibitor TAE684 *in vitro*…….……193

Appendix 3 Fes and Fer deficiency delayed tumor onset in MMTV-Neu transgenic mice in an additive manner…….……...……..……..196

List of Figures

Figure 1.1 Structure of Fes and Fer proteins and exon organization of the *fes* and *fer* loci……22

Figure 1.2 IL-4 signaling pathways……33

Figure 2.1 Expression levels of Fes kinase and GFP in parental AC2M2 and variant Fes expressing cell lines……57

Figure 2.2 Fes does not affect tumorigenesis in a tumor cell autonomous fashion. ……58

Figure 2.3 Fes does not play a tumor cell intrinsic role in term of lung metastasis ……59

Figure 2.4 Orthotopic tumor growth rates were reduced in *fes-null* mice……..61

Figure 2.5 Reduced metastasis in *fes-null* mice……..62

Figure 2.6 Reduced vascularity in *fes-null* tumor stroma……64

Figure 2.7 Immunoblotting analysis of PECAM-1 expression……...65

Figure 2.8 Fewer tumor-associated macrophages in *fes-null* mice……..68

Figure 2.9 *In vitro* macrophage phagocytosis of dextran beads……..69

Figure 2.10 Reduced macrophages in *fes-null* tumor-bearing mammary glands.. ……72

Figure 2.11 *Fes-null* macrophages are defective in promoting tumor cell migration and invasion……...73

Figure 2.12 Tail vein metastasis model……75

Figure 2.13 Fes-deficiency in the niche correlated with reduced CTC frequency… ……77

Figure 3.1 Delayed tumor onset in *fes*-deficient MMTV-Neu transgenic mice….. ……91

Figure 3.2 No difference in tumor growth rate between wild-type and *fes*-deficient MMTV-Neu transgenic mice……93

Figure 3.3 H&E and immunohistochemical stainings of pre-malignant normal mammary glands (NMG)……..95

Figure 3.4 Lower level of Ki67 and higher levels of CD3 and CD11b staining in *fes*-deficient normal mammary glands……..97

Figure 3.5 Elevated levels of NFκB activation in *fes*-deficient normal mammary glands……..100

Figure 3.6 Higher stromal grading in *fes*-deficient tumor-bearing mammary glands……..101

Figure 4.1 M2 macrophage activation and Jak3-Stat6 activation induced by tumor cell-derived IL-4……....119

Figure 4.2 Ectopic IL-4 expression does not affect tumor cell proliferation *in vitro*……...121

Figure 4.3 IL-4 expressing tumor cells did not develop tumors in CBA mice……

……..123

Figure 4.4 Reduced lung metastasis in CBA mice bearing IL-4 expressing tumors……..124

Figure 4.5 Tumor growth at the orthotopic site in nude mice was reduced when IL-4 was present……...126

Figure 4.6 Reduced lung metastasis in nude mice bearing IL-4 expressing tumors……..128

Figure 4.7 Orthotopic tumor growth rates were reduced in $Rag2^{-/-}$; $IL2R\gamma c^{-/-}$ mice bearing IL-4 expressing tumors……130

Figure 4.8 Complete elimination of lung metastasis in $Rag2^{-/-}$; $IL2R\gamma c^{-/-}$ mice bearing IL-4 expressing tumors……132

Figure 4.9 Complete elimination of lung metastasis in Rag2$^{-/-}$; IL2Rγc$^{-/-}$ mice bearing IL-4 expressing tumors when control and IL-4 expressing tumors were removed at the same size……..134

Figure 4.10 Elevated macrophages and macrophage phagocytosis of tumor cells in IL-4 expressing tumor-bearing mammary glands……137

Figure 4.11 High levels of arginase 1 expression in mammary glands bearing IL-4 expressing tumors…….140

Figure 4.12 Increased numbers of arginase 1 positively stained macrophages in IL-4 expressing tumor sections……141

Figure 4.13 Enlarged macrophages and more macrophage phagocytosis of tumor cells in IL-4 expressing co-culture……..143

Figure 4.14 Higher degree of macrophage phagocytosis of tumor cells in the presence of IL-4……145

Figure 5.1 Fes influences on macrophages in tumorigenesis……155

List of Abbreviations

2D/3D	Two-dimensional/three-dimensional
γc	Common gamma chain
AA	Antibiotic-antimycotics
Abl	Abelson murine leukemia viral oncogene homologue
AHR	Airway hyperresponsiveness
Alk	Anaplastic lymphoma kinase
ANOVA	Analysis of variance
Arg1	Arginase 1
Bcr	Breakpoint cluster region
BMM	Bone-marrow-derived macrophage
CAF	Cancer-associated fibroblast
CM	Condition medium
CTC	Circulating tumor cell
CSF-1	Colony-stimulating factor 1
CXCL12	C-X-C motif chemokine 12
DCIS	Ductal carcinoma in situ
DMEM	Dulbecco's Modified Eagle Medium
ECM	Extracellular matrix
EGF	Epidermal growth factor
EGFR	Epidermal growth factor receptor
EMT	Epithelial-mesenchymal transition
ER^+	Estrogen receptor positive
F-BAR	FCH-BIN/Amphiphysin/RSV
FCH	Fes-Fer CIP42 homology
FBS	Fetal bovine serum
Fes	Feline sarcoma
Fer	Fes-related
FGF	Fibroblast growth factor

Fps	Fujinami poultry sarcoma
Gag	Group associated antigen
GFP	Green fluorescence protein
GM-CSF	Granulocyte-macrophage CSF
Grb2	Growth factor receptor-bound protein 2
HBSS	Hank's Balanced Salt Solution
H&E	Hematoxylin and eosin
HGF	Hepatocyte growth factor
IL-4R	Interleukin-4 receptor
IL	Interleukin
IRS	Insulin receptor substrate
LDTA	Lymphocyte-defined tumor antigen
LPS	Lipopolysaccharides
MHC	Major histocompatibility complex
MMP	Matrix metalloproteinase
MMR	Macrophage mannose receptor
MMTV-LTR	Mouse mammary tumor virus long terminal repeat
MNG	Multinucleated giant cell
ND	Not detectable
NK	Natural killer
NMG	Normal mammary gland
NO	Nitric oxide
PAB	Phosphate-buffered saline with 1% (w/v) bovine serum albumin
PDGF	Platelet-derived growth factor
PE	Phycoerythrin
PI3K	Phosphatidylinositol 3-kinase
PIP_2	Phosphotidylinositol- (3,4)-bisphosphate
PIP_3	Phosphotidylinositol- (3,4,5)-trisphosphate
PR^+	Progesterone receptor positive
PTK	Protein-tyrosine kinase

PTB	Phosphotyrosine-binding
PyMT	Polyomavirus middle T
ROS	Reactive oxygen species
SDF-1	Stromal cell-derived factor 1
SH2	Src homology 2
Shc	Src homology 2 domain-containing transforming protein
Sos	Son of sevenless
Stat3/6	Signal transducer and activator of transcription 3/6
TAM	Tumor-associated macrophage
TGF-β	Transforming growth factor β
TIL	Tumor infiltrating lymphocyte
TLR	Toll-like receptor
TNF-α	Tumor necrosis factor α
VCAM-1	Vascular cell adhesion molecule-1
VEGF	Vascular endothelial growth factor
VLA-4	Very late activation antigen 4

Chapter 1

General Introduction

1.1 Breast cancer

1.1.1 Introduction

Breast cancer remains the most commonly diagnosed cancer among women worldwide and in Canada. One in 9 Canadian women is expected to develop breast cancer during her lifetime, and one in 29 Canadian women will die from breast cancer. In 2013, an estimated 65 new breast cancer cases will be diagnosed in Canadian women daily, and 14 Canadian women will die of breast cancer every day [1]. Although breast cancer mortality rates in Canada have decreased by 42 percent since 1986 as a result of better screening technologies, as well as improved treatments, breast cancer remains the leading cause of cancer-related death among Canadian women. This means that more work is required to study molecular targets that may ultimately lead to new treatment options for breast cancer patients.

1.1.2 Types of breast cancer

Breast cancer is a clinically heterogenous disease where origin and outcome can vary significantly. Based on histopathological presentation of the tumors, breast cancer can be classified as non-invasive, invasive, inflammatory breast cancer, and

Paget's disease of the nipple [2]. The most common type of non-invasive breast cancer is ductal carcinoma *in situ* (DCIS). This cancer originates inside the milk ducts and stays confined within the basement membrane and has not yet invaded into the surrounding stroma. DCIS is not life-threatening, but having DCIS can increase the risk of developing an invasive breast cancer later on. Invasive breast cancer, on the other hand, has invaded through the basement membrane into the surrounding stroma and can metastasize to distant organs. The most common types of invasive carcinomas are ductal and lobular carcinomas, which account for 50-80% of all invasive breast cancers. Other types of invasive breast cancer include invasive mucinous carcinoma (characterized by mucus produced by cancer cells), tubular carcinoma (characterized by the tubular phenotype exhibited by cancer cells), medullary carcinoma (characterized by a distinct boundary between tumor and normal tissue), and invasive micropapillary carcinoma (characterized by a nested papillary pattern). Inflammatory breast cancer and Paget's disease of the nipple are less common types of breast cancer, accounting for less than 5% of all breast cancers. In contrast, invasive ductal carcinoma (IDC) and ductal carcinoma *in situ* (DCIS) account for 85% of all breast cancer cases [3].

1.1.3 Risk factors

Breast cancer is a complex disease with no known single cause. There are a

number of risk factors that are linked to the development of the disease. Some established non-modifiable risk factors include gender and age, personal or family history of breast cancer, inherited genetic mutations, as well as early menstruation and late menopause. Being a woman is one of the strongest risk factors of breast cancer since the incidence among men is very rare with less than 1% of all breast cancer cases in Canada. The risk of developing breast cancer significantly increases with age; 82% of breast cancer cases and 90% of breast cancer deaths in Canada occur in women over the age of 50. A woman with cancer in one breast has a 3- to 4-fold increased risk of developing a new cancer in the other breast or in another part of the same breast. Having one first-degree relative (mother, sister, or daughter) with breast cancer approximately doubles a woman's risk, and having two first-degree relatives increases the risk by 3-fold. About 5% to 10% of breast cancer cases are thought to be hereditary, with the most common cause being an inherited mutation in the *BRCA1* and/or *BRCA2* genes, which play important roles in DNA damage repair. According to the most recent estimates, 55-65% of women who inherit a harmful *BRCA1* mutation and around 45% of women who inherit a harmful *BRCA2* mutation will develop breast cancer by the age of 70 [4][5]. A woman with early menstruation and late menopause may also have an increased risk of developing breast cancer, which may be due to a longer lifetime exposure to the hormones estrogen and progesterone.

Furthermore, other modifiable risk factors of developing breast cancer include few or no pregnancies, no breastfeeding, use of hormone replacement therapy, high

dose oral contraceptives, obesity, lack of physical activity, previous radiation exposure, high alcohol consumption, and smoking [6].

1.1.4 Molecular subtypes of breast cancer

Using gene expression profiling, studies of breast cancer have identified several major breast cancer subtypes, including normal-breast like, luminal A, luminal B, HER2 positive and basal-like subtypes [7-14]. Luminal A and luminal B subtypes are mostly identified among hormone receptor-positive cancers, whereas HER2 positive and basal-like are the major subtypes identified among hormone receptor-negative cancers. These breast cancer molecular subtypes differ with regard to their gene expression pattern, clinical features, response to treatment and prognosis.

Luminal A subtype accounts for about 40% of all breast cancer cases. Since tumors tend to be estrogen receptor positive (ER^+) and progesterone receptor positive (PR^+), patients respond well to hormone therapy; as a result, luminal A subtype showed the best prognosis with high 5-year survival (96%) and low 5-year local recurrence rate (0.8%), among all breast cancer subtypes [15-17]. Luminal B subtype is ER^+, PR^+ and $HER2^+$ with high Ki67 positivity indicating a large number of proliferating cancer cells. Women with luminal B tumors are often diagnosed at a younger age and have slightly poorer prognosis than those with luminal A tumors [15-17]. HER2 positive subtype is ER^-, PR^-, and $HER2^+$, and account for 10-15% of

all breast cancer cases. These tumors have a relatively poor prognosis and are prone to early and frequent recurrence and metastases [15-17]. Women with HER2+ breast cancers are treated with the drug Herceptin® (trastuzumab) as targeted therapy. Most basal-like tumors are triple negative (ER-, PR-, and HER-), and accounts for ~20% of all breast cancer cases. These tumors are often aggressive and have a poorer prognosis as compared to the estrogen receptor-positive subtype (luminal A and luminal B subtypes) [15-17]. These tumors tend to occur more often in younger women and African American women [18]. Women with basal-like breast cancers cannot be treated with hormone therapy or trastuzumab; and instead, they are usually treated with a combination of surgery, radiation therapy and chemotherapy. Normal breast-like is a less common molecular subtype of breast cancer. About 6-10% of all breast cancers fall into this category. These tumors are usually small and tend to have a good prognosis.

1.1.5 Breast cancer treatment

Treatment options for breast cancer patients include surgery, radiation therapy, chemotherapy, hormone therapy as well as targeted therapy [19]. Breast-conserving surgery is performed aiming to remove the cancer but not the breast itself, and includes lumpectomy (to remove the tumor only), partial or total mastectomy (to remove the part of the breast or the whole breast that has tumor), and modified radical

mastectomy (to remove the whole breast that has tumor, many of the lymph nodes under the arm, the lining over the chest muscles, and sometimes, part of the chest wall muscles). Radiation therapy is usually given following surgery to remove residual cancer cells remaining in the body by high-energy x-rays or other types of radiation. Chemotherapy may be given before surgery to shrink the tumor and reduce the amount of tissue that needs to be removed during surgery, which is called neoadjuvant chemotherapy. Or, chemotherapy may be given after the surgery to reduce the risk of cancer recurrence, which is called adjuvant chemotherapy. The most common chemotherapy drugs used for early breast cancer include Adriamycin® (doxorubicin), Ellence® (epirubicin), Cytoxan® (cyclophosphamide), Taxol® (paclitaxel) and Taxotere® (docetaxel) [20]. Tamoxifen is currently the most common hormone treatment for both early and advanced ER^+ breast cancer in pre- and post-menopausal women [21].

Unfortunately, conventional treatment options such as radiation therapy and chemotherapy lack tumor specificity and pose great toxicity to normal, rapidly proliferating cells, such as hair follicles and gastrointestinal cells. Hormonal therapy with tamoxifen can also act on cells all over the body and may increase the chance of developing endometrial cancer. These facts have led to the development of targeted therapy to attack specific cancer cells without harming normal cells. For example, monoclonal antibody, Herceptin® (trastuzumab), and tyrosine kinase inhibitor, lapatinib, have been used to target HER2 positive breast cancer [22-24]. Clinical trials

have been conducted to study the effect of targeted therapy in combination with chemotherapy; ultimately, providing more tailored treatment options to breast cancer patients [25-28].

1.1.6 Metastasis

Metastasis is a process by which tumor cells spread from the primary site to distant organs, and is the main cause of death from breast cancer due to its resistance to conventional therapies [29]. The metastatic cascade is divided into sequential stages including epithelial-mesenchymal transition (EMT), invasion, angiogenesis, intravasation, transport through vessels, extravasation and outgrowth of secondary tumors [30].

In normal breast tissues, luminal epithelial cells form the ducts and the secretory alveoli, and basal myoepithelial cells underlie the luminal epithelium and form a basal layer that rests on a basement membrane separating the stromal compartments [31, 32]. During EMT, initially polarized epithelial cells lose cell polarity and acquire phenotypes of mesenchymal cells, therefore inducing cellular invasion into neighboring stroma. EMT is characterized by loss of cell polarity, cell scattering and downregulation of epithelial proteins, particularly E-cadherin, which participate in regulating cell-cell adhesion. Loss of E-cadherin leads to decreased cell-cell contacts and increased cell motility [33]. Epithelial cells that have undergone

EMT also secrete matrix degrading proteases, such as matrix metalloproteinases (MMPs) [34], which are able to remodel the extracellular matrix (ECM) and release mitogenic and angiogenic factors into the tumor microenvironment [35]. Degradation of basement membranes and remodeling of ECM by MMPs facilitate tumor cell invasion into the surrounding tissue either as single cells or collectively in the form of clusters [36, 37]. Tumor cell invasion alone is not sufficient to produce distant metastases. It also requires the transport of malignant cells through blood and/or lymphatic vessels. Back in 1972, Dr Judah Folkman suggested that tumors cannot grow beyond a size of ~1mm in diameter and they stay dormant by prevention of neovascularization [38]. Most tumors start growing as small, avascular nodules. Due to lack of oxygen and other essential nutrients, they remain limited in size. Tumors induce angiogenesis to ensure exponential tumor growth by secreting pro-angiogenic signals, such as vascular endothelial growth factor (VEGF) [39]. VEGF binds to receptors on endothelial cells of nearby blood vessels, causing the endothelial cells to proliferate and bud from the existing blood vessels and migrate toward the tumor. Once the independent blood vessels have established around the tumor, it will start to grow to a larger size, and tumor cells intravasate into newly formed vessels and are transported through the vasculation. Indeed, angiogenesis is the rate-limiting step during tumor development and also one of the hallmarks of cancer [40-42]. Most tumor cells that entered the blood circulation are rapidly lost due to cell death [43], whereas a fraction of them will survive in the absence of adhesion, extravasate from blood vessels and

outgrow to micrometastases and eventually macrometastases in the secondary organs [44]. In 1889, the English surgeon Stephen Paget published the ‘seed and soil’ hypothesis, which states that the choice of the site for a secondary tumor is made not only by the tumor cells (the “seed”), but is largely influenced by the nature of the target organ (the “soil) [45, 46]. Therefore, a secondary tumor is established only if the seed can grow in the soil, that is, if the microenvironment of the target site is compatible with the properties and requirements of the disseminated tumor cells. The most common metastatic sites of breast cancer are the lung, liver, brain and bone.

1.1.7 Tumor microenvironment

Over the past decades, molecular cancer biologists have studied tumor development and progression from a tumor cell-centered perspective. However, emerging evidence indicates that the normal cells residing in the immediate vicinity of the tumor, the tumor stroma, also play an essential role in tumor initiation, progression, and metastasis [47, 48]. As the ‘seed and soil’ hypothesis originally postulated, both the tumor microenvironment (the “soil”) and tumor cells (the “seed”) are equally important to be investigated in order to better understand the biology of breast tumor development [46].

The tumor stroma is comprised mainly with fibroblasts, vascular endothelial cells, and a variety of infiltrating immune cells, including T and B lymphocytes,

macrophages, mast cells, granulocytes (neutrophils, basophils, eosinophils), dendritic cells, and natural killer cells. The tumor microenvironment constantly undergoes tissue remodeling by activating and recruiting fibroblasts and inflammatory cells to the tumor. These infiltrated cells, together with tumor cells, further remodel the microenvironment by secreting growth factors and proteinases. The tumor environment remains in an activated state; therefore, tumors are considered as ‘wounds that never heal’ [49, 50].

One of the largest components of the tumor stroma is constituted by cancer-associated fibroblasts (CAF). CAFs may be derived from resident fibroblasts, from bone marrow-derived mesenchymal stem cells, or from tumor cells that have undergone EMT [51-54]. Transforming growth factor β (TGF-β) and C-X-C motif chemokine 12/stromal cell-derived factor 1 (CXCL12/SDF-1) are the major tumor cell-derived factors that activate CAFs through the TGF-β and CXCL12/SDF-1 autocrine loop [55]. CAF-secreted CXCL12 stimulates tumor growth either by directly acting through the cognate receptor, CXCR4, expressed by tumor cells, or by promoting angiogenesis through the recruitment of endothelial progenitor cells into the tumor [56]. CAFs were found to induce the invasiveness of DCIS epithelial cells both *in vitro* and *in vivo* by increasing MMP9 and MMP14 expression [57], and also promote metastasis in breast cancer by secreting TGF-β [58].

Another crucial component of the tumor stroma corresponds to cells and

mediators of the innate immune system, that is, macrophages, granulocytes and mast cells. In 1863, Virchow hypothesized that the origin of cancer was at sites of chronic inflammation [59], and a growing body of evidence has indicated that inflammation contributes to a wide variety of tumors [60]. For example, colonic inflammation, such as that found in ulcerative colitis or Crohn's disease, predisposes patients to colorectal cancer [61]. Tumor-associated macrophages (TAMs) are a significant component of inflammatory infiltrates in the tumor microenvironment. TAMs are recruited to tumors by a range of growth factors and chemokines—including colony-stimulating factor 1 (CSF-1), granulocyte-macrophage CSF (GM-CSF), macrophage-stimulating protein (MSP), TGF-β1, chemokines CCL2, CCL7, CCL8, macrophage inflammatory protein-1α (MIP-1α), MIP-1β and macrophage migration inhibitory factor (MIF), which are often produced by tumor cells [62-64]. TAMs typically exhibit the M2 alternatively activated macrophage phenotype, as opposed to the classically activated M1 phenotype; and this often correlates with an immunosuppressive tumor microenvironment [65, 66]. Classical M1 macrophages exert anti-microbial and anti-tumorigenic effects by direct killing of microorganisms and tumor cells. In contrast, alternatively activated M2 macrophages provide many trophic functions that promote tumor progression and metastasis. For example, they stimulate angiogenesis by expressing VEGF, promote tumor invasion by producing MMP9, as well as promote tumor growth by providing proliferative signals, such as epidermal growth factor (EGF) [67-69]. TAMs have been directly visualized in association with tumor

cells intravasating into vessels, and increased TAM density strongly correlated with poor prognosis for breast, prostate, ovarian and cervical cancers [64, 70]. Furthermore, tumor-associated neutrophils (TANs) are another important cell in the tumor microenvironment. TANs can promote tumor destruction, but might also have an opposite effect of promoting tumor cell proliferation, angiogenesis and metastasis [71].

As part of adaptive immune responses, the role of T cells – the so-called tumor infiltrating lymphocytes (TILs) in the tumor microenvironment have been intensively studied [72]. $CD8^+$ cytotoxic T cells (among TILs) function as a direct cancer cell killers by recognizing peptides derived from tumor associated antigens that are presented by major histocompatibility complex (MHC) class I molecules. Following recognition, $CD8^+$ cytotoxic T cells are capable of cytokine release and killing of tumor cells by direct granule-mediated cytotoxity as well as delivering death signals mediated by FAS [73-75]. Recent meta-analysis studied the clinical significance of TILs in solid tumors, and suggested that the presence of $CD8^+$ T cells is a good prognosis marker with improved survival [76]. However, $CD4^+$ helper T cells are more plastic and play dual roles in the tumor microenvironment by converting from anti-tumorigenic to pro-tumorigenic behaviours. T_{reg} cells, a subset of $CD4^+$ helper T cells, constitutively express the high-affinity interleukin-2 (IL-2) receptor CD25, CTL antigen-4 (CTLA-4), and the lineage-specific transcription factor Foxp3 [77]. Evidence for the role of T_{regs} in the regulation of anti-tumor immunity was first

provided by Sakaguchi *et al.* using a syngeneic mouse heterotopic transplant model [78, 79]. This was later reproduced in several mouse tumor models, all of which demonstrated that depletion of T_{regs} via anti-CD25 mAb prior to tumor inoculation led to syngeneic tumor rejection [80]. T_{regs} have also been shown to suppress immune responses to tumors in non-small cell lung cancer and ovarian cancer [81].

1.1.8 Models to study breast cancer

Breast cancer is not a single disease. It is a collection of breast diseases that have diverse histopathologies, genetic and genomic variations, and clinical outcomes. Because of this complexity and heterogeneity, no single model would be expected to mimic all aspects of this disease. Therefore, we should be aware of the strengths and limitations of each experimental model, and be careful of choosing the right model when investigating different aspects of breast cancer [82].

1.1.8.1 Cell culture system

Breast cancer cell lines, such as MCF-7, T-47D, BT-474, SKBR3, MDA-MB-231 and Hs578T, have been the most widely used cell models to study how proliferation, apoptosis and migration are deregulated during the progression of breast cancer [83]. Recent studies compared the molecular profiles and genomic alterations of 51 breast cancer cell lines and primary human breast cancers, and

suggested that no single cell line was truly representative of the five common subtypes of breast cancer [84]. In order to overcome this limitation, cell lines were classified into luminal and basal subtypes, and subtype cell lines can be used as a system to provide powerful models for investigating breast cancer.

Most *in vitro* studies have been performed in two-dimensional (2D) cell culture. The major limitation of 2D culture is that cells grown on plastic plates lack exposure to components of the extracellular matrix as well as tumor-stromal cell interactions. Kenny and colleagues suggested that 3D reconstituted basement membrane cultures more faithfully recapitulated the tumor microenvironment *in vivo* after comparing gene expression, genomic alterations and morphologies of 27 breast cancer cells cultured in 2D versus 3D conditions [85-89]. Three-dimensional culture models have been widely used to investigate critical signaling interactions that are difficult to investigate *in vivo* [90-94].

1.1.8.2 Xenograft models

Orthotopic mouse models of breast cancer typically involve injecting tumor cells into the mammary fat pads of immunocompromised mice. These xenografts have allowed researchers to investigate many facets of breast cancer, including tumor initiation and growth, the role of the tumor microenvironment (tumor-stromal cell interaction, inflammation and angiogenesis), as well as metastasis. Xenografts can

also be used as preclinical models to predict whether anticancer agents will be effective in treating cancer patients. The advantages of xenograft mouse models include rapid and reproducible tumor growth, and the ease of generating sufficiently large cohorts of tumor-bearing mice for statistical analysis. However, there are several caveats to consider when using xenograft models. First, xenografts must be established in immunocompromised mice, and the absence of an intact immune system may profoundly affect tumor development and progression [95]. Second, the mouse mammary stroma is different from the human stroma [31, 96, 97]. The mouse mammary gland contains a large amount of fat with small amounts of interspersed fibrous connective tissue. Although the human breast also contains large areas of adipose tissue, the epithelium is generally not closely associated with adipose tissue; rather, it is associated with fibrous connective tissue. Furthermore, not all paracrine acting factors and their cell associated receptor systems are compatible between mouse and human. Xenograft models using a humanized fat pad in immunocompromised mice have been used in attempts to overcome some of these limitations [98].

From a technical perspective, there are two common ways to study metastasis using xenograft mouse models. In spontaneous metastasis assays, metastases arise from orthotopic tumors, and tumor cells must be highly metastatic to be capable of developing distant metastases at secondary sites. In experimental metastasis assays, tumor cells are introduced directly into the circulation via intravenous injection,

bypassing some crucial steps of metastasis [99]. While it has been controversial, some researchers claim that the direct introduction of cancer cells into the blood circulation should be considered as assay of organ colonization and not a true model of the metastatic process [100]. One problem of using xenografts to study metastasis is that metastatic nodules are most likely to be detected in the lungs, but not other common sites that occur in human breast cancer, including the liver, bone and brain. This makes it difficult to study the mechanisms of breast cancer metastasis in an unbiased way.

In chapter 2, we investigated the role of Fes kinase in human breast cancer using an orthotopic mouse engraftment model employing the AC2M2 mammary carcinoma cell line, which is a highly lung metastatic variant of the SP1 cell line, derived following three serial passages of lung metastatic nodules isolated after mammary fat pad engraftments in syngeneic mice [101]. The SP1 cell line was originally isolated from a spontaneous, poorly metastatic mammary intraductal adenocarcinoma that arose in an 18-month-old CBA/J female retired breeder [101, 102].

1.1.8.3 Transgenic mouse model

The most common transgenic mouse models of breast cancer were generated by targeting oncogenes such as *Myc*, *PyMT*, rat *Erbb2/Neu* and *Hras* to the mammary

gland using mouse mammary tumor virus long terminal repeat (MMTV-LTR) and whey acidic protein (Wap) promoters [103-106]. Although individual transgenic mouse models cannot faithfully recapitulate all aspects of human breast cancer, they have provided invaluable tools to expand our understanding of the genetics and biology of breast cancer.

The MMTV promoter drives high expression levels of transgene expression in ductal and alveolar luminal epithelial cells as well as myoepithelial cells during all stages of mammary gland development. ErbB2 (also known as HER2) is a member of the epidermal growth factor receptor (EGFR) family of receptor tyrosine kinases [107, 108]. ErbB2 is found to be overexpressed in 20-30% of human breast cancer due to gene amplification [24, 109], and ErbB2 overexpression strongly correlates with poor clinical prognosis [107, 110-112]. MMTV-driven overexpression of an activated form of the rat homolog of ErbB2 (Neu) in transgenic mice resulted in the development of multifocal adenocarcinomas with lung metastases by three months of age [105]. Subsequently, Guy and Muller generated transgenic mice with the overexpression of wild-type ErbB2 in mammary gland, since the primary mechanism in human breast cancer is the overexpression of wild-type ErbB2 and not its mutational activation [24, 113, 114]. These transgenic mice also provoke tumor formation and metastatic dissemination, but with longer latency (an average of 7 months) [104]. MMTV-Neu transgenic mice are powerful model to study the HER2 subtype of human breast cancer. In chapter 3, we explored the role of Fes kinase in human breast cancer using

this MMTV-Neu transgenic mouse model.

Mammary gland-specific expression of polyomavirus middle T oncogene (PyMT) under the control of the MMTV promoter in transgenic mice results in the development of multifocal mammary adenocarcinomas and metastatic lesions in the lungs [103]. In MMTV-PyMT mice, tumor formation and progression is characterized by four stages—hyperplasia, neoplasia, and early and late carcinoma, which is comparable to progression of human breast cancer from benign to invasive carcinoma. In addition to the morphological similarities, a gradual loss of hormone receptors (estrogen and progesterone) and β1-intergin as well as the overexpression of ErbB2 and cyclin D1 also closely recapitulates human breast cancer [115]. Hierarchical clustering analyses of the MMTV-PyMT tumors along with classified human tumors suggest that the status of MT tumors matches better with the luminal B subgroup of human breast tumors [116]. MMTV-PyMT transgenic mice are another excellent model to understand the biology of tumor progression in human breast cancer.

1.2 Fes kinase

1.2.1 Introduction

Protein-tyrosine kinases (PTKs) are found in all multi-cellular eukaryotic organisms, and play key roles in the regulation of a wide variety of cellular events, including cell growth, differentiation, adhesion, motility and apoptosis (reviewed in

[117, 118]). In humans, deregulation of PTKs has been demonstrated in the development of many disease states, including cancer (reviewed in [119, 120]). Due to their involvement in various forms of cancers, PTKs have become prominent targets for cancer therapeutic intervention [119]. PTKs are classified as receptor types and non-receptor types. Fes (Feline sarcoma), also known as Fps (Fujinami poultry sarcoma), and Fes-related Fer kinases are distinct from all other members of the PTK family, and make up subfamily IV of the non-receptor PTKs [121].

1.2.2 Discovery of *fes/fps* as transforming retroviral oncogenes

The *fes* and *fps* genes were originally identified as retroviral oncogenes isolated from feline and avian sarcomas, respectively [122-126]. Subsequent sequence analysis revealed that *v-fes/fps* alleles were homologous to cellular *c-fes/fps* proto-oncogenes, and the corresponding human and chicken orthologous were soon identified [127-131]. For simplicity, I will refer to this gene as *fes* and the protein as Fes for the remainder of this thesis.

The viral Fes (v-fes) proteins consist of amino-terminal retroviral group associated (Gag) sequences fused to either the full-length or varying portions of cellular Fes proteins (Figure 1.1 A) [132]. The viral Gag sequences confer unregulated tyrosine kinase activity upon Fes. Chicken myeloid progenitors infected with retroviruses containing the *v-fes* oncogene differentiated *in vitro* into macrophages

without exogenous macrophage colony stimulating factors [133]. Viral Fes activity has also been demonstrated to reduce or eliminate the need for exogenous growth factors in transformed fibroblasts [134]. Although several important signaling proteins have been implicated as putative targets of viral Fes kinases based on their increased tyrosine phosphorylation in viral Fes transformed cells, including p120RasGAP and the associated p190RhoGAP and p62Dok proteins [135-137], phosphatidylinositol 3-kinase (PI3K) [138], breakpoint cluster region (Bcr) [139], Src homology 2 domain-containing transforming protein (Shc) [140], signal transducer and activator of transcription 3 (Stat3) [141] and connexin 43 [142]), the molecular mechanism for the transforming potential of viral Fes is not yet understood.

1.2.3 Structural features of Fes and Fer proteins

Human Fes and Fer PTKs are 822 amino acids in length, and share a close structural similarity, consisting of an N-terminal FCH-BIN/Amphiphysin/RSV (F-BAR) domain, followed by a predicted coiled-coil (CC) motif, a central Src homology 2 (SH2) domain, and a C-terminal kinase domain (Figure 1, panel A; reviewed in [143]).

The F-BAR domain spans approximately 300 amino acids at the N-terminus. This unique amino-terminal structure distinguishes Fes and Fer from all other members of the PTK family. The F-BAR domain has been identified in members of *Pombe*

CDC15p homology (PCH) family of adaptor proteins, such as FBP17 and CIP4. These proteins have been shown to regulate cytoskeletal rearrangements, vesicular transport and endocytosis [145, 146]. F-BAR domains can dimerize to form banana-shaped curved structures, which bind to membranes through their positively charged concave surfaces and induce membrane curvature [146]. Although Fes and Fer kinases do not share all the characteristics of other F-BAR domain-containing proteins, it is likely that through their F-BAR domains they are able to bind phospholipids within the membrane. This may allow them to interact with and phosphorylate other proteins involved in regulating membrane processes, which represents important potential mechanistic functions for Fes kinase.

Fes and Fer proteins contain a central SH2 domain between the CC2 motif and the kinase domain (Figure 1.1 A). The SH2 domain is a non-catalytic domain found in a wide variety of signaling molecules and functions to mediate protein-protein interaction by binding to specific phosphotyrosine-containing peptide sequences. Phosphopeptide library screening using the Fes SH2 domain as an affinity matrix has identified a consensus-binding sequence YEXV/I (in which Y represents tyrosine; E, glutamate; X, any amino acid; V, valine; and I, isoleucine), which is present in many cellular proteins, including focal adhesion kinase (Fak), Tec, Lyn, Abelson murine leukemia viral oncogene homologue (Abl), haemopoietic cell kinase (Hck), CD72, CD3ε, SH2-domain-containing protein-tyrosine phosphatase-1 (SHPTP-1), leukocyte-antigen-related protein tyrosine phosphatase (LAR-PTP), FcγRI receptor,

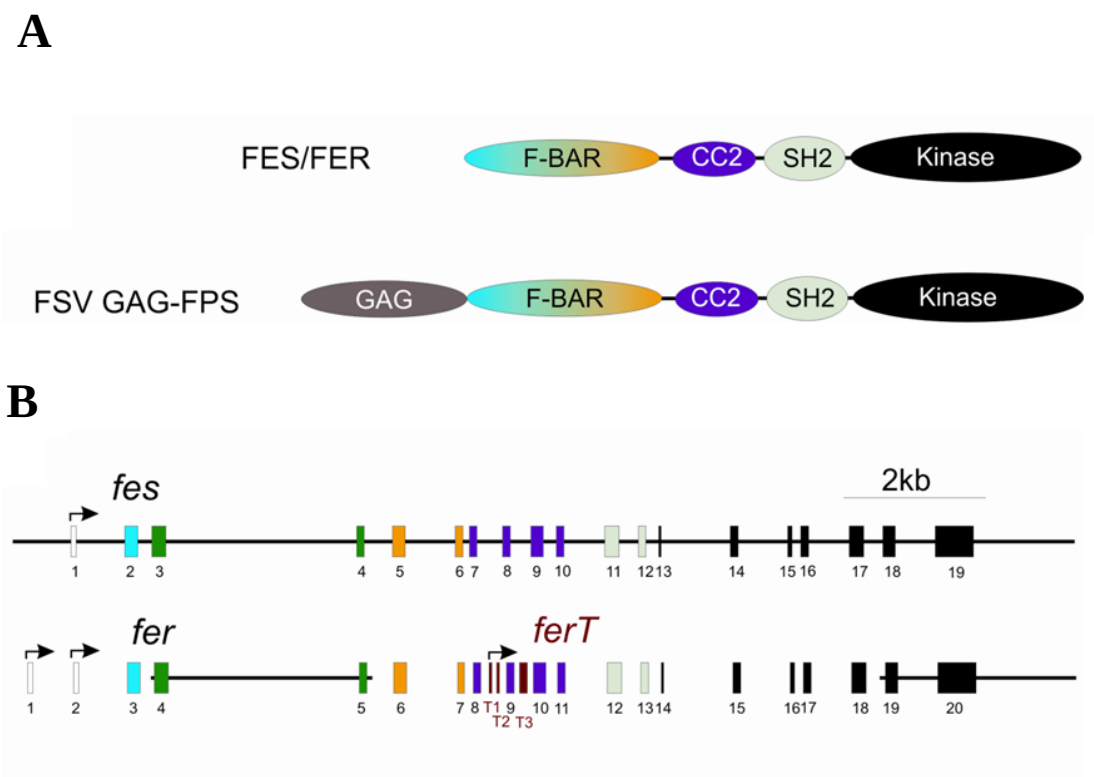

Figure 1.1 Structure of Fes and Fer proteins and exon organization of the *fes* and *fer* loci. A) Fes and Fer share a close structural similarity, consisting of an N-terminal F-BAR domain (blue/green/yellow oval), a predicted coiled-coil motif (CC2, purple oval), a central SH2 domain (ice blue oval), and a C-terminal kinase domain (black oval) [143]. FSV (Fujinami sarcoma virus) Gag-Fps consists of N-terminal retroviral Gag sequences (Gray oval) fused to the full-length of cellular Fps proteins [132]. B) The *fes* and *fer* proto-oncogenes are located on chromosomes 15.q26.1 and 5q.21, respectively [121]. The entire human *fes* locus spans approximately 13kb and consists of 19 exons. The exon organization of *fer* locus is almost identical to *fes*. The *fes* gene is illustrated as a continuous horizontal line, whereas the *fer* gene is indicated by the open line. Transcription start sites are indicated with right-pointing arrows. The first noncoding exons of *fes* (exon 1) and *fer* (exon 1 and 2) are represented as uncoloured rectangles, while the subsequent 18 coding exons are coloured to match the corresponding encoded protein domains shown in panel A. The *fer* gene has an internal promoter that drives the expression of *ferT* (shown in red) [144]. The three unique testes-specific exons (T1-3) are also indicated in red. (Adapted from [143])

G-CSF receptor, ezrin, Bcr, 3BP2A and γ-adaptin [147, 148]. It is surprising that although many potential SH2 binding partners of Fes have been proposed, there is very little biochemical evidence to support these interactions. Similarly, there is also little direct evidence of any intermolecular or intramolecular interactions mediated by the Fer SH2 domain, with the exception of cortactin, which appears to be a substrate for Fer [149, 150].

There are at least two tyrosine phosphorylation sites in the catalytic domain of Fes and Fer kinases, the first of which is a conserved tyrosine residue in the activation loop at Tyr713 in Fes [151] and Tyr715 in Fer (Craig, A. W. B. and Greer, P., unpublished observations). A second important site has been mapped to Tyr811 in Fes [152], two additional sites have been mapped in the N-terminal half of Fer at Tyr299 [153] and Tyr402 [154]. Tyr713 is the major autophosphorylation site in Fes, and phosphorylation of this site is diagnostic of the active form of the Fes kinase [152, 155]. The crystal structure of the SH2 domain of Fes kinase has been recently solved, which shows that the SH2 domain interacts with the N-terminal lobe of kinase domain to promote its activity [156].

1.2.4 Expression patterns and subcellular localization of Fes and Fer

The *fes* proto-oncogene is localized to human chromosome 15.q26.1, whereas the human *fer* locus maps to chromosome 5q.21 [121]. The complete human *fes* locus is

contained within 13kb of genomic sequence [130]. It consists of 19 exons, the first exon being non-coding. The exon organization of the *fer* locus is almost identical to *fes*. It also contains 18 coding exons which encode completely overlapping homologous amino acid sequence to Fes (Figure 1.1 B). Fes is expressed in a tissue-specific manner, with the highest levels present in myeloid, endothelial, and subsets of epithelial and neuronal cells [157]. Recently, it has been shown that Fes expression was induced during pregnancy and lactation, and its kinase activity was dramatically enhanced [158]. On the other hand, Fer is ubiquitously expressed, suggesting its general function common to all cells [159], but there is also a testis specific shorter FerT isoform lacking the N-terminal F-BAR and CC2 domains that results from the use of an internal promoter and several unique exons [144] (Figure 1.1 B).

1.2.5 Studies using transgenic and gene targeted mouse models of Fes kinase

Over the past two decades, several transgenic and gene-targeted mouse models have been created to explore the normal physiologic roles of the Fes kinase and its potential involvement in diseases.

The first transgenic mouse model of Fes was generated by microinjection of the 13kb fragment of human genomic DNA containing the entire *fes* coding sequence into mouse zygotes to achieve tissue-specific over-expression of wild type Fes. These transgenic mice displayed an appropriate tissue-specific expression pattern of the

human *fes* gene with the expected high levels observed in myeloid tissues, and showed no phenotypic changes [160].

Using the same zygote DNA microinjection method, our lab next generated a transgenic mouse line expressing kinase-activated Fes, encoded by a mutant human *fes* gene with an N-terminal Src myristoylation sequence [161]. These transgenic mice displayed widespread hypervascularity, eventually progressing to multifocal hemangiomas, and *fes* transcripts were localized to endothelial cells of both the vascular tumors and normal blood vessels [161]. These observations led to the discovery that Fes is normally expressed at high levels in endothelial lineages, and Fes may be involved in regulating endothelial cell proliferation and angiogenesis.

Subsequently, mice have been targeted with either null (*fes*-null) or kinase-inactivating (*fesKR*) mutations in the *fes* locus. The null targeting resulted in the replacement of exons 15 through 18 with the positive selection marker PGKneo [162]. This deletion eliminates coding sequences for most of the Fes kinase domain, resulting in the production of an unstable truncated Fes protein, which is rapidly degraded. Homozygous *fes*-null mice generated no detectable Fes protein and have no Fes kinase activity, both of which can be rescued by a human *fes* transgene [162]. The kinase-inactivating mutation was generated by converting the lysine (K) 588 codon, which is essential for Fes catalytic function, to an arginine (R) codon [163]. Both *fes*-null and *fesKR* mice were found to develop normally with only subtle defects in

hematopoiesis and essentially normal vasculogenesis and angiogenesis [162, 163]. However, *fes*-knockout mice generated by Hackenmiller *et al.* exhibited abnormal myeloid proliferation and functional defects in the macrophage lineage [164]. The differences in the phenotypes observed by our group and Hackenmiller group may be due to mouse strain background differences and the specific molecular approaches used to target the *fes* locus [162].

When challenged with LPS to mimic a gram-negative bacterial infection, *fps*-null mice showed a hyper-inflammatory phenotype, which may due to the fact that macrophages in these mice secreted higher levels of pro-inflammatory cytokine tumor necrosis factor α (TNF-α) in response to LPS challenge. This correlated with a defect in Toll-like receptor (TLR) 4 internalization and prolonged activation of the NF-κB signaling pathway in *fps*-null macrophages [165]. These results suggest that Fps may play an important role in regulating the innate immune response to endotoxin through controlling production of the key cytokine, TNF-α, by macrophages.

Given the importance of angiogenesis and inflammation in tumor initiation and progression, it has become apparent that Fes might contribute to cancer through its role in stromal cells such as vascular endothelial cells and macrophages.

In addition, a more recent study has also revealed that the Fes kinase is highly expressed in breast epithelial cells during lactation, and it is a component of the E-cadherin-based adherens junction in the mammary gland during lactation [158]. So,

it seems reasonable to suspect that Fes may also play tumor cell intrinsic roles in tumorigenesis.

1.2.6 An identity crisis for Fes: Oncogene or Tumor suppressor?

1.2.6.1 Evidence for oncogenic functions of Fes

So far, with our knowledge, we do not know yet if Fes kinase plays an oncogenic or tumor suppressor role in human breast cancer, since there is evidence supporting either role of Fes.

fes/fps was originally identified as an oncogene from feline (*fes*) or avian (*fps*) retroviruses [122-126]. Viral Fps proteins, encoded by *fps* fused to an N-terminal retroviral Gag sequence, were among the first members of the PTK family to be characterized as dominate-acting oncoproteins. When expressed under the control of a heterologous promoter in transgenic mice, *v-fps* induced tumors in lymphoid and mesenchymal tissues [166]. This observation strongly argued that *fes/fps* might be an oncogene and activating mutations in the *fes/fps* proto-oncogene might contribute to human cancer.

To further support oncogenic function for Fes in human cancer, Fes protein expression has been reported in renal cell carcinomas [167]. Small interfering RNA-mediated knockdown of Fes expression inhibited cellular proliferation of renal carcinoma cells, however, ectopic expression of either wild-type or kinase-inactive

Fes in these cells failed to alter their proliferation *in vitro* and *in vivo* [168].

1.2.6.2 Evidence for tumor suppressor functions of Fes

An exciting report by Bardelli *et al.* [169] at first seemed to provide the biological evidence that *fes* could indeed behave like a dominant-acting oncogene in human cancer. They performed a mutational analysis of sequences encoding the catalytic domains of 89 tyrosine kinases in a panel of 182 human colorectal cancers, and revealed four missense mutations in sequences encoding the kinase domain of Fes. They speculated that these mutations might have activated the Fps kinase and thereby contributed to cancer. However, subsequent biochemical and theoretical structural analysis demonstrated that these mutations found in human colorectal cancer actually result in the inactivation, rather than activation of Fes [170]. This suggested the possibility that *fes* might also function as a tumor suppressor.

Using the MMTV-polyomavirus middle T transgenic breast cancer model, it was shown that tumor onset occurred earlier in mice targeted with either *fps*-null or kinase-inactive mutations as compared to wild type mice [170]. This earlier tumor onset phenotype was rescued by interbreeding with a human *fes* transgene [170]. These observations provided the first compelling genetic evidence that Fes could play a tumor suppressor role in epithelial tumorigenesis.

More recently, findings from Smithgall's group implicated Fes kinase as a

tumor suppressor in colorectal cancer [171, 172]. In contrast to normal colonic epithelium, Fes expression was reduced or absent in most colon tumor sections. Fes protein levels were also low or absent in a panel of human colorectal cancer cell lines. Ectopic expression of wild type Fes in these cell lines inhibited their anchorage-independent growth [171]. The *fes* promoter was observed to be methylated in colorectal cancer cell lines, and this correlated with down-regulation of Fes protein expression [172]. These colon cancer studies provided more evidence for a potential tumor suppressor role for Fes in epithelial cancer.

In summary, the current literature suggests Fes may have a very complex involvement in cancer, including oncogenic and tumor suppressor functions that are intrinsic to cancer cells, as well as specific to stromal cells, such as macrophages and vascular endothelial cells. The main focus of this research project is to understand the multiple roles of Fes, and ultimately determine if Fes inhibition might represent a therapeutic option for treating breast cancer patients.

1.3 Interleukin-4

1.3.1 Introduction

Interleukin-4 (IL-4) is a pleiotropic type I cytokine that plays a critical role in the regulation of immune responses [173, 174]. IL-4 consists of three intra-chain disulfide bridges and adopts a bundled four α-helix structure [175, 176]. IL-4 is

produced and secreted by many immune cells, including, $CD4^+$ Th2 helper T cells [177], $CD4^+NK1.1^+$ NKT cells [178, 179], basophils [180-182], mast cells [183, 184], and activated eosinophils [185].

1.3.2 Biological functions of IL-4

IL-4 was first described as B-cell growth factor isolated from a mouse thymoma based on its ability to induce the proliferation of mouse B lymphocytes which had been purified with anti-IgM antibodies [186]. The designation B-cell stimulatory factor-1 was proposed when it was shown to act on resting B cells to induce expression of class II MHC molecules [187] and to enhance their subsequent proliferative responsiveness to anti-IgM antibodies [188, 189]. IL-4 has also been shown to promote immunoglobulin class switching of human B cells from IgM to IgE and IgG4 [190] and mouse B cells to IgE and IgG1 [191, 192].

Besides being a B-cell differentiation and stimulatory factor, IL-4 has broad functions in multiple cell types of hematopoitic and non-hematopoietic origin. Upon exposure to IL-4, naïve T (Th0) cells differentiate into Th2 helper T cells while differentiation toward the Th1 cell phenotype is inhibited. IL-4 stimulated Th2 cells are also capable of producing additional IL-4 and a series of other cytokines including IL-5, IL-10 and IL-13 [193, 194]. IL-4 induces vascular endothelial cells to express vascular cell adhesion molelcule-1 (VCAM-1) [195], but not intracellular adhesion

molecule-1 (ICAM-1) and E-selectin [196, 197]. The interaction between VCAM-1 expressed by vascular endothelial cells and very late activation antigen 4 (VLA-4) expressed by immune cells promotes the adhesion of immune cells to the lining of vessels in a selective manner, facilitating the recruitment of VLA-4-expressing T cells, eosinophils and basophils, but not VLA-4-nonexpressing neutrophils, to sites of inflammation [196, 198, 199].

IL-4 is also a potent macrophage fusion factor, capable of inducing macrophages to form large multinucleated giant cells (MNG) that are central players in the inflammatory response to foreign materials and in adverse responses to implants. IL-4-induced MNG formation *in vitro* is dependent on many factors, including the concentration of IL-4, the source of macrophages, macrophage density, the length of incubation, and even tissue culture surface material [200]. In addition, IL-4 is a survival factor, protecting lymphocytes and myeloid progenitors from apoptosis [201-205].

In response to lipopolysaccharides (LPS) expressed by bacteria or IFN-γ released from $CD8^+$ Th1 T cells and NK cells, macrophages undergo classical (M1) activation which is characterized by increased expression of TNF-α, IL-12, IL-6, and nitric oxide (NO) [206-208]. Through these pro-inflammatory mediators, classically activated M1 macrophages exert anti-microbial and anti-tumorigenic effects, including direct killing of microorganisms and tumor cells [209]. In contrast to

M1-like classical activation, macrophages have been shown to undergo alternative M2-like activation in the context of wound healing or within the tumor microenvironment [66, 210, 211]. IL-4 and IL-13 secreted from $CD4^+$ Th2 cells, mast cells and basophils are capable of inducing macrophages to undergo this alternative M2 activation. This leads to increased expression of IL-10, TGF-β, arginase 1, the macrophage mannose receptor (MMR), and CD23 [206, 210, 212-214]. Instead of killing tumor cells, M2 activated macrophages are believed to promote tumor cell growth, invasion and metastasis by secreting paracrine acting factors and extracellular matrix remodeling factors including EGF, MMP and VEGF [209].

1.3.3 IL-4 receptor complex

IL-4 receptors (IL-4R) are present in hematopoietic, endothelial, epithelial, muscle, fibroblast, hepatocyte and brain tissues and are usually expressed at between 100 and 5000 molecules per cell [215, 216]. IL-4 initiates signal transduction through one of two different receptor complexes, a type I or type II receptor (Figure 1.2). The type I receptor is a heterodimeric complex comprising a 140kDa IL-4Rα chain and a common gamma chain (γc), which is a signal-transducing unit shared by receptors for members of the IL-2 subfamily of hematopoietins [217-219]. The type II receptor also consists of the IL-4Rα chain but the γc is substituted by the IL-13 low affinity receptor 1 (IL-13Rα1) [220]. The type I receptor is specific for IL-4, whereas the type

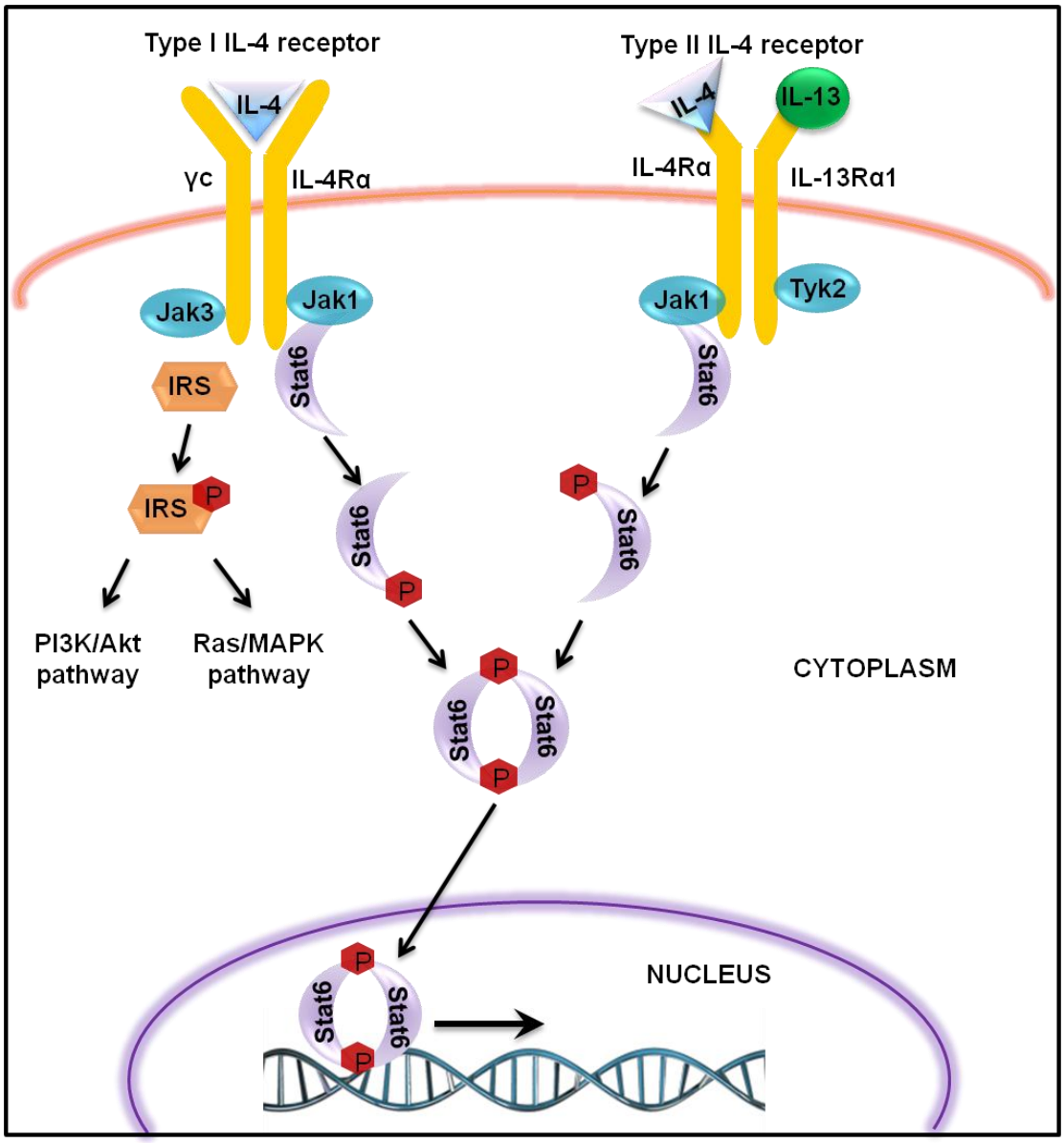
Type I IL-4 receptor
Type II IL-4 receptor
IL-4
IL-13
γc
IL-4Rα
IL-4Rα
IL-13Rα1
Jak3
Jak1
Jak1
Tyk2
Stat6
Stat6
IRS
IRS
P
Stat6
P
P
Stat6
PI3K/Akt pathway
Ras/MAPK pathway
CYTOPLASM
P
Stat6
Stat6
P
NUCLEUS
P
Stat6
Stat6
P

Figure 1.2 IL-4 signaling pathways. IL-4 initiates signal transduction through either type I or type II receptor. The type I receptor is a heterodimeric complex comprising a IL-4Rα chain and a common gamma chain (γc), while the type II receptor consists of the IL-4Rα chain and the IL-13 low affinity receptor 1 (IL-13Rα1). The type I receptor is specific for IL-4, whereas the type II receptor can be activated by either IL-4 or IL-13. Upon activation by ligand binding, Jak1 and Jak3 are recruited to IL-4Rα and γc, respectively; whereas, Jak1, and Tyk2 are recruited to IL-4Rα and IL-13Rα1, respectively. Stat6 is then recruited to the receptor through its SH2 domain, and becomes phosphorylated by Jak kinases. Phosphorylated Stat6 disengages from IL-4Rα and homodimerizes with a second Stat6 molecule. Stat6 homodimers translocate into the nucleus and initiate the transcription of IL-4 target genes. In addition to Stat6, IL-4R recruits and activates IRS molecules through an N-terminal PTB domain. When IRS molecules become phosphorylated, they interact with the p85 regulatory subunit of phosphoinositide 3-kinase (PI3K) and the adaptor molecule growth factor receptor-bound protein 2 (Grb2). These interactions lead to the activation of the PI3K—Akt and Ras—MAPK signaling pathway, respectively.

II receptor can be activated by either IL-4 or IL-13. This explains why IL-4 and IL-13 share many similar biological functions [221, 222]. Hematopoietic cells such as T and B cells express only the type I receptor, whereas cells of the myeloid lineage such as monocytes, macrophages, and fibroblasts express both type I and type II IL-4Rs. Non-hematopoietic cells such as smooth muscle cells and epithelial cells predominantly express the type II receptor [223].

The IL-4Rα chain is 785 amino acids long, with 553 residues comprising the cytoplasmic domain [217]. There are five highly conserved tyrosine residues (Y497, Y575, Y603, Y631 and Y713) in the cytoplasmic domain which are potential sites of phosphorylation and subsequent interaction with downstream signaling molecules through their SH2 or phosphotyrosine-binding (PTB) domains [174]. Based on biological functions associated with them, these five highly conserved tyrosine residues can be grouped into three distinct regions. The first region containing Y497 is required for relaying proliferation signals through recruitment of several intracellular messengers such as insulin receptor substrate (IRS) proteins and Shc [224-226] [227]. The second region contains tyrosine residues Y575, Y603 and Y631, and is critical for transducing downstream signals through Stat6 activation and subsequent gene expression [228]. Finally, Y713 residing within an immunoreceptor tyrosine-based inhibitory motif (ITIM) is involved in the activation of phosphatases and plays an important role in down-regulating cell responses [229].

IL-4 Rα alone is able to bind IL-4 with high affinity (K_d 20 to 300 pM) [174]. IL-4 engagement allows the γc chain to recognize the IL-4 bound IL-4Rα complex in the plasma membrane, and the resulting heterodimerization of these subunits in turn initiates the signaling cascade. However, cells lacking γc chain can still respond to IL-4 and transduce signals by homodimerization of IL-4Rα. Reichel *et.al.* have shown that the binding of stem cell factor (SCF) to the chimeric receptor kit/IL-4Rα is sufficient to activate Jak1 and Stat6, and to induce IL-4-specific gene expression in the absence of γc chain [230].

1.3.4 IL-4 signaling pathways

1.3.4.1 JAK—STAT pathway

In hematopoietic cells, the binding of IL-4 to IL-4Rα brings γc in close proximity, and heterodimerization of these two chains results in the recruitment of the Janus family of tyrosine kinases Jak1 and Jak3 to IL-4Rα and γc, respectively [231, 232]. However, in non-hematopoietic cells, type II IL-4R recruits Jak1, Jak2, and Tyk2 [222] [223]. These Jak kinases then become phosphorylated through tyrosine *trans*-autophosphorylation [174]. Once activated, Jak kinases mediate the phosphorylation of tyrosine residues Y575, Y603, and Y631 in the IL-4Rα cytoplasmic tail [174, 233], creating docking sites for signal transducer and activator of transcription 6 (Stat6). Stat6 is recruited to the receptor through its SH2 domain,

and becomes phosphorylated by Jak kinases at tyrosine residues including Y641; a C-terminal tyrosine that is very important for Stat6 dimerization [234, 235]. Phosphorylated Stat6 then disengages from IL-4Rα and homodimerizes through interaction of its SH2 domain with the C-terminal phosphotyrosine residue of a second Stat6 molecule [236]. Stat6 homodimers then translocate into the nucleus, where they recognize specific cis-acting sequences in the promoter regions of responsive genes, and thereby initiate the transcription of IL-4 target genes [237]. Stat6 mediated IL-4 target genes include those that encode for MHCII, CD23, germline immunoglobulin ε, IL-4Rα, VCAM1 and E-selectin [197, 234, 235, 238-240].

In this way, Stat6 plays a central role in exerting the biological responses of IL-4. Mice deficient in Stat6 displayed defects in CD23 and MHC-II expression, Th2 helper T cell differentiation and proliferation, and immunoglobulin class switching [241-243]. Similar phenotypes were also observed in IL-4 deficient mice or in animal challenged with neutralizing antibodies to IL-4 and the IL-4R [241].

1.3.4.2 PI3K—AKT pathway

In addition to Stat6, IL-4R recruits and activates IRS molecules through an N-terminal PTB domain [244, 245]. IRS-1/2 binds to an insulin IL-4 receptor (I4R) motif within the cytoplasmic region of IL-4Rα. Once phosphorylated, this conserved

tyrosine-497 residue within the I4R motif is thought to be a site of interaction with the IRS-1/2 PTB domain [224]. Studies have shown that cell lines expressing an IL-4Rα Y497F mutant consistently failed to activate the IRS pathway and did not proliferate in response to IL-4 [246]. When IRS-1/2 molecules become phosphorylated, they act as cytosolic docking sites linking a variety of SH2 domain-containing signaling molecules to phosphorylated receptor complexes [247-249]. Phosphorylated IRS-1/2 interacts with the p85 regulatory subunit of phosphoinositide 3-kinase (PI3K) and the adaptor molecule growth factor receptor-bound protein 2 (Grb2). These interactions lead to the activation of the PI3K—Akt and Ras—MAPK signaling pathway, respectively.

Interaction of the p85 regulatory subunit with IRS-1/2 causes a conformational change in the PI3K complex, resulting in the activation of the p100 catalytic subunit. Once activated, the p100 catalytic subunit then phosphorylates membrane lipid phosphotidylinositol-(3,4)-bisphosphate (PIP_2), converting it to phosphotidylinositol-(3,4,5)-triphosphate (PIP_3). PIP_3 is capable of activating a number of downstream kinases, including protein kinase C and Akt (also known as protein kinase B) which plays a central role in anti-apoptosis and cell survival. IL-4 has been shown to protect T and B lymphocytes from death via apoptosis [201, 202]; and PI3K appears to be a key player in exerting this effect since inhibitors of PI3K, such as wortmannin and LY294002, block the ability of IL-4 to prevent apoptosis in 32D myeloid cells and in B cells [204].

1.3.4.3 RAS—MAPK pathway

Phosphorylated IRS-1/2 can also interact with adaptor protein Grb2 through its SH2 domain to initiate the Ras—Raf—MAPK signaling cascade [249]. Grb2 mediates this by recruiting the guanine nucleotide exchange factor, Son of sevenless (Sos), to the cell membrane [250]. Sos then catalyzes the exchange of GDP in inactive Ras at the cell membrane for GTP, and Ras becomes activated [251]. Raf is the downstream effector of activated Ras [252]. Active Raf initiates a signaling cascade which ultimately leads to the phosphorylation and activation of the mitogen activated protein kinases ERK-1/2 [253]. However, IL-4 mediated Ras—MAPK signaling is not consistently observed. Several studies have suggested that IL-4 fails to activate Ras—Raf—MAPK mediated mitogenic signaling in a number of hematopoietic cell lines [254-256].

Shc is another adaptor molecule that can mediate interactions between IL-4R and Grb2/Sos. In human B cells and keratinocytes but not in T lymphocytes, Shc was found to be involved in the Ras—MAPK signaling pathway upon stimulation with IL-4 [257, 258]. In addition, activation of Shc has also been observed in the myeloid progenitor cell line 32D and in the IL-4 responsive cell line CT.4R [174, 259]. Thus, activation of the Ras—MAPK pathway by IL-4 may depend on cell type and signaling molecules present within them.

Nonreceptor tyrosine kinase Fes has been found to be activated by IL-4

[260-262]. Fes associates with IL-4Rα through interaction of tyrosine phosphorylated Fes and PI3K after IL-4 engagement in mouse T cells [261]. However there have been no reports yet linking Fes to IL-4 or IL-13 signaling in macrophages. Overexpression of kinase-inactive Fes blocks the IL-4 activation of IRS-2, but not Stat6. Therefore, in the context of Fes, signals downstream of IL-4 can be categorized into Fes dependent (IRS-1/2 and PI3K) and Fes independent (Stat6 and MAPK) pathways [262].

1.3.5 IL-4 and disease

1.3.5.1 Asthma

$CD4^+$ Th2 cells and Th2 cytokines, mainly IL-4 and IL-13, are the key players in the development of allergic asthma through Stat6-dependent mechanisms [241-243, 263-265]. IL-4 is important during allergen challenge through its involvement in promoting the differentiation and proliferation of Th2 cells, induction of the IgE isotype switch, whereas IL-13 has a critical role in mediating airway hyperresponsiveness (AHR) and mucus hypersecretion in order to manifest the allergic reaction [266]. IL-4 mutant protein receptor antagonists were able to inhibit IL-4- and IL-13-induced Stat6 phosphorylation and IgE production *in vitro* as well as the development of allergic airway eosinophilia and AHR in mice [267, 268]. Clinical trials have also provided promising results suggesting that recombinant human soluble IL-4R as an IL-4 antagonist is safe and effective in the treatment of moderate

persistent asthma [269, 270]. However, more recent studies have described different asthma phenotypes, and the initial view that asthma is a purely Th2-mediated disease had to be revised [271]. IL-4 together with IL-13 requires further investigations as a therapeutic target for treating asthma.

1.3.5.2 Rheumatoid arthritis

In contrast to allergic diseases, IL-4 acts as an anti-inflammatory cytokine in autoimmune diseases such as rheumatoid arthritis. Rheumatoid arthritis is an inflammatory process that involves Th1 proinflammatory cytokines such as IL-1, IL-6, IL-8, IL-12, and TNF-α as the origin of this disease [272]. IL-4 is capable of inhibiting Th1 cell formation and the secretion of Th1 cytokines, by driving naïve Th0 cells to differentiate towards the Th2 cell type [193, 273]. Based on the role of IL-4, it has been proposed that IL-4 may be a potential therapeutic agent for treating rheumatoid arthritis [274]. Using animal models, IL-4 treatment has been shown to inhibit the development of proteoglycan-induced arthritis by regulating IL-12 production [275, 276]. A single injection of adenovirus-producing IL-4 was able to reduce joint inflammation, levels of proinflammatory cytokines and bone destruction in rat adjuvant-induced arthritis [277]. Moreover, engineered bone marrow-derived dendritic cells that express IL-4 also showed the ability to control collagen-induced arthritis [278]. Therefore, these results support the feasibility of using IL-4 gene

therapy for the treatment of arthritis.

1.3.5.3 Cancer

The role of IL-4 in cancer has long been investigated. Numerous *in vitro* studies have suggested contradictory findings that IL-4 could either enhance or inhibit cancer cell proliferation depending on the cancer cell type. IL-4 alone or in combination with other cytokines such as IFN-γ and TNF-α has been shown to inhibit cell growth of human renal cell carcinoma [279, 280]. IL-4 has also been reported to inhibit anchorage-dependent and –independent growth of breast cancer cell lines MCF-7 and MDA-MB-231 by acting through IL-4R expressed on them [281]. There are several more studies showing that IL-4 is growth inhibitory to breast cancer cells *in vitro* [282-284]. In contrast, Prokopchuk *et al.* showed that high levels of endogenous IL-4 expressed by human pancreatic cancer cells can promote their cell proliferation in an autocrine fashion [285]. Moreover, IL-4 is a survival factor for tumor cells, and it can protect tumor cells from apoptosis induced by multiple agents. IL-4 treatment significantly reduced CD95- and chemotherapeutic drug-induced apoptosis in prostate, breast, thyroid, and bladder tumor cell lines through the up-regulation of the antiapoptotic protein Bcl-X_L[286, 287].

High levels of IL-4 production have been detected among the tumor-infiltrating T lymphocytes of several advanced solid cancers [288]. Besides the

increased levels of IL-4 expression in cancer patients, the number of IL-4R has also been shown to be elevated on many tumor cells, including renal cell carcinoma [279], malignant melanoma [283], glioblastoma [289], as well as head and neck cancer [290]. Several studies have shown that malignant tumor cells genetically engineered to produce IL-4 displayed potent anti-tumor effects *in vivo*, suggesting the potential use of IL-4 secreting tumor cells as tumor vaccines for treating patients with advanced cancers [291-293]. In a rat brain glioblastoma model, transfer of retrovirus expressing IL-4 and primary neural progenitor cells transfected with IL-4 has been shown to be effective, leading to the survival of most tumor-bearing mice [294]. Unfortunately, almost no positive responses have occurred in clinical trials of recombinant human IL-4 in patients with renal cell carcinoma, chronic lymphocytic leukemia, and non-Hodgkin's lymphoma [295-297]. However, a subsequent clinical trial performed by Gitlitz, B.J. *et al.* found that systemic administration of IL-4 in combination with GM-CSF led to the differentiation of dendritic cells and enhanced their number and function in cancer patients [298]. This study suggests that IL-4 and GM-CSF may be used as adjuvants for cancer treatments.

1.4 Goals of this work

Although Fes was originally identified as oncogene [122-126], subsequent studies have suggested that Fes may also function as a tumor suppressor in human

epithelial cancers [170-172]. The main focus of this thesis was to elucidate the roles of Fes in breast cancer development using an orthotopic engraftment model (Chapter 2) as well as a HER2 transgenic mouse model (Chapter 3). Ultimately, I sought to determine whethter Fes inhibition might represent a future therapeutic option for treating breast cancer patients. Chapter 4 developed from our interest in understanding how cytokine and interleukin signaling contributes to the pro- and anti-tumorigenic involvement of tumor-associated macrophages. Unexpectedly, my observations suggested that IL-4 might be a good canadidate for immunotherapy.

Chapter 2

Fes tyrosine kinase expression in the tumor niche correlates with enhanced tumor growth, angiogenesis, circulating tumor cells, metastasis, and infiltrating macrophages

2.1 Abstract

Fes is a protein tyrosine kinase with cell autonomous oncogenic activities that are well established in cell culture and animal models, but its involvement in human cancer has been unclear. Abundant expression of Fes in vascular endothelial cells and myeloid cell lineages prompted us to explore roles for Fes in the tumor microenvironment. In an orthotopic mouse model of breast cancer, we found that loss of Fes in the host correlated with reductions in engrafted tumor growth rates, metastasis, and circulating tumor cells. The tumor microenvironment in Fes-deficient mice also showed reduced vascularity and fewer macrophages. In co-culture with tumor cells, Fes-deficient macrophages also poorly promoted tumor cell invasive behavior. Taken together, our observations argue that Fes inhibition might provide therapeutic benefits in breast cancer, in part by attenuating tumor-associated angiogenesis and the metastasis-promoting functions of tumor-associated macrophages.

2.2 Introduction

The *fes* proto-oncogene (also known as *fps*), encodes a SH2 domain-containing cytoplasmic PTK which has been implicated in signaling downstream of receptors for cytokines, growth factors, immunoglobulin, collagen and endotoxin [132, 299]. Fes expression is restricted to myeloid, endothelial, and subsets of epithelial and neuronal cells [132, 157, 158]. Fes was originally identified as a dominant-acting oncoprotein encoded by transforming retroviruses isolated from avian (*fps*) [125, 126] or feline (*fes*) [122-124] tumors. When expressed in transgenic mice, viral *fps* induced tumors in lymphoid and mesenchymal tissues [166]. These observations suggested that activating mutations in the human *fes* proto-oncogene might contribute to cancer.

Missense mutations were subsequently identified in human colorectal cancers [169], leading to the speculation that activated Fes kinase contributed to these cancers. However, subsequent biochemical and structural modeling analysis revealed that these mutations attenuated rather than activated Fes kinase [170]. This revelation raised the novel possibility that Fes might also function as a tumor suppressor.

Genetic evidence to support this hypothesis came from studies of transgenic mice expressing polyomavirus middle T (PyMT) antigen in the mammary glands. Tumors developed earlier in mice targeted at the *fes* locus with either null or kinase-inactivating missense mutations [170]. The *fes* promoter was also found to be silenced by methylation in colorectal cancer cell lines, and this correlated with

downregulation of Fes expression [172]. These apparently contradicting observations argued that Fes may play both oncogenic and tumor suppressor roles.

Furthermore, considering the different cell types which express Fes, the cumulative effect on tumorigenesis may depend on both tumor autonomous cell roles and roles in cells of the tumor niche. For example, tissue-specific expression of an activated *fes* allele in transgenic mice led to hypervascularity and multifocal hemangiomas correlating with expression in vascular endothelial cells [161], and this same activated *fes* allele was able to partially rescue the vasculogenesis defect in VEGF knockout embryos [300]. In other studies using *fes* knockout mice, we observed hypersensitivity to endotoxin, which correlated with abundant Fes expression in macrophages where it regulates TLR4 endocytosis, NFκB signaling and TNF-α expression [162, 165]. These phenotypes in transgenic and knockout mice suggested possible roles for Fes in both vascular endothelial and myeloid cells, which might influence tumor progression. Tumor cell autonomous roles for Fes in breast cancer initiation were also suggested by a recent study showing Fes is highly expressed and activated in mouse mammary epithelial cells during lactation, where it associates with E-cadherin based adherens junctions [158]. Fes expression level and enzymatic activity are also found to be upregulated in transformed, highly proliferative MDA-MB-231 breast cancer cells [301].

To elucidate the involvement of Fes in breast cancer, we have employed a tumor

cell orthotopic mouse mammary gland engraftment model designed to separately examine tumor cell autonomous and niche roles of Fes. Manipulation of Fes expression in the engrafted breast carcinoma cells had no effect on growth at the orthotopic injection site or metastasis. However, when Fes expression was eliminated in the niche, significant reductions in tumor growth rates and metastasis were observed. These defects correlated with reductions in tumor-associated vascularity, macrophages, and circulating tumor cells. Bone marrow-derived *fes-null* macrophages were less proficient at promoting the *in vitro* invasive properties of cocultured tumor cells, or of being induced to invade by tumor cells. These observations are consistent with tumor progression roles of Fes acting at the level of the vascular endothelial cells and macrophages. This study provides novel genetic evidence that the Fes protein-tyrosine kinase represents a potential therapeutic target in breast cancer, where Fes inhibition in macrophages and vascular endothelial cells would attenuate their tumor promoting roles.

2.3 Materials and methods

2.3.1 Cell culture

The highly metastatic AC2M2 mouse mammary carcinoma cell line, that contains an hepatocyte growth factor (HGF)-Met autocrine loop [102], was routinely cultured in Dulbecco's Modified Eagle Medium (DMEM, Invitrogen) supplemented

with 10% fetal bovine serum (FBS, Sigma), 2mM L-glutamine and 2mM antibiotics-antimycotics (Invitrogen), and maintained at 37℃ with 5% CO_2 in a humidified incubator. These cells were transduced with lentivirus expressing green fluorescence protein (GFP). For some experiments, these GFP-expressing AC2M2 cells were transduced with pMSCVpuro (Clontech) retroviruses encoding C-terminally Myc-epitope tagged wild type, kinase-dead (K558R[163]), or kinase-activated (*N*-terminally myristoylated) Fes [161].

2.3.2 Mice

The previously established *fes-null* ($fes^{-/-}$) strain [162] was crossed with nude mice (NCr-$Foxn1^{nu/nu}$; Taconic) to produce hybrid wild-type ($fes^{+/+}$; *nu/nu*) and *fes-null* nude ($fes^{-/-}$; *nu/nu*) mice. Mice were housed in the Animal Care Facility and procedures were carried out according to the guidelines of the Canadian Council on Animal Care, with the approval of the institutional animal care committee.

2.3.3 Orthotopic mammary gland engraftment model

After being anesthetized with 250mg/kg avertin, age-matched wild-type and *fes-null* female nude mice were injected with 7,500 GFP-expressing AC2M2 cells into the fourth mammary gland [102]. Tumor growth at the orthotopic site was measured by ultrasound imaging (VisualSonics Vevo 770) 12, 14, 16, 19, and 22 days after

engraftment. On day 23, the tumors were removed and mice were kept alive to assess metastasis. On day 35, mice were euthanized, lungs were dissected, and GFP-expressing metastatic nodules were biophotonically imaged using a Pan-A-See-Ya Panorama imaging system. Images were captured using a Hamamatsu B/W ORCA-ER digital camera with excitation filter at 470nm/20nm and an emission filter at 525nm/20nm.

2.3.4 *In vivo* macrophage imaging

Mice were engrafted with AC2M2 cells as described earlier. On day 13, these tumor-bearing mice were injected with 200μL of 20mg/mL tetramethylrhodamine conjugated dextran beads (Invitrogen,). After 2 hours, mice were perfused with 1% paraformaldehyde in PBS and mammary glands were dissected and imaged by Leica TCS SP2 confocal microscopy.

2.3.5 Flow cytometry measurement of macrophages and endothelial cells

Tumor-bearing mammary glands were harvested from wild-type and *fes-null* nude mice 7 days after engraftment as described earlier, and digested in tissue digestion buffer containing 0.1mg/mL collagenase (Sigma), 0.072mM $CaCl_2$ and 20% FBS at 37℃ for 3 hours. Single-cell suspensions were obtained by filtering twice through 70μm cell strainers (BD Biosicence). Samples were centrifuged at 700rpm for

5 min, and resuspended in 2mL ice-cold PAB [phosphate-buffered saline with 1% (w/v) bovine serum albumin]. Aliquots were incubated with 0.1μg/mL phycoerythrin (PE)-conjugated rat anti-mouse F4/80 antibody (Caltag) for macrophages, PE-conjugated rat IgG2a (Molecular Probes) for isotype control, or propidium iodide (Invitrogen) for cell viability. Samples were then washed with ice-cold PAB, fixed for 15 min with 2% formaldehyde (Sigma) at 37℃, resuspended in 500μl PAB, and analyzed by flow cytometry. Peritoneal macrophages were used as positive controls.

2.3.6 Immunoblotting

Lysates from mammary glands or tumors were prepared in RIPA lysis buffer (10mM Tris pH 7.2, 158mM NaCl, 1mM EDTA, 0.1% SDS, 1% sodium deoxycholate, 1% Triton 100 with 10μg/mL aprotinin, 10μg/mL leupeptin, 100μM sodium orthovanadate, 100μM phenylmethylsulfonyl fluoride using a Ultra-Turrax T25 homogenizer (Terochem Scientific). For cell cultures, cells were washed with ice-cold PBS containing 100μM vanadate, and then lysed with RIPA lysis buffer for 20min. The remaining procedures have been described in detail previously [158, 302]. Briefly, lysates were centrifuged at 13,000 $\times g$ for 15 min at 4℃ to obtain the soluble fractions. After protein quantification, samples were diluted with SDS sample buffer and heated for 5 min at 95℃. Proteins were then resolved by SDS-PAGE and transferred to membranes using a semi-dry transfer apparatus (Bio-Rad). Membranes were blocked

with either 5% skimmed milk or 5% BSA for 1 hr, and incubated overnight with primary antibody at 4℃. After washing in TBST, membranes were incubated with the appropriate secondary antibody for 1 hr at room temperature, and proteins were detected by using enhanced chemiluminescence reagents (NEN Life Science Products).

Protein levels were determined by densitometry using Image Pro software. Antibodies used for immunoblotting included anti-Fes, which is a rabbit polyclonal serum that cross-reacts with Fes and Fer [157], anti-Myc ascites (1-9E10.2 mouse hybridoma from American Type Culture Collection), anti-RasGap rabbit polyclonal [135], anti-tubulin mouse monoclonal (Sigma), or anti-PECAM-1, which is rabbit polyclonal serum raised against a GST-fusion protein containing the complete cytoplasmic domain of mouse PECAM-1 [303].

2.3.7 Immunofluorescence analysis of tumors and stroma

Tumors and associated mammary glands were removed from age-matched wild-type and *fes-null* mice 7 days after engraftment, fixed in 4% paraformaldehyde, and paraffin embedded. Tissue sections (5μm) were deparaffinized with toluene and rehydrated through an ethanol gradient. Antigen was retrieved by heating sections in 10mM sodium citrate (pH 6.0) at 95℃ in a steam cooker for 20 min. After cooling at RT for 20 min, sections were rinsed 3 times with PBS, and incubated in 0.2%

Triton/PBS for 10 min, followed with 3 PBS rinses. Sections were then blocked with 3% BSA for 20 min. Following 3 washes in PBS, sections were incubated overnight with PECAM-1 rabbit polyclonal antibody (1:50 dilution in blocking buffer) at 4℃. Sections were washed 3 times in PBS before addition of Alexa Fluor 546 goat anti-rabbit IgG (1:200 dilution in blocking buffer, Invitrogen) for 1 hour at room temperature. After thorough washing with PBS, sections were mounted with Mowiol (Calbiochem) and imaged using Olympus BX51 fluorescence microscopy with excitation filter at 545nm and emission filter at 576nm. Quantification of vasculature in tumor stoma was performed using Image Pro software.

2.3.8 Peritoneal lavage

Peritoneal macrophages were harvested as described previously [165]. Briefly, after mice were euthanized by deep isoflurane inhalation and cervical dislocation, peritoneal lavage were performed twice with 5ml of pre-warmed lavage media [RPMI1640 (Invitrogen), 10mM HEPES, 5mM EDTA, 10U/ml heparin, 1% antibiotic-antimycotic, 50μM α-monothioglycerol] each using a 5ml syringe and 23 gauge needle. Cells were pelleted at 700rpm for 5 minutes, and resuspended in 5ml of erythrocyte lysis buffer (154mM NH_4Cl, 10nM $KHCO_3$, 100μM EDTA) for 5 minutes at 4℃ to lyse red blood cells. For flow cytometry, cells were then resuspended in 500μl PAB and ready to use for staining. Otherwise, cells were resuspended in

pre-warmed peritoneal macrophage media [RPMI1640 (Invitrogen), 5% FBS, 1% antibiotic-antimycotic, 1% glutamine, 1mM HEPE, 50μM α-monothioglycerol], plated and incubated in a 5% CO_2 humidified incubator at 37℃. After 2 hours, non-adherent cells were washed off with PBS, and adherent cells (i.e. peritoneal macrophages) were used for subsequent experiments.

2.3.9 *In vitro* macrophage phagocytosis of dextran beads

1×10^6 wild-type and *fes-null* peritoneal macrophages were seeded into each well of 12-well plates, and incubated overnight. The next morning, macrophage medium were replaced with HBSS containing 1mg/ml BSA, and cells were incubated for 1 hour. Tetramethylrhodamine conjugated dextran beads were then added to the cells at a final concentration of 1mg/ml for 2 hours. After nucleus staining with DAPI, cells were imaged by Leica TCS SP2 confocal microscopy. The density of dextran beads phagocytosed by macrophages was quantified using Image Pro software.

2.3.10 Tail vein injection lung metastasis model

5×10^5 GFP-expressing AC2M2 cells were injected into the tail veins of wild-type or *fes-null nu/nu* mice, and 3 weeks later lungs were dissected and biophotonically imaged as described above. Numbers and sizes of metastatic lesions were determined using Image Pro software.

2.3.11 Detection of circulating tumor cells

Twenty-two days after engraftment with GFP-expressing AC2M2 cells, peripheral blood was collected by cardiac punctures performed under deep anesthesia with isofluorane. 500μL of blood samples were subjected to hypotonic shock with 5mL distilled water, followed by isotonic restoration with 1.5mL 0.6M KCl. Samples were then washed with 50mL PBS to remove red blood cell debris, resuspended in 500μL PAB, and analyzed by flow cytometry.

2.3.12 Collagen invasion assay

Primary bone marrow-derived macrophages were obtained as previously described [304]. MTLn3-GFP rat breast cancer cells were cocultured for 18 hours with bone-marrow-derived macrophages (BMM) from wild-type or *fes-null* mice in the presence of CSF-1 and 10% FBS. Cocultures were then overlaid with collagen I gels and invasion into the collagen gel after 24 hours was quantified as previously described [305]. This assay was performed by Dr. Violeta Chitu in Dr Richard Stanley's laboratory at the Albert Einstein College of Medicine.

2.3.13 Statistics

All statistical analysis was done by using GraphPad Prism 5 software. All error

bars represent standard error of the mean. P values were calculated by Student's *t*-test and 2-way analysis of variance (ANOVA) analysis. Data sets with $P \leq 0.05$ were considered statistically significant.

2.4 Results

2.4.1 Fes does not affect tumorigenesis in a tumor cell autonomous fashion

Preliminary experiments were performed to explore potential tumor cell autonomous roles for Fes in mammary tumorigenesis. GFP-expressing AC2M2 mouse breast carcinoma cells were transduced with retroviruses encoding wild-type (WT Fes), kinase-dead (KR Fes) or activated Fes (Myr Fes) (Figure 2.1). These cells were engrafted into the mammary glands of *nu/nu* mice and tumor growth was monitored by ultrasound measurement for 22 days. Primary tumors were then removed to promote metastatic growth and lung metastasis was examined 13 days later. No significant differences in tumor growth rates at the orthotopic injections site were observed (Figure 2.2) and there were no significant differences in the frequency of metastasis to the lungs (Figure 2.3). Thus, Fes did not appear to play a tumor cell autonomous role in this AC2M2 tumor engraftment model.

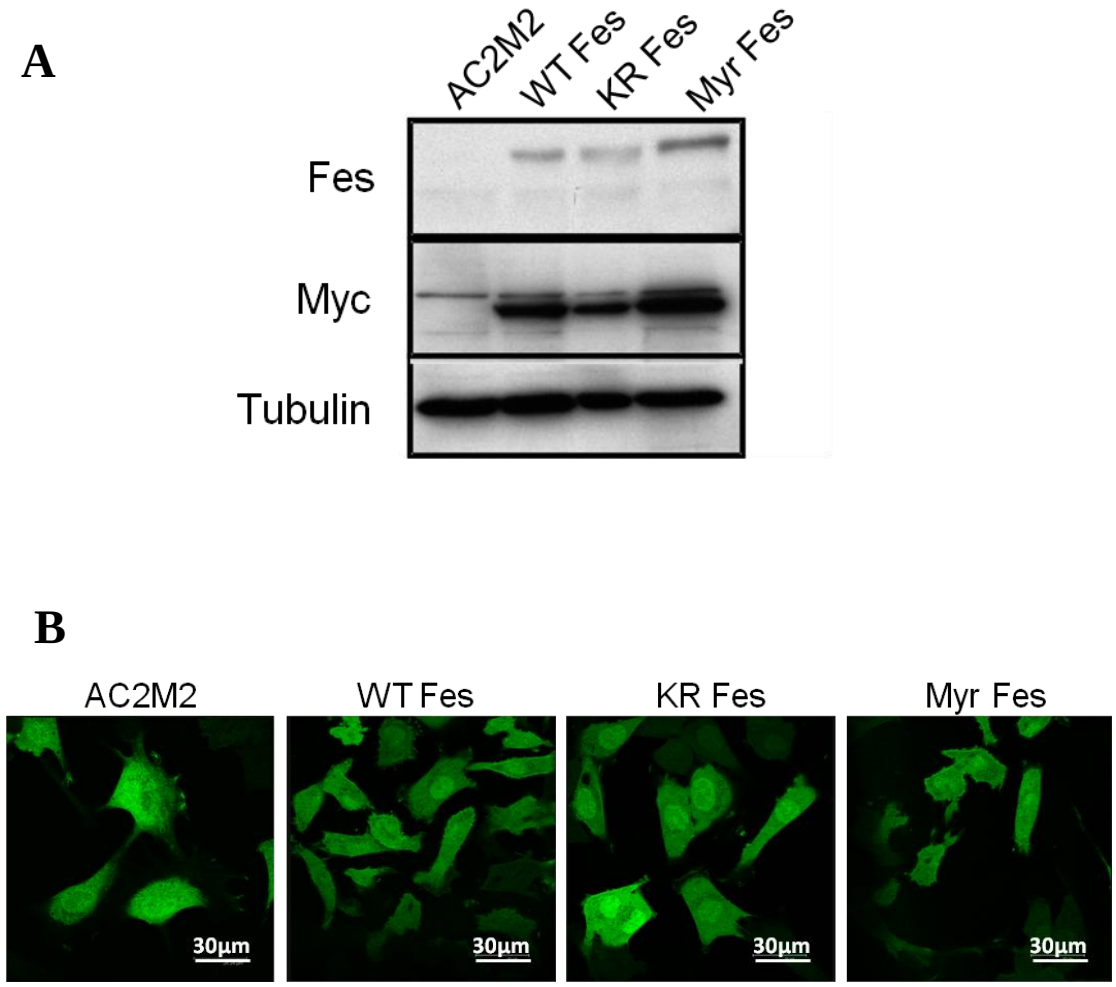

Figure 2.1 Expression levels of Fes kinase and GFP in parental AC2M2 and variant Fes expressing cell lines. Parental AC2M2 cells were transduced with retroviruses encoding C-terminally myc-epitope tagged wild type (WT Fes), kinase-dead (KR Fes) or activated Fes (Myr Fes). A) Protein lysates from these four cell lines were assessed by immunoblotting with the indicated antibodies; Myc for ectopic Fes expression, Fes for ectopic and endogenous Fes expression, and tubulin for protein loading. Endogenous Fes expression was not apparent in parental AC2M2 cells. Comparable levels of ectopic Fes-Myc protein expression were observed in each transduced cell line. B) Confocal microscopy confirmed that the three transduced cell lines expressed the same level of GFP as parental AC2M2 cells.

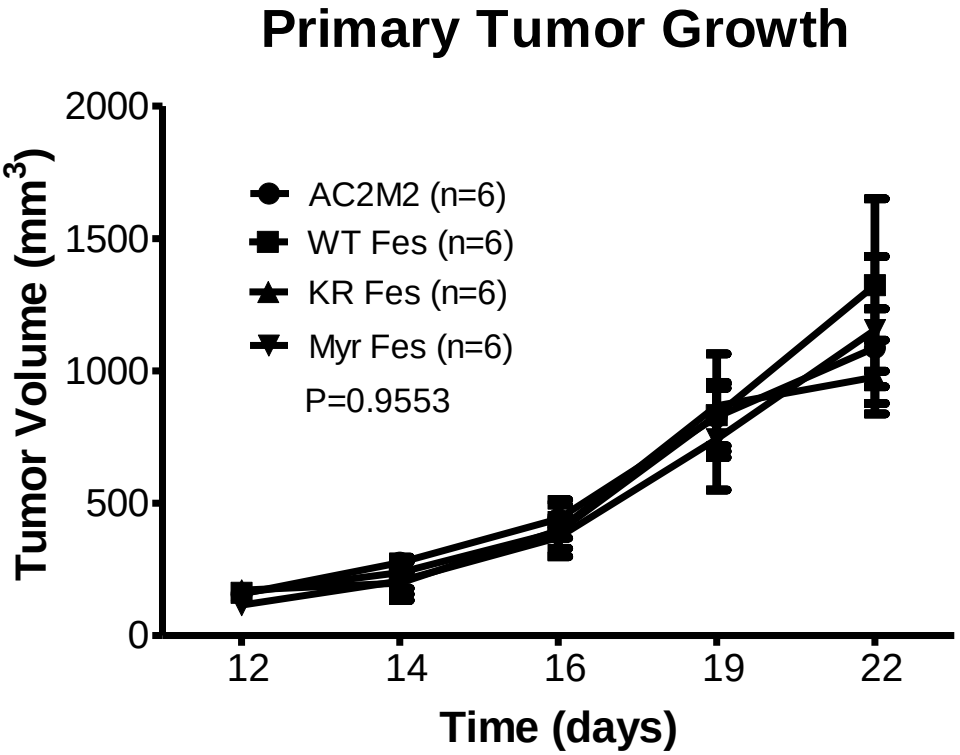

Figure 2.2 Fes does not affect tumorgenesis in a tumor cell autonomous fashion. 7,500 parental AC2M2 cells or those expressing wild type Fes (WT Fes), kinase-dead Fes (KR Fes) or kinase-activated Fes (Myr Fes) were engrafted into the fourth mammary glands of nude mice and tumorigenesis was assessed by ultrasound imaging over a period of 22 days. All four cell lines grew tumors at indistinguishable rates (n = 6 for each cell line; P = 0.9553).

A

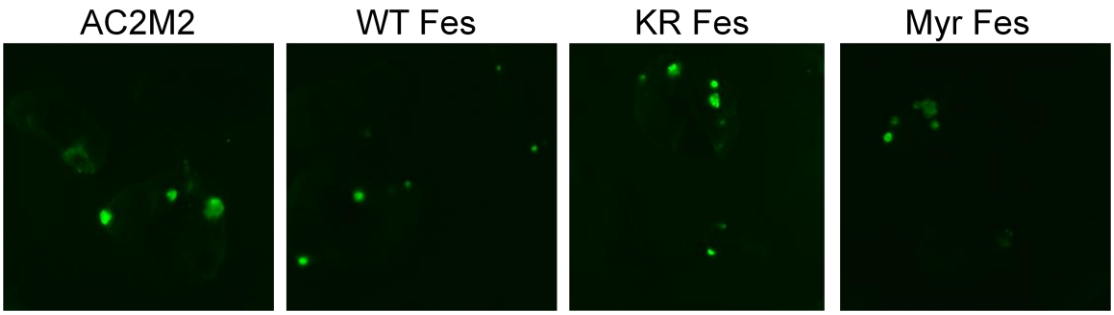

B

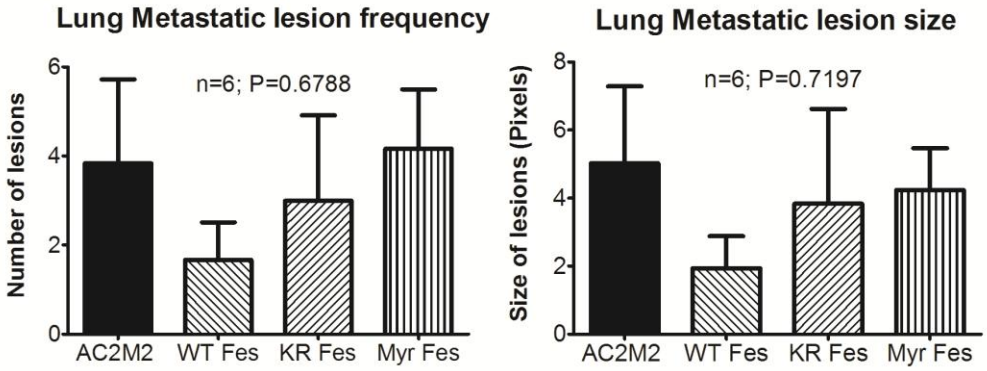

Figure 2.3 Fes does not play a tumor cell intrinsic role in term of lung metastasis. 7,500 cells of GFP–expressing parental AC2M2 or three variant Fes expressing cell lines (wild-type Fes, WT Fes; kinase-dead Fes, KR Fes; kinase-activated Fes, Myr Fes) were engrafted into the fourth mammary fat pad of nude mice. After monitoring primary tumor growth, tumor resection surgery was performed on day 23 post engraftment of tumor cells, in order to promote tumor growth at metastatic sites. Mice were euthanized 13 days after resection surgery, lungs were dissected and imaged by biophotonic imaging to assess lung metastasis. A) Photographs indicate representative images of lungs from each group. B) Biophotonic images of lung metastasis were assessed by Image Pro software to quantify number of lesions and size of lesions in pixels. No significant differences were observed in the frequency of metastasis to the lung and the size of lung metastatic lesions (n=6 for each cell line; P = 0.6788 for the frequency of lung metastasis, P = 0.7197 for the size of lung metastatic lesion).

2.4.2 Fes plays a tumor promoting role in the niche

We next asked whether Fes expression in the niche cells, rather than in tumor cells, might influence tumor growth and metastasis. To facilitate these experiments, we crossed *nu/nu* mice with *fes* knockout mice [162] and established colonies of wild-type and *fes-null nu/nu* mice. GFP-expressing AC2M2 cells were orthotopically engrafted into the mammary glands of wild-type and *fes-null nu/nu* mice and tumor growth and metastasis was monitored as described earlier. Tumor growth at the orthotopic site was significantly slower in *fes-null* mice ($P < 0.0001$) relative to wild-type mice (Figure 2.4) and the frequency of lung metastasis was also significantly reduced in *fes-null* mice, with 79% of wild-type mice versus 55% of *fes-null* mice developing metastasis (Figure 2.5A). Also, among mice displaying lung metastasis wild-type mice displayed significantly more metastatic nodules ($P = 0.0055$; Figure 2.5B). Although there was a trend toward smaller sized metastatic lung nodules in the *fes-null* mice, this difference did not achieve statistical significance ($P = 0.1215$; Figure 2.5B).

2.4.3 Reduced vascularity in the *fes-null* tumor niche

The reduction in tumor engraftment growth rate and metastasis frequency in *fes-null* mice suggested Fes might be playing a tumor promoting role, which is intrinsic to cells making up the tumor niche. Angiogenesis promotes tumor growth

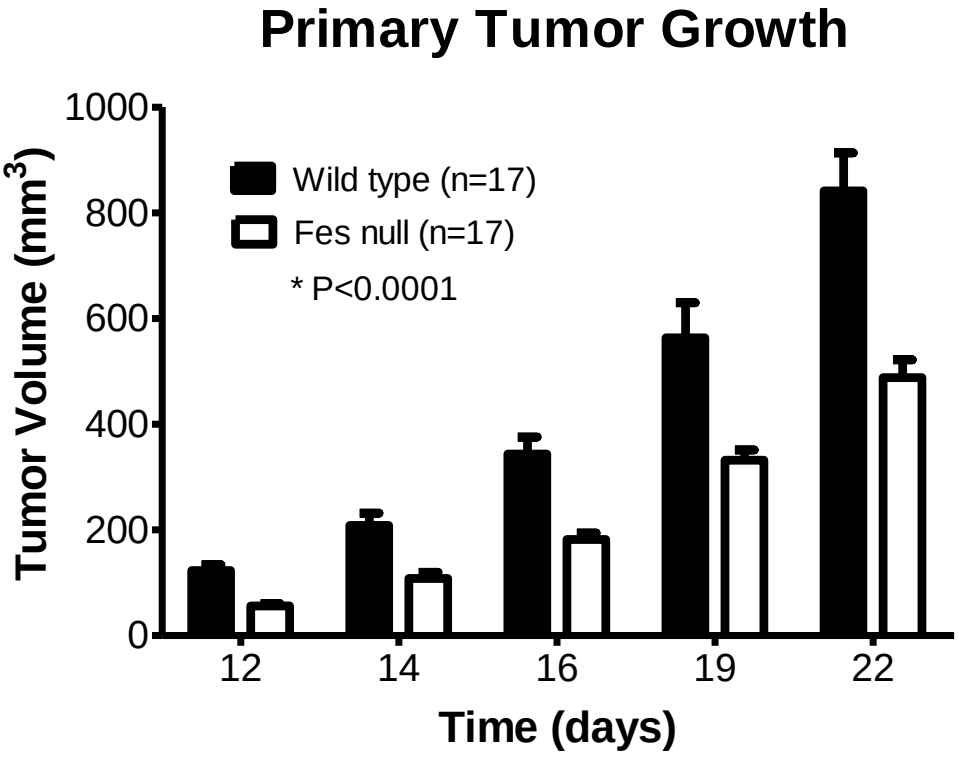

Figure 2.4 Orthotopic tumor growth rates were reduced in *fes-null* mice. AC2M2 cells were engrafted into mammary glands of wild type and *fes-null* nude mice and tumorigenesis was assessed by ultrasound imaging over a period of 22 days. Tumor growth rates were significantly slower in *fes-null* relative to wild-type mice ($P < 0.0001$; n=17 for both groups)

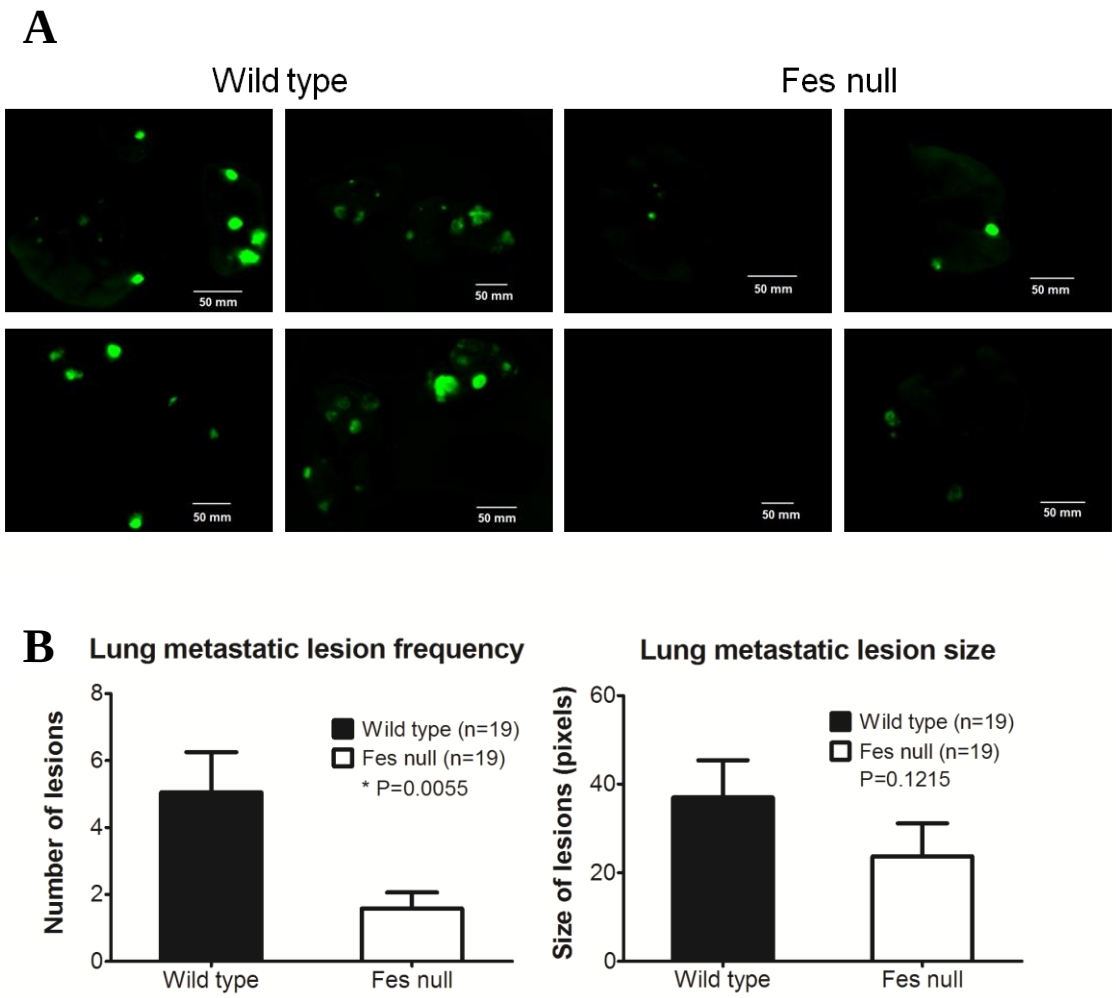

Figure 2.5 Reduced metastasis in *fes-null* mice. 7,500 GFP-expressing AC2M2 cells were engrafted into the fourth mammary glands of wild-type and *fes-null* mice and allowed to grow for 22 days. Tumors were then removed to promote tumor growth at metastatic sites and lungs were removed for biophotonic imaging of metastatic lesions 13 days later. A) 79% (15 of 19) of wild type lungs harbored detectable metastasis while only 55% (10 of 19) of the *fes-null* mice displayed lung metastasis. n=19 for each group. Photographs indicate representative images of lungs from four different mice of each group. B) Significantly more metastatic lesions per lung were observed in wild-type relative to *fes-null* mice lungs (P = 0.0055; n=19 for each group). The size of metastatic lesions (as assessed by pixel numbers per lesion) in *fes-null* mice appeared somewhat smaller than in wild-type mice, but this difference did not reach statistical significance (P = 0.1215).

and metastasis, and Fes is expressed in vascular endothelial cells and has been implicated in angiogenesis [161, 306-308]. We therefore examined the vascularity in wild-type and *fes-null* tumors and associated tissues. PECAM-1 immunofluorescencestaining (Figure 2.6A) revealed reduced numbers of blood vessels in *fes-null* stroma. Quantification of these data showed a significant reduction in vessel density in *fes-null* tumor stroma (P = 0.0251; Figure 2.6B). When the percentages of vessels of different sizes were compared, we found that the reduced vascularity was not associated with any particular size of vessels (Figure 2.6B).

To further quantify the vascular content of tumors and associated stroma, we performed quantitative immunoblotting analysis using PECAM-1 antibody. Tumors were allowed to grow for 7 days after AC2M2 cell injection. Lysates were then prepared from dissected tumors (stroma-free), the tumor-associated stroma (tumor-free), as well as from uninvolved mammary glands of tumor-bearing mice or mammary glands of non-tumor-bearing mice. PECAM-1 immunoreactivity was significantly reduced in tumors (P = 0.0124; Figure 2.7Aa and Figure 2.7B) and tumor-associated stroma (P = 0.0284; Figure 2.7Ab and Figure 2.7B) from *fes-null* mice relative to wild type mice. There was also a trend toward less PECAM-1 levels in *fes-null* uninvolved mammary glands from tumor-bearing mice (P = 0.0580; Figure 2.7Ac and Figure 2.7B) and mammary glands from non-tumor bearing control mice (P = 0.1233; Figure 2.7Ad and Figure 2.7B), but these differences were not

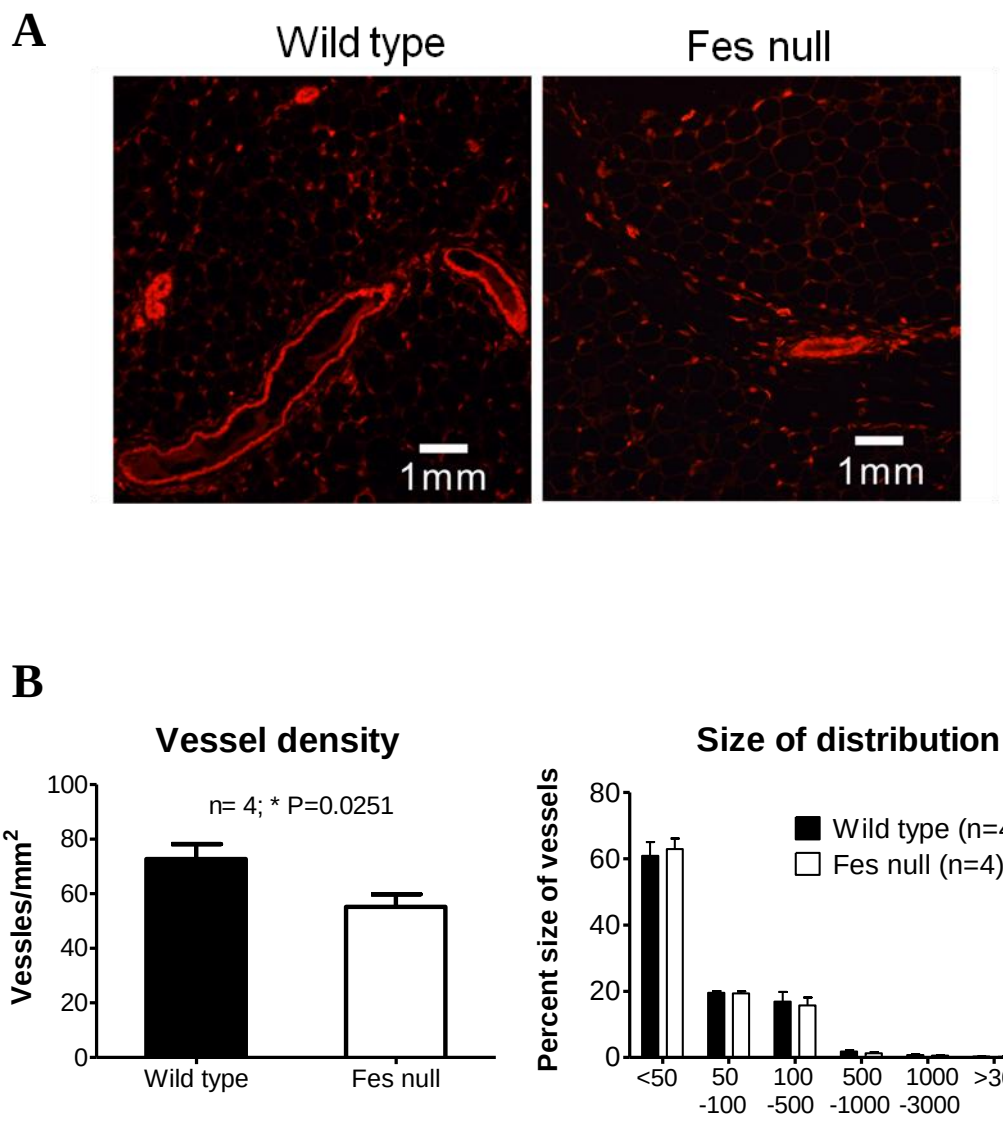

Figure 2.6 Reduced vascularity in *fes-null* tumor stroma. 7,500 GFP-expressing AC2M2 cells were injected into mammary glands of wild type and *fes-null* mice. On day 7 post injection, tumor-bearing mammary glands were dissected, fixed and paraffin-embedded. 5μm tissue sections were deparaffinized and stained with PECAM-1 antibody. A) Stromal blood vessels were detected by PECAM-1 staining. In addition to large gauge vessels, smaller vessels were also apparent. B) Composite images of the stromal tissue surrounding each tumor were assembled and fluorescent pixels in this tumor boundary area were quantified using Image Pro software. The density and size distribution of the blood vessels were determined. Significantly fewer vessels per mm^2 were present in *fes-null* tumor stroma (P = 0.0251), but there was no difference in the size distribution of these vessels (<50 pixels, P = 0.3562; 50-100 pixels, P = 0.4460; 100-500 pixels, P = 0.1226; 500-1000 pixels, P = 0.2371; 1000-3000 pixels, P = 0.2222; >3000 pixels, P = 0.0790; n = 4 for each group).

A

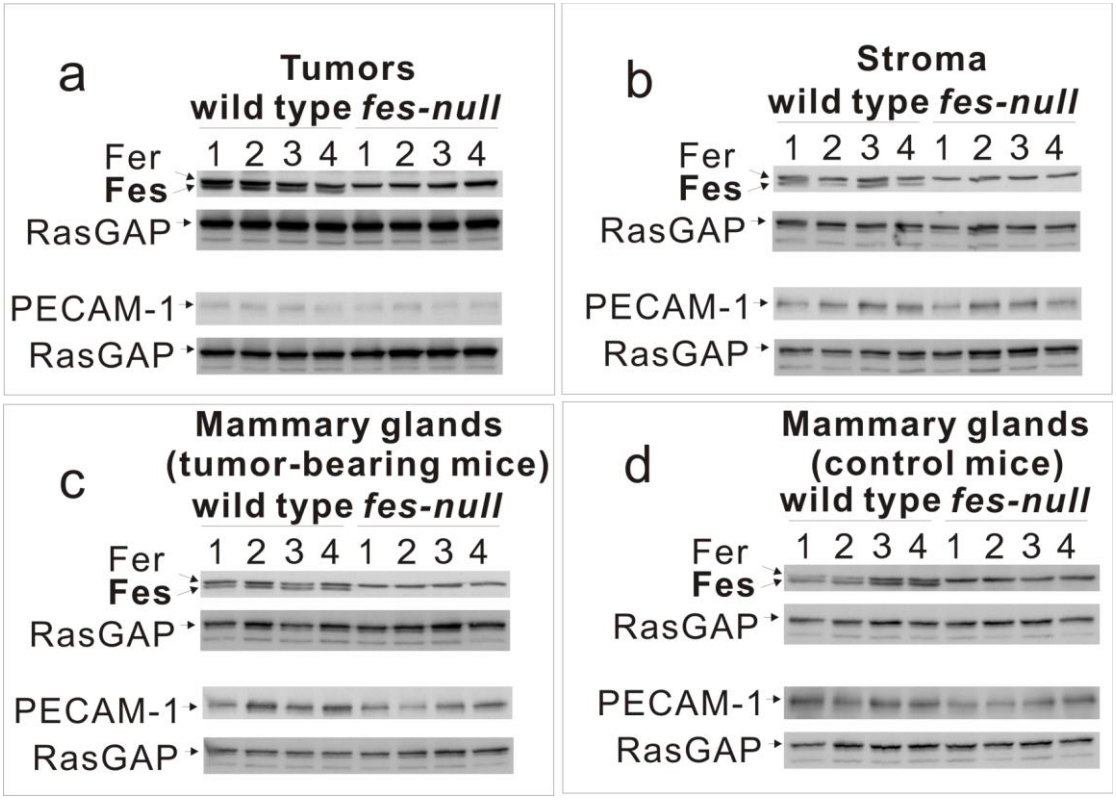
a
Tumors
wild type fes-null
Fer
Fes
1 2 3 4 1 2 3 4
RasGAP
PECAM-1
RasGAP
b
Stroma
wild type fes-null
Fer
Fes
1 2 3 4 1 2 3 4
RasGAP
PECAM-1
RasGAP
c
Mammary glands
(tumor-bearing mice)
wild type fes-null
Fer
Fes
1 2 3 4 1 2 3 4
RasGAP
PECAM-1
RasGAP
d
Mammary glands
(control mice)
wild type fes-null
Fer
Fes
1 2 3 4 1 2 3 4
RasGAP
PECAM-1
RasGAP

B

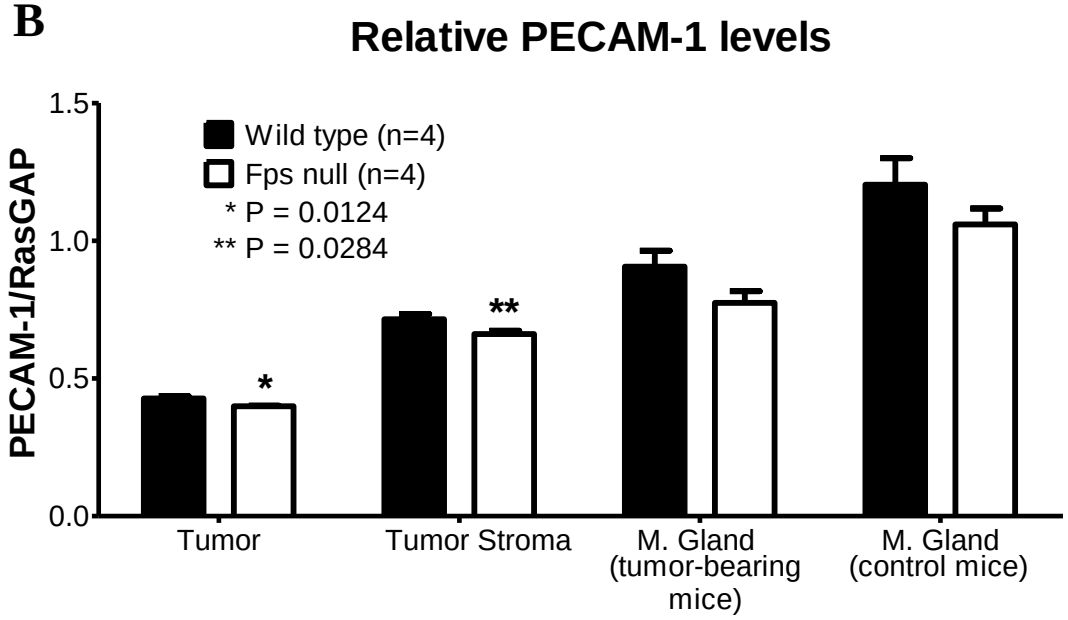
Relative PECAM-1 levels
PECAM-1/RasGAP
1.5
1.0
0.5
0.0
Wild type (n=4)
Fps null (n=4)
* P = 0.0124
** P = 0.0284
*
**
Tumor
Tumor Stroma
M. Gland (tumor-bearing mice)
M. Gland (control mice)

Figure 2.7 Immunoblotting analysis of PECAM-1 expression. Wild-type and *fes-null* mice were engrafted with AC2M2 cells and tumors were allowed to grow for 7 days. Tumors were dissected away from associated stroma and separate lysates were analyzed by immunoblotting with the indicated antibodies. A) An antibody that recognizes both Fes and the related Fer protein was used to confirm genotypes and anti-PECAM-1 was used to assess vascular endothelial content. These blots were stripped and reprobed with anti-RasGAP to normalize for protein loading and to quantify relative PECAM-1 levels by densitometry. B) Uninvolved mammary glands from tumor-bearing mice as well as mammary glands from non-tumor bearing control mice were also assessed (n = 4 for each group). Significantly lower levels of PECAM-1 were observed in both tumors (a, P = 0.0124) and tumor-associated stroma (b, P = 0.0284) from *fes-null* mice. A trend toward reduced PECAM-1 levels was also observed in uninvolved mammary glands from tumor-bearing mice (c, P = 0.0580) and mammary glands from non-tumor bearing control mice (d, P = 0.1233); but these were not statistically significant.

statistically significant.

2.4.4 Reduced involvement of tumor-associated macrophages in *fes-null* mice

Another Fes-expressing cell type that has been implicated in regulating tumorigenesis is the macrophage. In particular, alternatively activated M2-like macrophages are implicated in promoting tumor-associated angiogenesis and metastasis [209, 309, 310]. We therefore examined the involvement of macrophages in this engraftment model. Macrophages were initially detected *in vivo* by taking advantage of their propensity to phagocytose dextran beads. Tetramethylrhodamine -conjugated beads were injected i.v. into tumor-bearing mice 13 days after engraftment of GFP-expressing AC2M2 cells. Tumor-bearing mammary glands were removed 2 hours later and imaged by confocal fluorescence microscopy. In wild-type mice, large numbers of dextran-labeled macrophages were clearly observed at the tumor front and within the tumor (Figure 2.8). In contrast, few macrophages were apparent in *fes-null* tumors and associated stroma.

Because Fes-deficiency may have compromised macrophage phagocytosis of dextran beads (Figure 2.9), we also used surface antigen labeling and flow cytometry to quantify macrophages in tumors and surrounding stromal tissues. Single-cell suspensions were prepared from intact tumor-bearing mammary glands removed 7 days after tumor cell injection and the surface antigen F4/80 was used to quantify macrophages. There was a significant reduction in the $F4/80^{+}$ tumor-associated

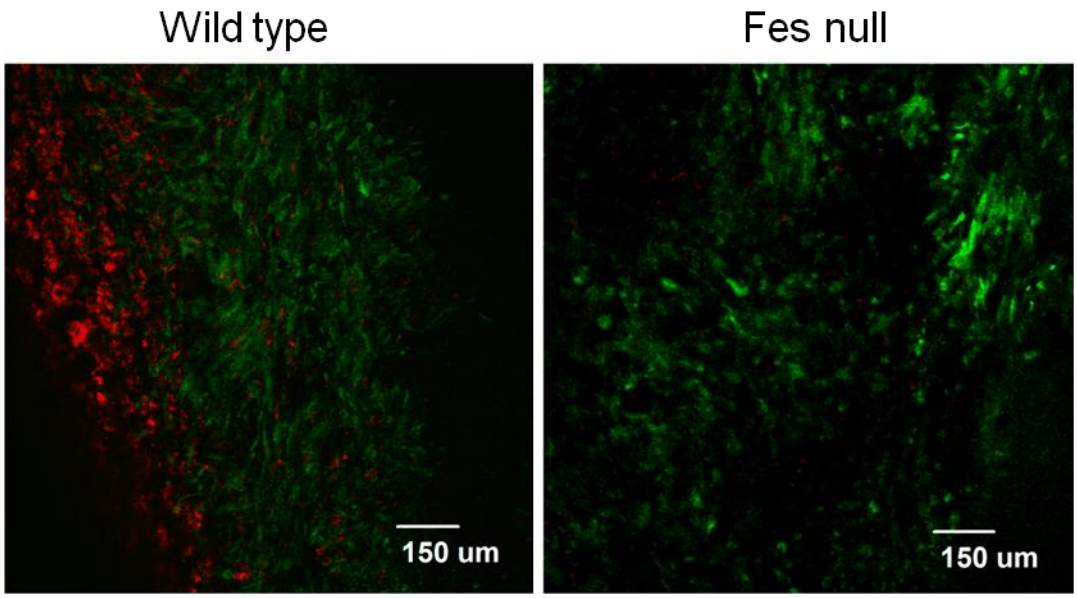

Figure 2.8 Fewer tumor-associated macrophages in *fes-null* mice. Tumor-bearing wild-type and *fes-null* littermates were injected with tetramethylrhodamine -conjugated dextran beads. 2 hours later, tumors were resected, fixed and imaged by confocal fluorescence microscopy. Large numbers of activated macrophages (red) were apparent in association with tumors (green) from wild-type, but not from *fes-null* mice.

A

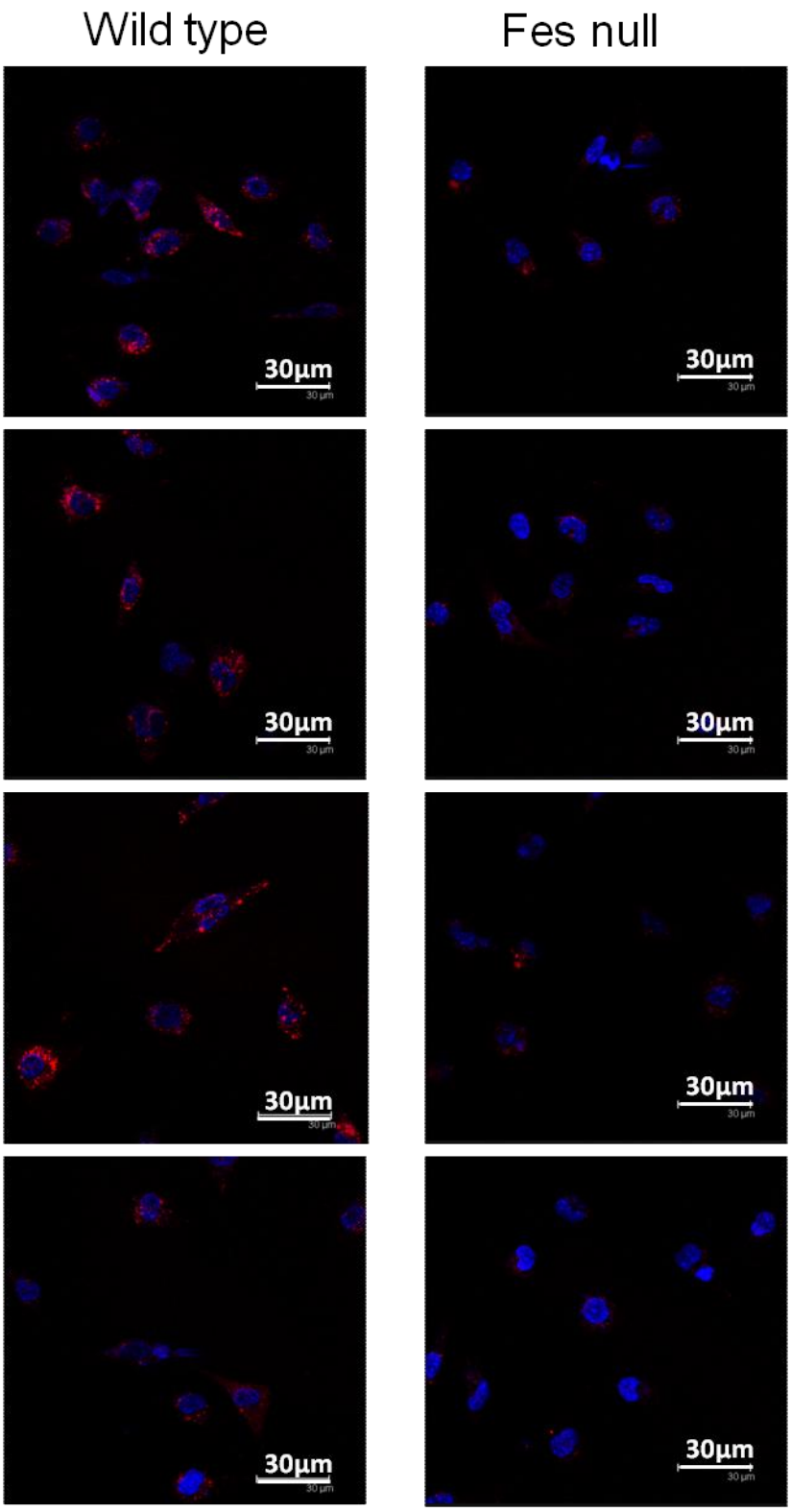

B

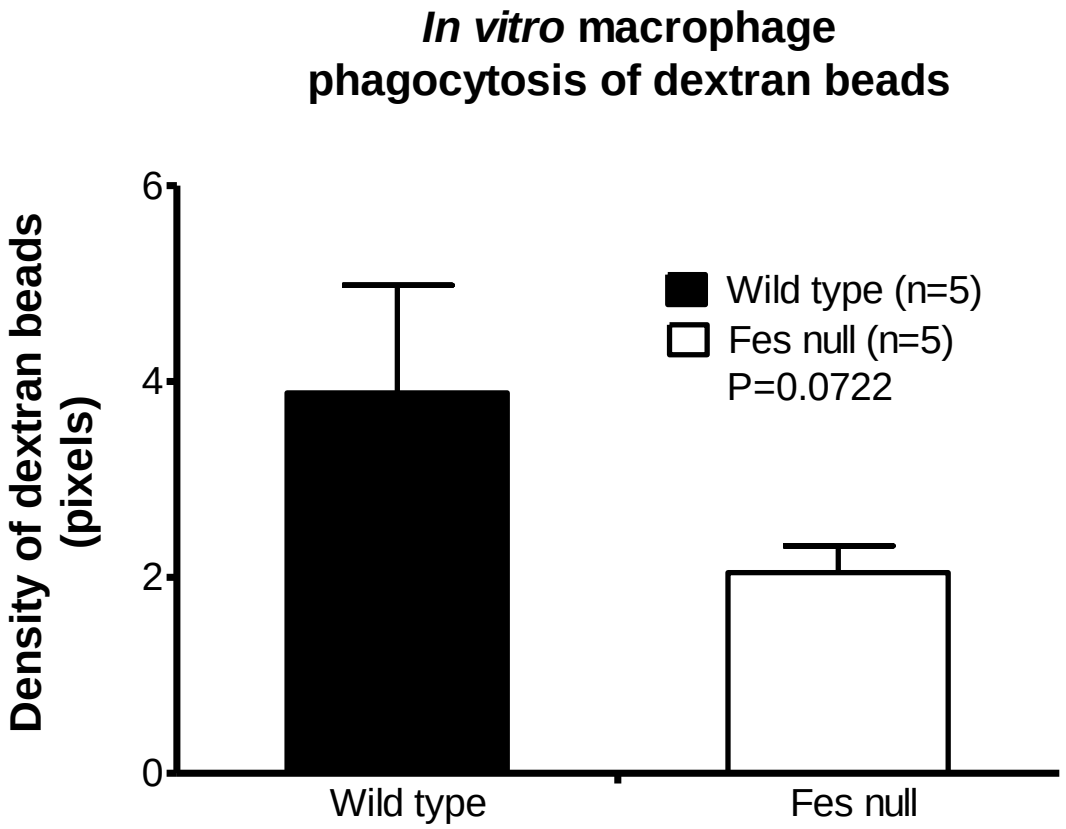

Figure 2.9 *In vitro* macrophage phagocytosis of dextran beads. 1×10^6 wild-type and *fes-null* peritoneal macrophages were cultured with tetramethylrhodamine-conjugated dextran beads at a final concentration of 1mg/ml for 2 hours. Nuclei were stained with DAPI. Confocal microscopy images (A) showed that both wild type and *fes-null* macrophages were able to phagocytose dextran beads. Although *fes-null* macrophages were slightly deficient in phagocytosing dextran beads, this difference did not reach statistical significance (P = 0.0722).

macrophage content in *fes-null* tumor-bearing mammary glands (P = 0.0369; Figure 2.10).

2.4.5 *Fes-null* macrophages are deficient in promoting tumor cell migration and invasion

Tumor-associated macrophages have been shown to correlate with increased neovascularization and poor prognosis in human breast cancer [311]. Alternatively activated tumor-associated macrophages are thought to promote angiogenesis and metastasis, in part through paracrine interactions with vascular endothelial cells [312-314] and with tumor cells which promote their invasive potential [305, 315, 316]. We therefore asked if *fes-null* macrophages were deficient in these properties. To examine this we cultured primary BMMs from wild-type or *fes-null* mice in isolation or in cocultures with MTLn3 rat mammary adenocarcinoma cells in a collagen matrix-based invasion assay model [305]. BMMs from each genotype or MTLn3 cell invaded to the same degree when cultured in isolation. In cocultures, BMMs from both genotypes promoted the invasion of MTLn3 cells, but *fes-null* BMMs were significantly less effective in doing so (P=0.005; Figure 2.11). MTLn3 cells also promoted the invasion of BMMs in cocultures, but the *fes-null* BMMs were significantly less responsive (P=0.002; Figure 2.11).

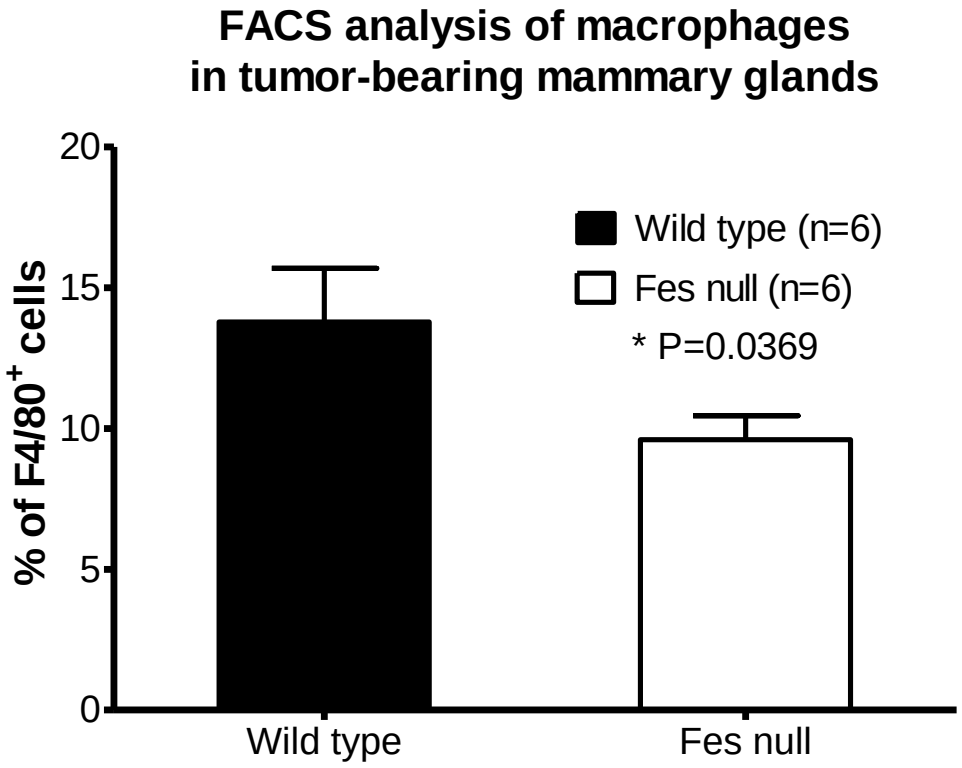

Figure 2.10 Reduced macrophages in *fes-null* tumor-bearing mammary glands. Single-cell suspensions were prepared from tumor-bearing mammary glands of wild-type and *fes-null* mice 7 days posttumor cell injection. Cells were stained with PE-conjugated F4/80 antibody to identify macrophages and the relative percentages of stained cells were determined by flow cytometry. There were significantly fewer macrophages in tumor and associated stroma from *fes-null* relative to wild-type mice ($P = 0.0369$; $n = 6$ for both groups).

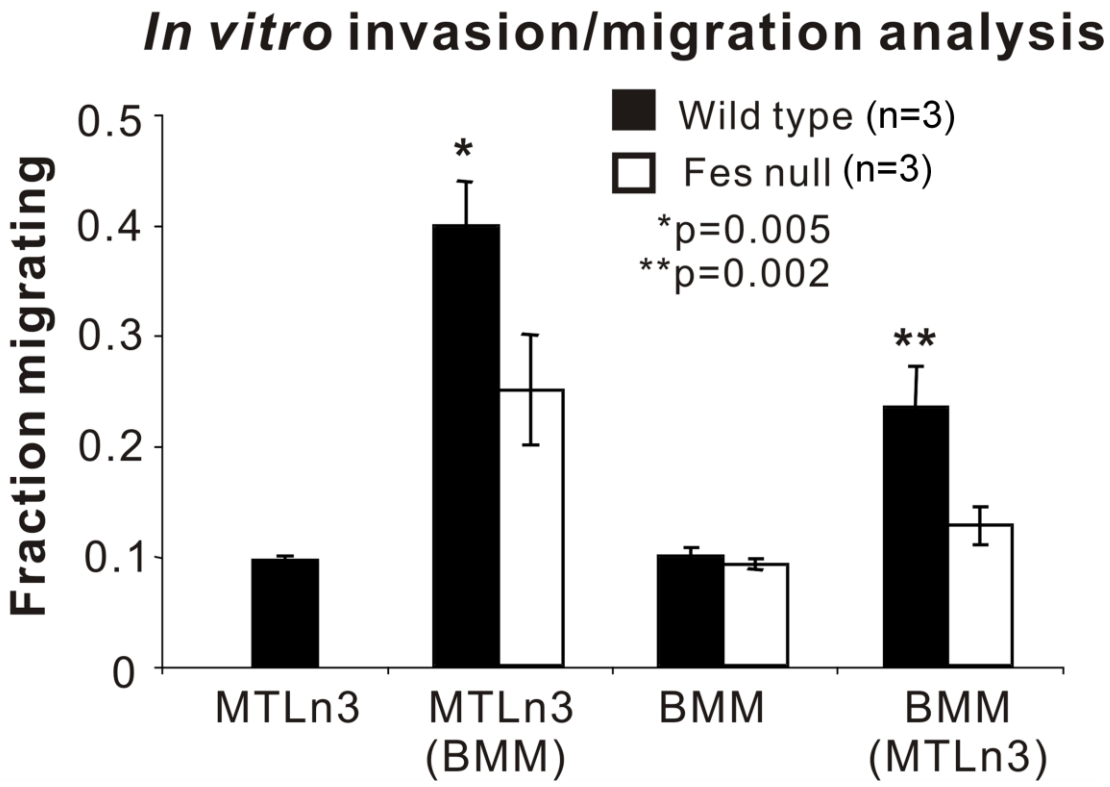

Figure 2.11 *Fes-null* macrophages are defective in promoting tumor cell migration and invasion. BMMs were obtained from wild-type and *fes-null* mice and plated in monolayers in isolation or with MTLn3 breast tumor cells. After 16 hours they were overlayed with collagen I gels. Migration/invasion into the collagen after 24 hours was assessed by confocal microscopy and the fraction of each cell type that migrated/invaded 20μM or more was determined. For the cocultures, the histograms indicate migration of the unbracketed cell type. In cocultures, *fes-null* BMMs were significantly less effective at promoting the migration/invasion of MTLn3 cells than wild-type BMMs (P= 0.005). Tumor cell-induced migration/invasion of BMMs was also significantly reduced in *fes-null* relative to wild-type BMMs (P= 0.002). The data are the average of 3 independent experiments. This experiment was performed by Violeta Chitu in Dr Richard Stanley's laboratory at the Albert Einstein College of Medicine.

2.4.6 Fes deficiency in the lung niche does not compromise tumor cell invasion and initial growth rates at the metastatic site

Angiogenesis is believed to play a rate-limiting effect on tumor growth [42]. Reduced tumor growth rates at the primary site in *fes-null* mice might therefore be due in part to roles for Fes in promoting vascular endothelial cell migration, proliferation and establishment of new vessel structures. However, metastasis also involves interactions between tumor and endothelial cells, both at the level of escape from the primary site and extravasation at the metastatic site. To explore this latter event we injected GFP-expressing AC2M2 cells into the tail veins of wild-type and *fes-null nu/nu* mice and quantified the number and sizes of lung metastatic lesions that formed after 22 days using biophotonic imaging of resected lungs (Figure 2.12). No significant differences were seen, suggesting that Fes-deficiency in the lung microvascular bed did not influence the process of tumor cell adhesion and invasion through the endothelium, or the initial metastatic growth rate.

2.4.7 Fes deficiency in the niche compromises the escape of tumor cells from the primary tumor site

Paracrine signaling between tumor cells and macrophages at the primary tumor site may play an important role in metastasis by promoting the ability of tumor cells to gain access to the vasculature [70, 315, 316]. Reduced metastasis in *fes-null* mice

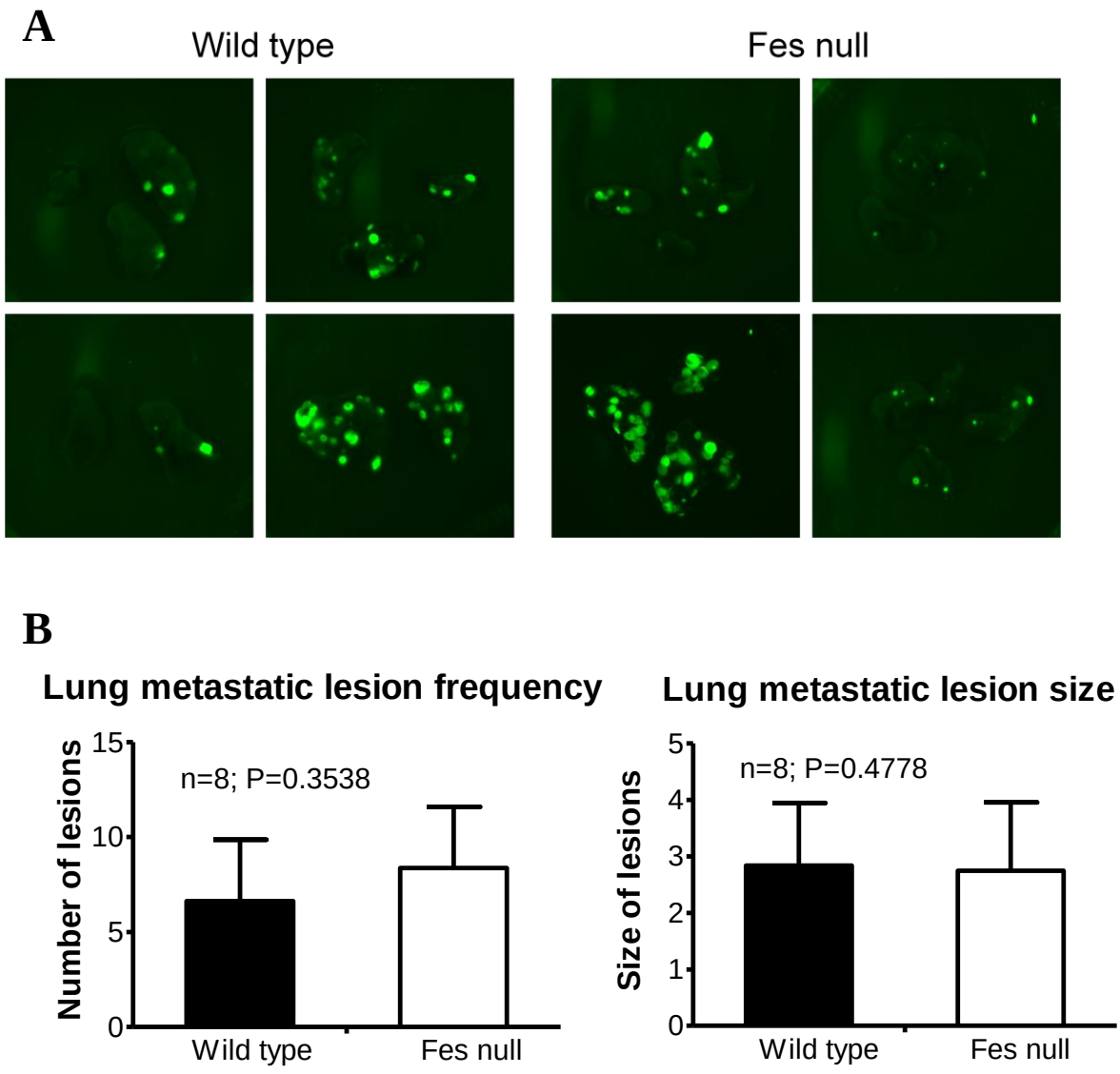

Figure 2.12 Tail vein metastasis model. 5×10^5 GFP expressing AC2M2 cells were injected into the tail veins of wild-type or *fes-null* nude mice and 22 days later lungs were dissected and biophotonically imaged. A) Photographs indicate representative images of lungs from four different mice of each group. B) Numbers of lesions per lung and sizes of metastatic lesions (positive pixels) were determined using Image Pro software. No significant differences were seen in the number of lesions per lung (P = 0.335) or the size of the lesions (P = 0.478) (n = 8 for each genotype).

(Figure 2.6) coupled with observations suggesting that Fes may potentiate paracrinesignaling between macrophages and tumor cells contributing to mutually enhanced invasive potential (Figure 2.11) led us to examine the number of circulating tumor cells (CTCs) in this engraftment model. GFP-expressing AC2M2 cells were injected into the mammary glands of wild-type and *fes-null nu/nu* mice and tumors were allowed to grow for 22 days. Peripheral blood was then assessed for the presence of CTCs by flow cytometry (Figure 2.13). A significantly higher percentage of GFP^+ nucleated cells were detected in the blood of tumor-bearing wild-type relative to *fes-null* mice (P=0.047; Figure 2.13A). Although tumor sizes were smaller in all but one of the *fes-null* mice at the time of analysis, there was no apparent correlation between levels of CTCs and tumor sizes in the wild-type or *fes-null* mice (Figure 2.12B)

2.5 Discussions

Mammalian Fes and orthologous avian Fps were initially discovered as viral oncogenic PTKs encoded by tumor-causing retroviruses [124, 126]. Subsequent studies demonstrated the transforming and tumorigenic potential of those viral Fps/Fes oncoproteins [166]. Collectively, those observations argued that cellular Fes, when activated by mutation or inappropriately overexpressed, could promote tumorigenesis through dominant acting tumor cell autonomous functions. We were therefore surprised

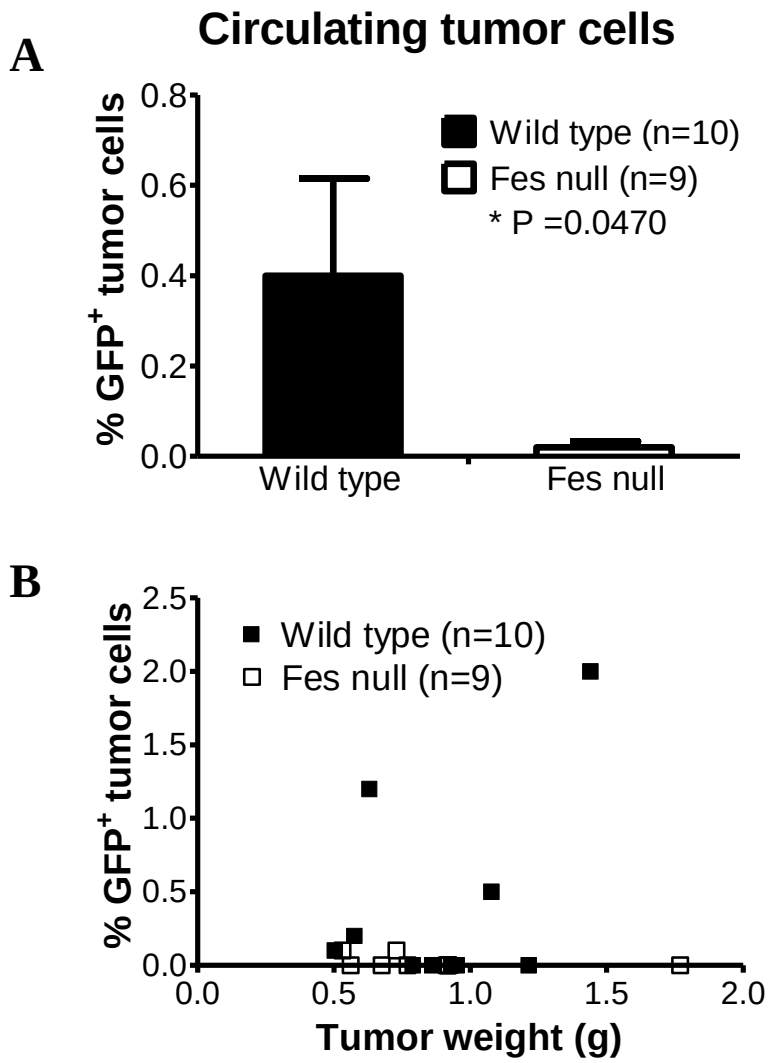

Figure 2.13 Fes-deficiency in the niche correlated with reduced CTC frequency. Peripheral blood was isolated by cardiac puncture of control mice or tumor-bearing mice 22 days after engraftment with GFP-expressing AC2M2 cells. RBCs were removed by hypotonic lysis and the remaining nucleated cells were assessed for GFP fluorescence by flow cytometry. A) Percent GFP^+ nucleated circulating cells (P = 0.047; n = 10 wild-type, n = 9 *fes-null*). B) Percent GFP^+ cells were plotted against the weight of excised tumors. There were no significant detectable levels of GFP^+ cells in 9 tumor-bearing *fes-null* mice. In contrast, 3 of 10 wild-type tumor-bearing mice had significant levels of GFP^+ cells. Positive and negative controls were nontumor bearing mouse blood with or without spiked addition of GFP-expressing AC2M2 cells.

to find that ectopic overexpression of wild-type, kinase-activated or kinase-dead cellular Fes had no apparent effect on the *in vivo* tumorigenic potential of the tumor cell line used in these engraftment studies. It should also be noted that we were unable to detect endogenous Fes expression in AC2M2 cells. A very recent study has suggested that both the protein expression level and the enzymatic activity of Fes are upregulated in transformed, highly proliferative MDA-MB-231 breast cancer cells [301]. Perhaps, MDA-MB-231 cells are a more appropriate model to study the tumor cell intrinsic role of Fes in tumorigenesis.

Considering that Fes is also expressed in vascular endothelial and myeloid lineages, we next explored the possibility that it might influence tumorigenesis through effects on cells in the tumor niche. We had previously shown that transgenic expression of an activated *fes* allele correlated with hypervascularity, and this led to the original observation of Fes expression in vascular endothelial cells [161]. Subsequent studies have linked Fes activation to signaling in endothelial cells downstream of angiogenic growth factors including VEGF, platelet-derived growth factor (PDGF), and fibroblast growth factor (FGF) [317-319]. Using PECAM-1 expression as a marker of endothelial cells, we observed a significant reduction in the vascularity of tumors and associated stroma in *fes-null* mice. There was also a trend toward reduced vascularity in unaffected mammary glands in tumor-bearing mice as well as in glands of control mice; consequently, reduced angiogenesis in *fes-null* mice may not be strictly tumor-associated. However, these latter reductions were not statistically significant,

suggesting that tumor-associated angiogenic signaling may be more sensitive to Fes deficiency. Because angiogenesis is linked to tumor growth and metastasis [41], these observations were consistent with the observed differences in growth rate and lung metastasis. Thus, reduced tumorigenesis in *fes-null* mice may be, at least in part, due to loss of proangiogenic Fes signaling functions intrinsic to vascular endothelial cells, and could reflect differential responsiveness to tumor-produced paracrine acting factors including VEGF, PDGF, and FGF.

Other cells of the niche can interact in a paracrine fashion with the endothelium and with tumor cells to promote tumor growth and metastasis. Fes is expressed in hematopoietic cell types, including platelets [320], mast cells [321], granulocytic cell types [322] and macrophages [163]. Although we cannot rule out any particular cell type, we focused our attention on macrophages because of the high level of Fes expression in these cells and accumulating evidence linking them to tumorigenesis [70, 309, 312-314, 323-325]. Given our observation of decreased numbers of CTCs in *fes-null* mice, we were particularly intrigued with the recent report correlating tumor cell interactions with macrophages and endothelial cells with clinical metastasis in breast cancer [324]. *In vitro* co-culture experiments revealed a significant defect in the ability of *fes-null* bone marrow derived macrophages to promote tumor cell invasion into collagen I gels. Furthermore, the tumor cell-induced invasive properties of the macrophages were compromised in Fes-deficient cells. These observations strongly argue that Fes plays roles in metastasis by promoting paracrine interactions between

macrophages and tumor cells. However, it should be considered that BMMs were used in these coculture collagen gel invasion studies, so their phenotype may not be expected to precisely recapitulate that of tumor-associated macrophages *in vivo*. Furthermore, the *in vivo* niche contains many other cytokines, growth factors, and extracellular matrix components, as well as many other cell types, including fibroblasts, lymphocytes, and vascular and lymphatic endothelial cells. Further studies are required to elucidate the roles of Fes in differentiation of monocytic progenitors into specialized macrophage phenotypes and the ability of these cells to interact with the *in vivo* tumor niche.

Classically, activated inflammatory M1-like macrophages are induced by IFN-γ as well as other factors including LPS, TNF-α, and GM-CSF; and they mediate resistance to microbial infections as well as anti-tumorigenic properties [208]. Alternatively, activated M2-like macrophages are induced by IL-4 and IL-13; and in response to other cytokines, including TGF-β, IL-10, and CSF-1, they acquire tumor-promoting properties, and also suppress inhibitory M1 macrophage functions [95]. We observed fewer phagocytic F4/80^{+} macrophages in *fes-null* tumor-associated stroma, and we speculate that tumor promoting M2-like macrophages may be reduced in *fes-null* tumor stroma.

Fes-deficient mice had slightly reduced numbers of circulating myeloid cells and slightly increased numbers of GM-CSF induced colony-forming unit

granulocyte-macrophage colonies in methylcellose assays [162, 163]. These and other studies have implicated Fes in hematopoietic differentiation along the granulocyte-monocyte lineage. However, there have been no studies that specifically addressed the effects of Fes deficiency on macrophage polarization into M1- versus M2-like phenotypes. However, *in vitro* studies have shown that activated Fes can promote differentiation of bi-potential U937 cells into macrophages at the expense of the alternative granulocytic fate [326] and can also promote survival and granulocytic differentiation of 32D cells upon IL-3 removal [327]. These observations indicate subtle roles for Fes in regulating myeloid differentiation that merit further analysis. Perhaps of more relevance to this study, it will be important to determine if Fes modulates the response of monocytes to IFN-γ or IL-4/IL-13, which drive M1- or M2-like polarization, respectively [65, 209]. Based on our observations, we speculate that Fes-deficient macrophages will be relatively refractory to IL-4- or IL-13- induced M2-like polarization. Previous studies reported that Fes interacts with the IL-4Rα chain in B cells, and potentiates recruitment of PI3K to IRS2 [260-262]. However, we are unaware of reports linking Fes to IL-4/IL-13 signaling in macrophages. We also speculate that Fes-deficient macrophages will be hypersensitive to M1-polarization. We have previously shown that *fes-null* mice display hyperinflammatory responses to LPS [162], which were further characterized *in vivo* by increased leukocyte recruitment to locally inflamed tissues and increased levels of systemic TNF-α [328]. Cultured *fes-null* macrophages displayed prolonged LPS-induced activation of NFκB, increased

TNF-α production, and reduced internalization of the TLR4 receptor complex [165]. It will be important to determine if Fes-deficiency promotes an M1-like polarization at the expense of M2 macrophages. In that case, Fes inhibition might not only interfere with tumor-promoting functions of M2 polarized macrophages, but might also promote the M1-based antitumor functions. In our current working model, Fes-deficiency may skew macrophages toward a proinflammatory M1 polarity that could contribute to tumor initiation. This might have played a role in the earlier tumor onset seen in the Fes-deficient MMTV-PyMT transgenic mouse model of mammary tumorigenesis [170]. At later stages of tumorigenesis where tumor-associated macrophages tend to skew more towards to protumorigenic M2 polarized state, Fes-deficiency might attenuate that process, leading to reduced tumor progression, as observed in the orthotopic engraftment model used in this study.

In summary, our observations suggest that systemic inhibition of Fes might provide antitumorigenic benefits in cancer by inhibiting endothelial cell intrinsic angiogenic signaling as well as inhibiting the tumor promoting properties of tumor-associated macrophages.

Chapter 3

Deficiency of Fes kinase expression correlates with delayed mammary tumor onset in a MMTV-Neu transgenic mouse model

3.1 Abstract

Fes is a cytoplasmic protein tyrosine kinase that is highly expressed in breast epithelial cells during lactation, as well as in vascular endothelial and myeloid cells. Retrovially encoded oncogenic alleles of Fes are associated with tumors in chickens and cats and cause tumors in transgenic mice; however, a role for Fes in human cancer has not been established.

Using a transgenic mouse model of breast cancer driven by an activated HER2/Neu allele expressed in the mammary epithelium, we observed delayed tumor onset in *fes*-deficient mice compared to wild-type mice. However, there was no significant difference in tumor growth rates. The delayed tumor onset correlated with reduced levels of epithelial dysplasia and increased levels of lymphocyte and granulocyte infiltrates as well as NFκB activation in *fes*-deficient normal mammary glands prior to detection of tumors. In addition, higher stromal grading was identified as a reflection of numbers of immune cells relative to tumor size in *fes*-deficient tumor-bearing mammary glands, suggesting increased levels of immune infiltration in those tissues. These observations argue that Fes inhibition might provide therapeutic

benefits in breast cancer by attenuating the carcinogenic process associated with HER2 overexpression.

3.2 Introduction

Fes is a non-receptor protein tyrosine kinase, which consists of an N-terminal F-BAR domain, a predicted coiled-coil motif, a central SH2 domain, and a C-terminal kinase domain [143]. Fes is expressed in a tissue specific manner, with highest expression levels in myeloid, endothelial, and subsets of epithelial and neuronal cells [157]. Recently, Fes expression and kinase activity were found to be upregulated during pregnancy and lactation [158], as well as in transformed, highly proliferative MDA-MB-231 breast cancer cells [301]. So far, with our knowledge, we do not know yet whether Fes kinase plays an oncogenic or tumor suppressor role in human breast cancer, since there is evidence supporting either role of Fes.

Fes was originally identified as a dominant-acting oncoprotein encoded by transforming retroviruses isolated from avian (*fps*) [125, 126] or feline (*fes*) [122-124] tumors. When expressed in transgenic mice, viral *fps* induced tumors in lymphoid and mesenchymal tissues [166]. These observations suggested that activating mutations in the human *fes* proto-oncogene might contribute to cancer.

In 2003, four missense mutations were identified in human colorectal cancers [169], leading to the speculation that activated Fes kinase contributed to these cancers.

However, subsequent biochemical and structural modeling analysis revealed that these mutations attenuated rather than activated Fes kinase [170]. This revelation raised the novel possibility that Fes might also function as a tumor suppressor.

The first compelling genetic evidence to support this hypothesis came from studies using the MMTV-PyMT transgenic breast cancer model. Tumors developed earlier in mice targeted at the *fes* locus with either null or kinase-inactivating missense mutations [170]. The *fes* promoter was also found to be silenced by methylation in colorectal cancer cell lines, and this correlated with downregulation of Fes expression [172]. These apparently contradicting observations argued that Fes may play both oncogenic and tumor suppressor roles.

Based on gene expression profiles, breast cancer can be classified into five major subtypes, including luminal A, luminal B, normal breast-like, basal-like, and HER2 subtype [11]. Basal-like and HER2 breast cancers are the most aggressive subtypes with poor prognosis, where more targeted therapies are urgently required [15-17]. In previous studies using the AC2M2 orthotopic mouse mammary engraftment model, we demonstrated that wild-type mice developed significantly larger tumors and higher degree of lung metastasis as compared to *fes-null* mice [302], suggesting the tumor promoting role of Fes in the tumor niche in this particular basal-like breast cancer model. Here, we utilized transgenic mice with overexpression of an activated form of the rat homolog of HER2 (Neu) driven by the MMTV

promoter (MMTV-Neu) to mimic the HER2 subtype of breast cancer [105], and found *fes*-deficient transgenic mice developed mammary tumors with a significantly longer latency as compared to wild-type mice. This delayed tumor onset correlated with reduced levels of epithelial dysplasia and increased levels of lymphocyte and granulocyte infiltrates as well as NFκB activation in *fes*-deficient normal mammary glands. Higher stromal grading was also identified in *fes*-deficient tumor-bearing mammary glands, based on the number of immune cells. These observations suggested that Fes may play a stromal-specific tumor promoting role in HER2 subtype of breast cancer, and Fes inhibition might provide therapeutic benefits in breast cancer by attenuating the carcinogenic process associated with HER2 overexpression.

3.3 Materials and methods

3.3.1 Mice

Mice targeted with a kinase-inactivating mutation in *fes* ($fes^{KR/KR}$) was previously described [163]. Briefly, the fes^{KR} allele was generated by targeting the mouse *fes* locus with a missense mutation (Lys588Arg), resulting in a stable Fes protein that lacks detectable kinase activity [163]. Transgenic mice with MMTV-driven overexpression of an activated Neu transgene were purchased from Jackson Lab [105]. Hereafter, we refer it as $Neu^{NT/o}$ transgenic mice.

The previously established *fes*$^{KR/KR}$ strain was crossed with *Neu*$^{NT/o}$ transgenic mice to produce wild-type (*fes*$^{+/+}$, *Neu*$^{NT/o}$), heterozygous (*fes*$^{KR/+}$, *Neu*$^{NT/o}$) and homozygous *fes*-deficient (*fes*$^{KR/KR}$, *Neu*$^{NT/o}$) mice. Mice were housed in the Animal Care Facility and procedures were performed according to the guidelines of the Canadian Council on Animal Care, with the approval of the institutional animal care committee.

3.3.2 Spontaneous mammary tumor model

All thoracic and abdominal mammary glands were examined every week by physical palpation for initial tumor occurrence after mice reached 180 days old. Once initial tumors were detected, tumor growth was monitored every week and tumor size was recorded according to a circle template. When tumors grew to a certain size, mice were euthanized and tumor-bearing mammary glands were harvested, and then either snap-frozen and kept in a -80℃ freezer for immunoblotting analysis or fixed in 4% paraformaldehyde and paraffin embedded for immunohistochemistry analysis. For each genotype, the following tissues were accumulated: normal mammary glands (NMG) at 60 days old, small size tumors (size 1-3), medium size tumors (size 6-8), and large size tumors (size 10-12). Tumor volumes in mm^3 were calculated corresponding to each size on circle template using the equation of Volume = $4/3\pi R^3$ (R, radius of the tumor). Tumor onset and tumor growth rate were analyzed using

GraphPad Prism software.

3.3.3 Immunoblotting

Frozen mammary glands or tumors were removed from the -80℃ freezer and defrosted on ice. Tissue lysates were generated by homogenizing with 2mL RIPA lysis buffer (10mM Tris pH 7.2, 158mM NaCl, 1mM EDTA, 0.1% SDS, 1% sodium deoxycholate, 1% Triton 100 with 10μg/mL aprotinin, 10μg/mL leupeptin, 100μM sodium orthovanadate, 100μM phenylmethylsulfonyl fluoride) using a Ultra-Turrax T25 tissue homogenizer (Terochem Scientific), and centrifuged at 13,000rpm for 15min at 4℃ to remove fat. All samples were normalized to the same protein concentration using BioRAD kit. After diluted in SDS sample buffer, 200μL aliquots were made from each tissue lysates and kept in -20℃ before running on SDS-PAGE. Protein levels were determined by densitometry using Image Pro Software. Primary antibodies used for immunoblotting analysis included anti-phospho-NFκB (Cell Signaling) and anti-tubulin (Sigma).

3.3.4 Histopathological assessment of H&E sections

Normal mammary glands or mammary glands containing different sizes of tumors were harvested, fixed in 4% paraformaldehyde and paraffin embedded. 5μm tissue sections were cut, stained with hematoxylin and eosin (H&E) stain, and then

assessed for histopathologic features in a blinded fashion. Each H&E section was scored with a stroma grade of one, two or three, which corresponds to low, intermediate or high level of immune cell infiltration. Stroma grades were then matched with tumor size and tissue genotype, and further data analysis were performed using GraphPad Prism software.

3.3.5 Immunohistochemical staining

Five μm sections of formalin fixed paraffin embedded either normal or tumor-containing mammary gland tissues were stained with antibodies against Ki67 (Ventana) for proliferating cells, CD3 (Ventana) for T cells and CD11b (Abcam) for granulocytes by automated Ventana staining system Discovery XT. Stained slides were scanned with an Aperio scanner and images were analyzed using Aperio ImageScope software.

3.3.6 Statistics

All statistical analysis was done by using GraphPad Prism software. All error bars represent standard error of the mean. P values were calculated by Student's *t* test analysis or one-way ANOVA (where specified). Data sets with $P \leq 0.05$ were considered significant.

3.4 Results

3.4.1 Fes deficiency correlates with delayed tumor onset in *Neu*$^{NT/o}$ transgenic mice

In previous studies, we have shown that Fes expression in the tumor niche promotes tumorigenesis and metastasis in the AC2M2 mouse mammary carcinoma cell line orthotopic mouse engraftment model. Since AC2M2 cells are a basal-like breast cancer cell line, we next investigated the role of Fes in a distinct HER2 breast cancer model. These experiments involve the use of an immune-competent MMTV-Neu (*Neu*$^{NT/o}$) transgenic mouse model of mammary tumorigenesis [105].

By crossing our previously established *fes*^{KR} (targeted Fes kinase inactivating mutation) strain with *Neu*$^{NT/o}$ transgenic mice, we accumulated 46 wild-type (*fes*$^{+/+}$, *Neu*$^{NT/o}$), 47 heterozygous (*fes*$^{KR/+}$, *Neu*$^{NT/o}$) and 49 homozygous *fes*-deficient (*fes*$^{KR/KR}$, *Neu*$^{NT/o}$). Wild-type mice had the earliest tumor onset, whereas homozygous *fes*-deficient mice developed tumors with a significantly longer latency. Mice with only one kinase-inactivated *fes* allele had intermediate tumor latencies (average tumor onset: *fes*$^{+/+}$, *Neu*$^{NT/o}$, 274 days; *fes*$^{KR/+}$, *Neu*$^{NT/o}$, 316 days and *fes*$^{KR/KR}$, *Neu*$^{NT/o}$, 389 days; $P < 0.0001$; Figure 3.1).

3.4.2 Fes deficiency does not affect tumor growth rates in *Neu*$^{NT/o}$ transgenic mice

We have determined that Fes plays an oncogenic role in tumor initiation in the

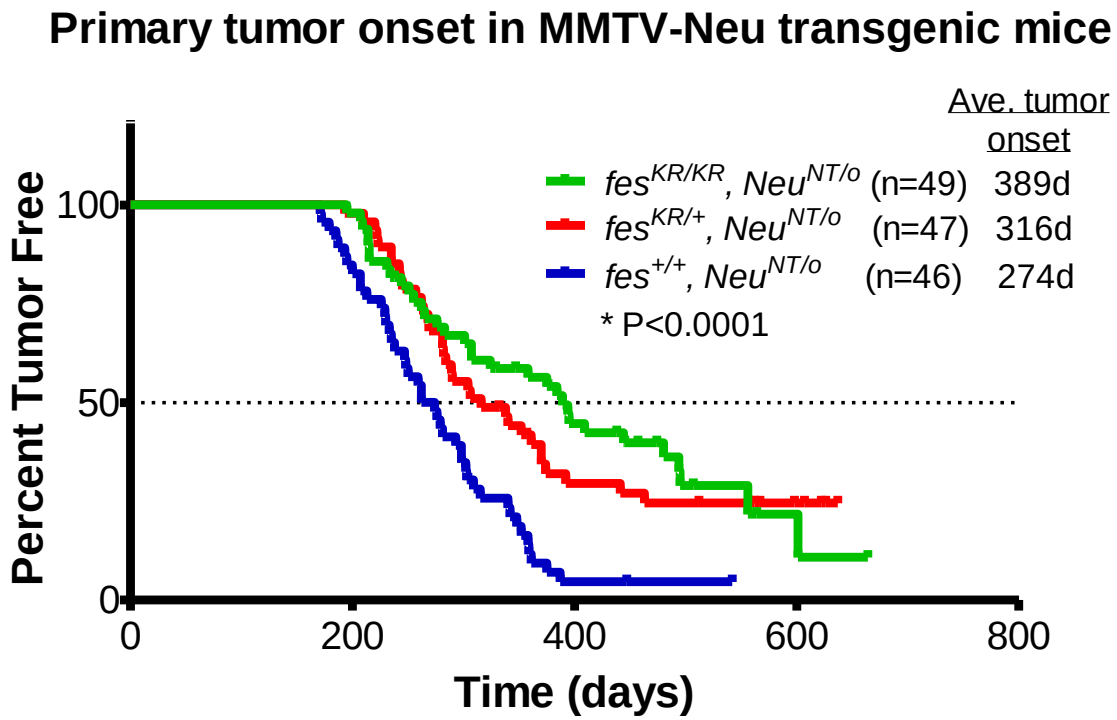

Figure 3.1 Delayed tumor onset in *fes*-deficient MMTV-Neu transgenic mice. Mice targeted with Fes kinase-inactivated mutation (fes^{KR}) were crossed with MMTV-Neu ($Neu^{NT/o}$) transgenic mice, and primary tumor onsets of these mice were monitored by physical palpation weekly. On average, wild-type ($fes^{+/+}$, $Neu^{NT/o}$) MMTV-Neu transgenic mice developed spontaneous tumors at 274 days of age. However, in homozygous *fes*-deficient ($fes^{KR/KR}$, $Neu^{NT/o}$) mice, the average tumor onset was delayed for over 100 days (389 days). Mice with only one kinase-inactivated *fes* allele showed intermediate latencies of 316 days ($P< 0.0001$; n= 46 for $fes^{+/+}$, $Neu^{NT/o}$; n= 47 for $fes^{KR/+}$, $Neu^{NT/o}$; and n= 49 for $fes^{KR/KR}$, $Neu^{NT/o}$).

HER2-driven transgenic mouse model of breast cancer. Next, we assessed whether Fes deficiency has an effect on tumor growth rate kinetics in this model. After initial tumors were detected, tumor size was followed every week by physical palpation. Tumor growth rate was calculated as a rate constant of mm^3 per day by GraphPad Prism software. The average tumor growth rates were the same in wild-type ($fes^{+/+}$, $Neu^{NT/o}$), heterozygous ($fes^{KR/+}$, $Neu^{NT/o}$) and homozygous *fes*-deficient ($fes^{KR/KR}$, $Neu^{NT/o}$) mice (P= 0.6790 by one-way ANOVA; Figure 3.2). These observations show that Fes deficiency does not affect tumor growth rates in established tumors in MMTV-Neu transgenic mice. In addition, we did not find any significant differences in the length of time taken from initial tumor detection to onset of exponential tumor growth among the three genotypes, suggesting that Fes does not have an effect on the angiogenic switch associated with accelerated tumor growth.

3.4.3 Decreased levels of epithelial dysplasia and increased numbers of lymphocytes and granulocytes in Fes-deficient normal mammary glands

In order to determine the underlying mechanism of delayed tumor onset in *fes*-deficient MMTV-Neu transgenic mice, we harvested pre-malignant NMG tissues and stained with hematoxylin and eosin (H&E) for histopathological assessment. Histopathologic analysis suggested that there were higher levels of epithelial dysplasia in wild type NMG as well as more lymphocytes and granulocytes in

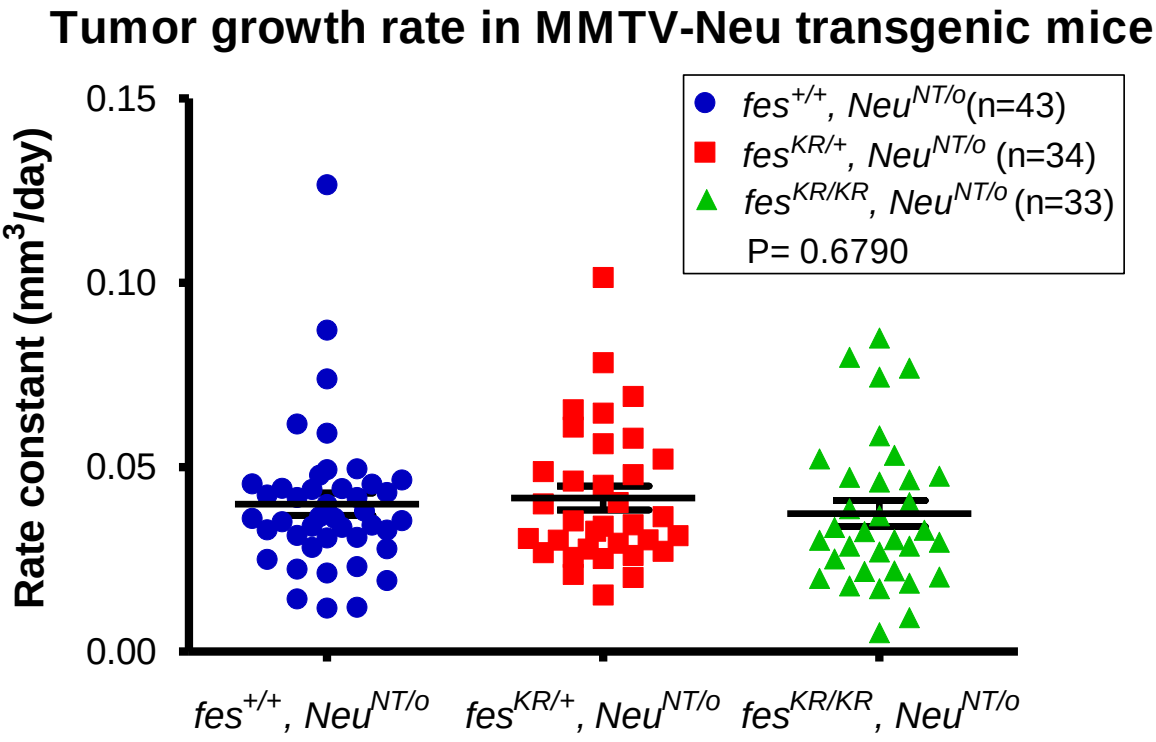

Figure 3.2 No difference in tumor growth rate between wild-type and *fes*-deficient MMTV-Neu transgenic mice. Mice targeted with Fes kinase-inactivated mutation (fes^{KR}) were crossed with MMTV-Neu ($Neu^{NT/o}$) transgenic mice, and primary tumor onsets of these mice were monitored by physical palpation. Once initial tumors were detected, tumor volumes were assessed every week and tumor growth rate was calculated as a rate constant of mm^3 per day. There was no significant difference in term of tumor growth rate among wild-type ($fes^{+/+}$, $Neu^{NT/o}$), heterozygous ($fes^{KR/+}$, $Neu^{NT/o}$) and homozygous *fes*-deficient ($fes^{KR/KR}$, $Neu^{NT/o}$) mice (P=0.6790 by one-way ANOVA; n= 43 for $fes^{+/+}$, $Neu^{NT/o}$, n= 34 for $fes^{KR/+}$, $Neu^{NT/o}$, and n= 33 for $fes^{KR/KR}$, $Neu^{NT/o}$).

fes-deficient NMG (Figure 3.3A-C).

Using initial histopathological assessment on H&E staining as guidance, we next stained the same NMG tissues with specific cell markers, including Ki67 (Figure 3.3 D) for proliferating cells indicative of dysplasia, CD3 (Figure 3.3 E) for T lymphocytes, and CD11b (Figure 3.3 F) for granulocytes, and then quantified the staining using the Aperio system. Statistical analysis showed significantly lower levels of Ki67 (P= 0.0413; Figure 3.4A) as well as higher levels of CD3 (P= 0.0275; Figure 3.4B) and CD11b (P= 0.0098; Figure 3.4C) positive cells in *fes*-deficient pre-malignant NMG. This was consistent with the blinded histopathological assessment.

3.4.4 Elevated levels of NFκB activation in *fes*-deficient normal mammary glands at the pre-malignant stage

We previously found higher numbers of $CD3^+$ T lymphocytes and $CD11b^+$ granulocytes in *fes*-deficient normal mammary glands by immunohistochemical staining. This observation suggested that there might be an increased level of inflammation in these tissues, resulting in a delayed tumor onset in *fes*-deficient MMTV-Neu transgenic mice. We next performed immunoblotting analysis with phospho-p65 NFκB antibody as an inflammatory marker to verify the inflammation status of both wild-type and *fes*-deficient normal mammary glands. The phospho-p65

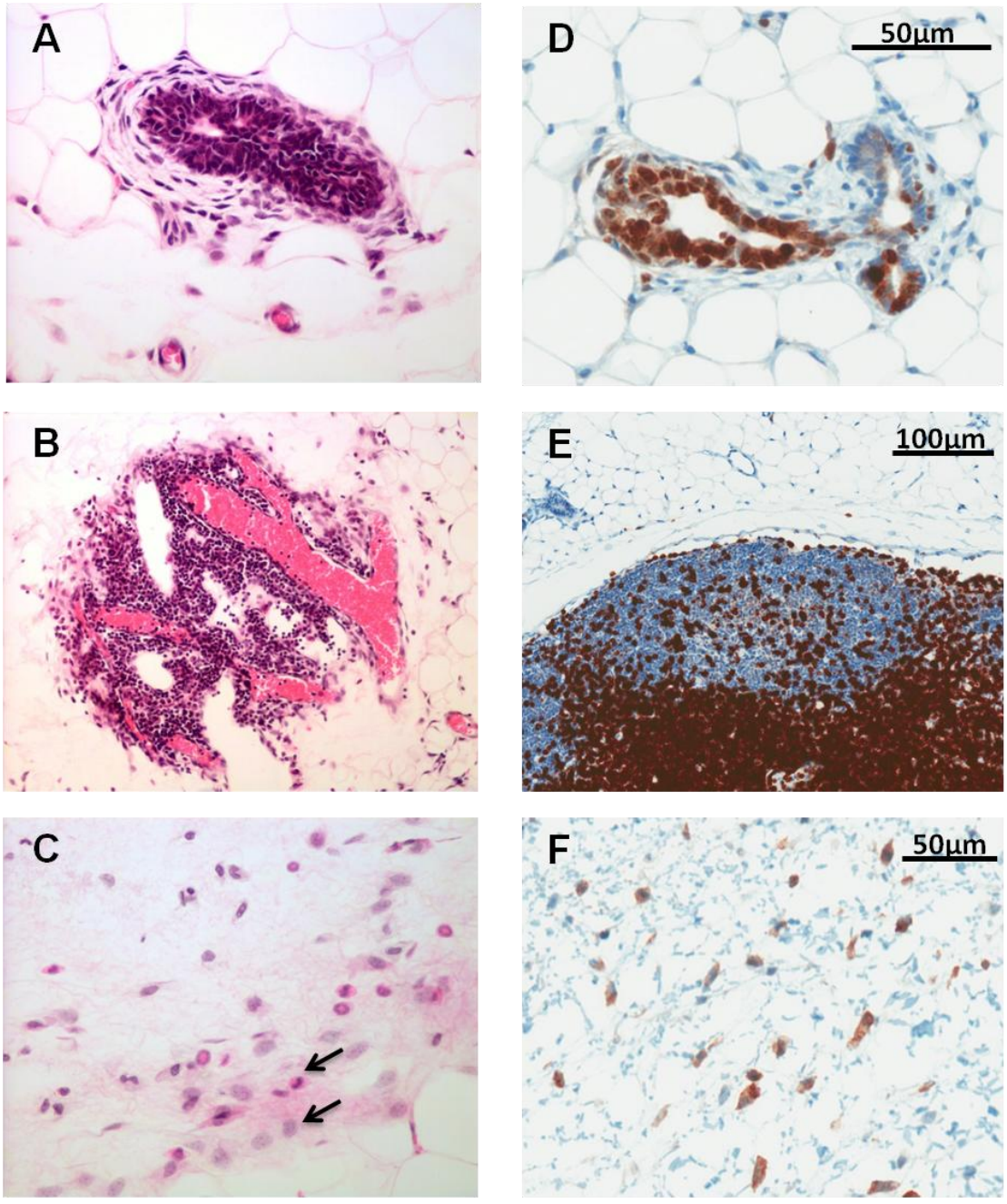
A
D
50µm
B
E
100µm
C
F
50µm

Figure 3.3 H&E and immunohistochemical stainings of pre-malignant normal mammary glands (NMG). Wild-type (*fes*$^{+/+}$, *Neu*$^{NT/o}$) and *fes*-deficient (*fes*$^{KR/KR}$, *Neu*$^{NT/o}$) MMTV-Neu transgenic mice were euthanized at 60 days of age before the development of any detectable tumors. NMGs were dissected, fixed in 4% paraformaldehyde and paraffin embedded. 5μm sections were stained with hematoxylin and eosin (A-C). A) A representative image of epithelial dysplasia, where the lumen is filled with proliferating epithelial cells and myoepithelial cell layer is disorganized. B) A representative image of a lymph node with large amount of lymphocytes. C) A representative image of highly inflamed mammary tissue with arrows pointing at granulocytes. After histopathological assessment on H&E stainings, sections were made from the same tissue blocks and stained with various cell markers, including Ki67 for proliferating cells (D), CD3 for T lymphocytes (E) and CD11b for granulocytes (F) using a Ventana automated staining system.

A

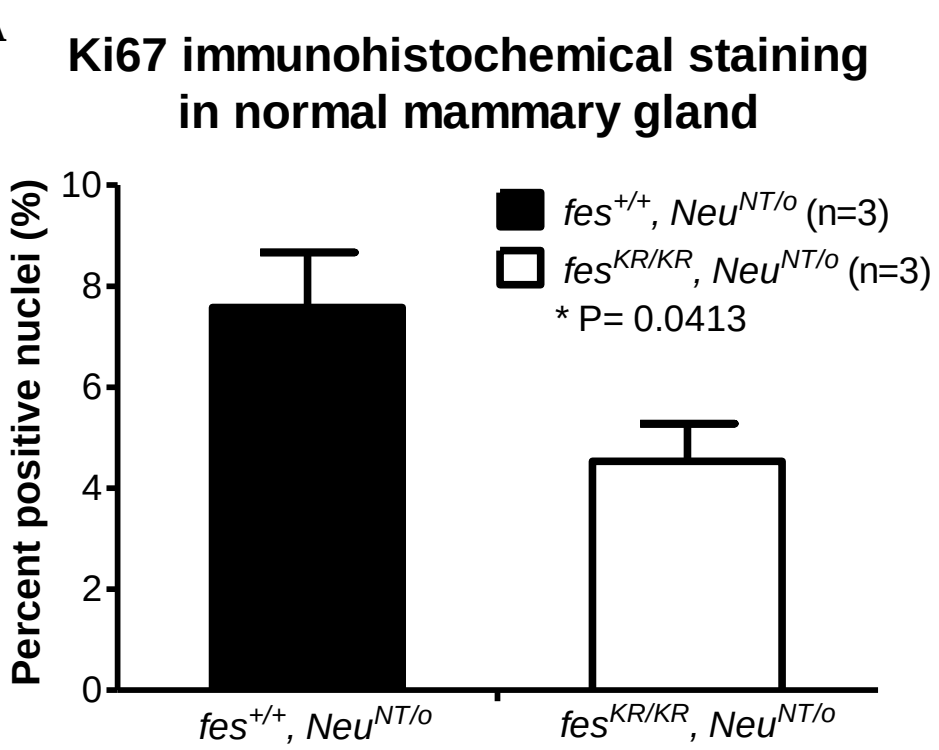
Ki67 immunohistochemical staining
in normal mammary gland
Percent positive nuclei (%)
10
8
6
4
2
0
fes+/+, NeuNT/o (n=3)
fesKR/KR, NeuNT/o (n=3)
* P= 0.0413
fes+/+, NeuNT/o
fesKR/KR, NeuNT/o

B

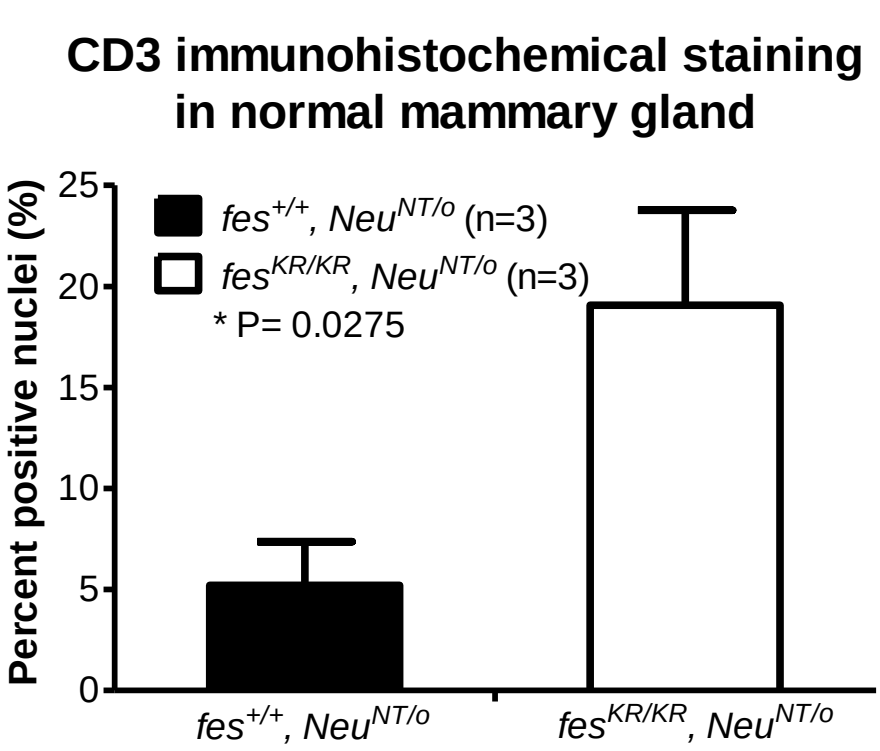
CD3 immunohistochemical staining
in normal mammary gland
Percent positive nuclei (%)
25
20
15
10
5
0
fes+/+, NeuNT/o (n=3)
fesKR/KR, NeuNT/o (n=3)
* P= 0.0275
fes+/+, NeuNT/o
fesKR/KR, NeuNT/o

C

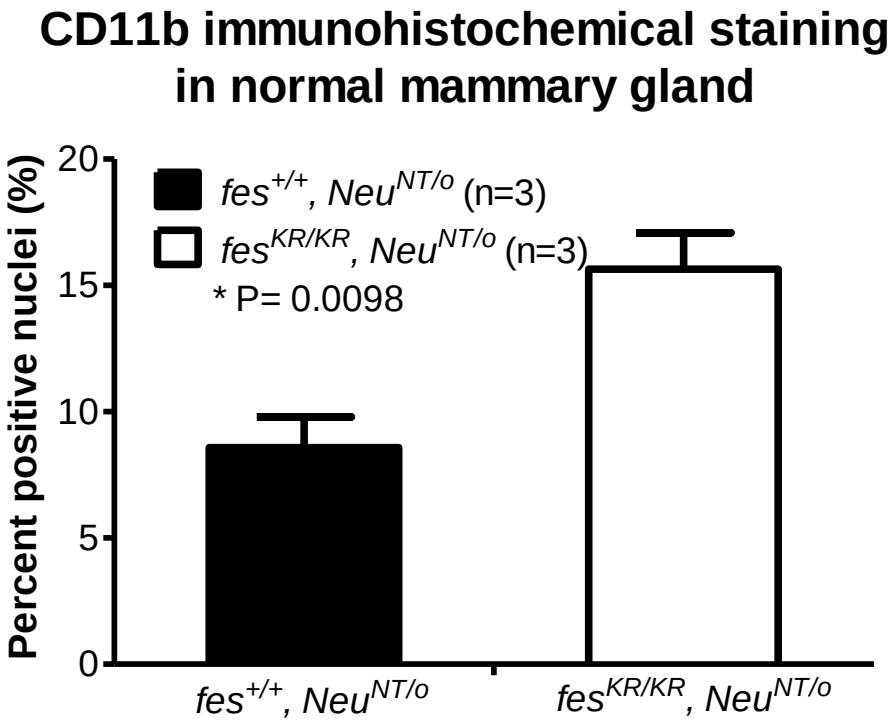

Figure 3.4 Lower level of Ki67 and higher levels of CD3 and CD11b staining in *fes*-deficient normal mammary glands. Wild-type (*fes*$^{+/+}$, *Neu*$^{NT/o}$) and *fes*-deficient (*fes*$^{KR/KR}$, *Neu*$^{NT/o}$) MMTV-Neu transgenic mice were euthanized at 60 days of age before the development of any detectable tumors. NMGs were dissected, fixed in 4% paraformaldehyde and paraffin-embedded. 5μm sections were stained with Ki67 for proliferating cells, CD3 for T lymphocytes and CD11b for granulocytes. Staining was quantitated by Aperio, and statistical analysis was performed using GraphPad Prism software. There was significantly higher Ki67 (panel A) staining in wild-type NMG as well as higher levels of CD3 (panel B) and CD11b (panel C) staining in *fes*-deficient NMG (P= 0.0413 for Ki67, P= 0.0275 for CD3, P= 0.0098 for CD11b; n=3 for both groups).

NFκB level was elevated in *fes*-deficient NMG as compared to wild-type NMG (P= 0.0018; Figure 3.5A, B), suggesting a higher level of inflammation in *fes*-deficient NMG, which was consistent with the results obtained by immunohistochemical staining.

3.4.5 Higher stromal grading in *fes*-deficient malignant tumor-bearing mammary glands

We next assessed mammary glands containing comparably sized tumors from both wild-type and *fes*-deficient MMTV-Neu transgenic mice. Blinded histopathologic assessment of H&E stained sections of tumor-containing mammary glands was performed to determine a stromal grading of 1 to 3 based on the numbers of immune cells (for example, T and B lymphocytes, macrophages, granulocytes) present in the tumor and surrounding gland. The stromal grade was found to be significantly higher in *fes*-deficient tumor-bearing mammary glands, which correlated with more immune cells in *fes*-deficient tumor stroma as well as a higher level of inflammation in *fes*-deficient tumor-containing mammary glands (P= 0.042; Figure 3.6).

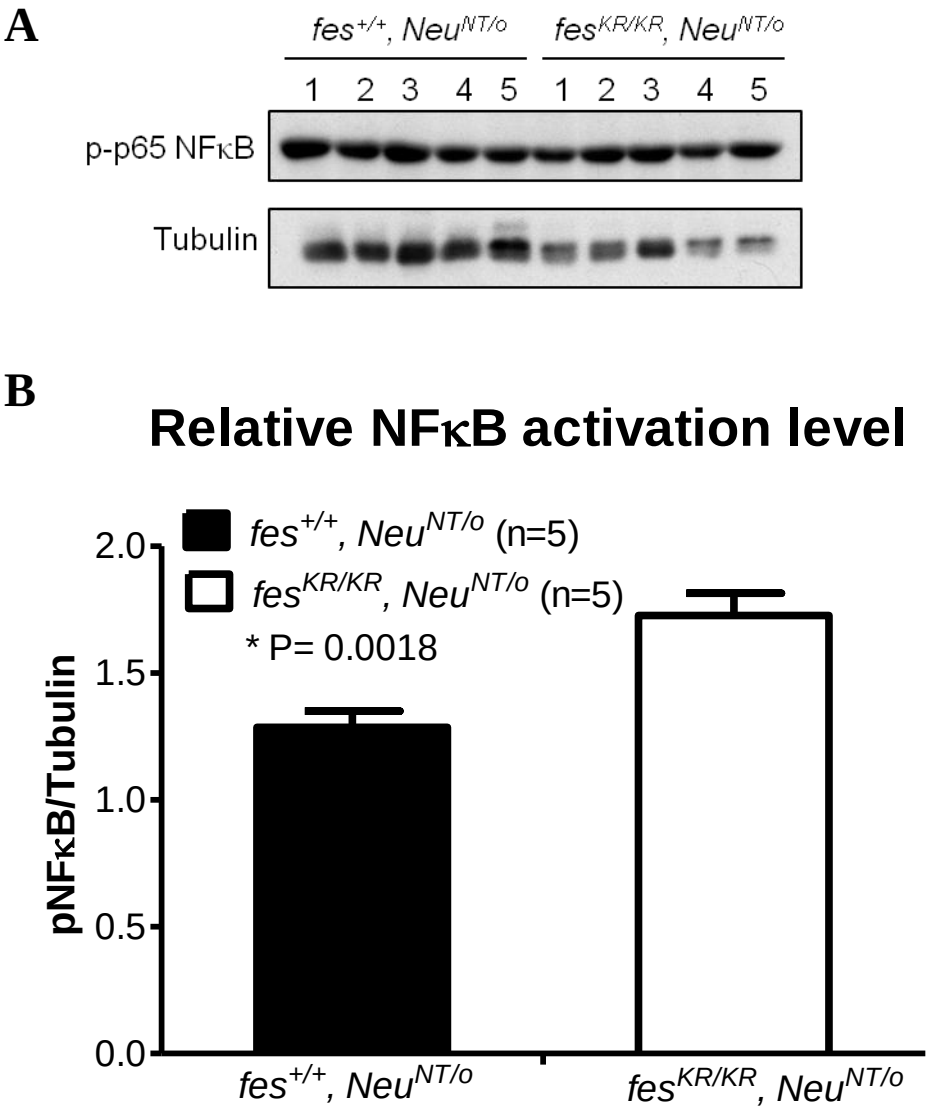

Figure 3.5 Elevated levels of NFκB activation in *fes*-deficient normal mammary glands. (A) Wild-type (*fes*$^{+/+}$, *Neu*$^{NT/o}$) and *fes*-deficient (*fes*$^{KR/KR}$, *Neu*$^{NT/o}$) MMTV-Neu transgenic mice were euthanized at 60 days of age, and normal mammary glands were dissected and frozen at -80℃ freezer. Tissues were homogenized with RIPA lysis buffer, and lysates were analyzed by immunoblotting analysis with anti-phospho-p65 NFκB (p-p65 NFκB) antibody and anti-tubulin antibody for protein loading control. (B) Densitometry analysis revealed that NFκB activation was significantly elevated in *fes*-deficient normal mammary glands (P= 0.0018; n= 5 for both groups).

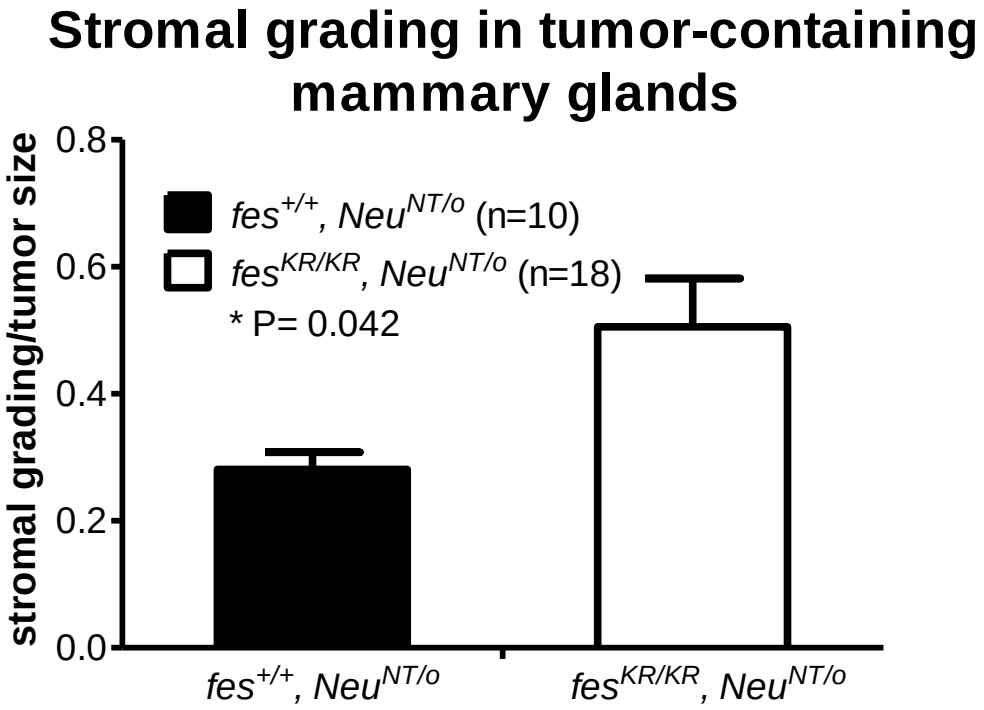

Figure 3.6 Higher stromal grading in *fes*-deficient tumor-bearing mammary glands. Wild-type ($fes^{+/+}$, $Neu^{NT/o}$) and *fes*-deficient ($fes^{KR/KR}$, $Neu^{NT/o}$) MMTV-Neu transgenic mice were allowed to develop spontaneous tumors, and tumor onset as well as tumor size were monitored every week by physical palpation. Mammary glands containing comparable size of tumors were removed from both genotypes at different time, and then fixed in 4% paraformaldehyde and paraffin embedded. 5μm sections were stained with H&E and subjected to blinded histopathological assessment. Each tumor-containing mammary gland was assigned with a stromal grading based on the number of immune cells present in the tumor stroma, and stomal grading relative to tumor size was plotted. Statistical analysis showed that stromal grading was significantly higher in *fes*-deficient tumor-containing mammary glands (P= 0.042; n= 10 for $fes^{+/+}$, $Neu^{NT/o}$ and n= 18 for $fes^{KR/KR}$, $Neu^{NT/o}$).

3.5 Discussions

With the advent of gene and protein microarray profiling, breast tumors were grouped into five subtypes based on their gene-expression patterns, that are, luminal A, luminal B, normal breast-like, basal-like and HER2 subtypes [11]. Previously, we used the AC2M2 orthotopic mouse mammary engraftment model as a basal-like breast cancer model, and demonstrated that Fes kinase plays an oncogenic role in promoting breast tumorigenesis and distant metastasis. The tumor promoting role of Fes in that model was associated not with the cancer cells but with cells of the tumor niche, including tumor-associated macrophages and vascular endothelial cells [302]. In this study, we used transgenic mice with MMTV-driven overexpression of an activated HER2 transgene, the rat neuoblastoma derived *Neu* oncogene [105], which is a spontaneous breast tumor model recapitulating HER2 subtype of breast cancer. In this particular model, we found the average tumor onset in *fes*-deficient transgenic mice was delayed by over 100 days as compared to wild-type littermates. However, once tumors started to grow, there was no difference in the rate of growth between wild-type and *fes*-deficient mice. These observations suggested that Fes kinase plays an oncogenic role in the early phase of tumor development, i.e. tumor initiation, but not during tumor growth, in this HER2 overexpressing transgenic mouse model of breast cancer.

As Muller and colleagues originally suggested, these MMTV-Neu transgenic

mice would develop metastatic nodules in the lungs simultaneously [105]. One caveat of this study is that we did not assess the effect of Fes deficiency in the development of distant metastasis, and future experiments are required to address this question. Notably, wild-type MMTV-Neu transgenic mice in our study developed tumors at around 274 days of age, which was slightly delayed as compared to a median tumor incidence of 205 days reported by Muller group [104]. This might be due to a slight difference in mouse strain background. Besides that, no other phenotypic differences were observed as far as wild-type animals were concerned.

The same study was done in the context of Fes-related Fer kinase, and similar results indicated that Fer deficiency also correlated with delayed primary tumor onset in the MMTV-driven HER2 transgenic mouse model of breast cancer [329]. When both Fes and Fer kinases are inactivated, we found even longer tumor latency as compared to Fes kinase alone ($P< 0.0001$; Appendix 3). This result suggested an additive effect of Fes and Fer in promoting the initiation of spontaneous tumors in HER2 transgenic mice, and suggests that inhibition of both Fes and Fer kinases would be beneficial for treating women with HER2 overexpressing breast cancer.

In order to explore the underlying mechanism of delayed tumor onset in *fes*-deficient transgenic mice, we collected normal mammary glands (NMG) before the development of any detectable tumors, and assessed the inflammatory status of these tissues. By immunoblotting and immunohistochemical staining, we found an

elevated level of NFκB activation as well as more lymphocytes and granulocytes in *fes*-deficient NMG, suggesting the hyperinflammatory status of these glands. These observations were consistent with the hyperinflammatory phenotype observed in *fes*-knockout mice after LPS challenge [165]. All together, it suggested that Fes may play a role in regulating inflammation; and the absence of Fes may lead to a higher level of inflammation in general.

As Virchow hypothesized in 1983, cancer may originate at sites of chronic inflammation, and increasing evidence has indicated that inflammation is a contributor of a wide variety of tumors [59, 60]. Accordingly, one might speculate that the absence of Fes would be associated with a higher level of inflammation, which would lead to an earlier tumor onset in a spontaneous tumor model. However, this is contradictory to our observations in the MMTV-Neu model. The increased numbers of $CD3^+$ T lymphocytes and $CD11b^+$ granulocytes we observed in *fes*-deficient normal mammary glands indeed indicated a higher level of adaptive and innate immune response in these tissues. But, these immune responses may have been acting to eliminate neoplastic epithelial cells, which would otherwise have progressed to dysplasia, and eventually to carcinoma. This explanation is supported by reduced dysplasia in *fes*-deficient normal mammary glands, detected by histophathological assessment and immunohistochemical staining with Ki67. In contrast, inflammation induced in the MMTV-PyMT model may be some what different. We speculate that the PyMT oncogene may induce a much greater degree of inflammation than

activated HER2/Neu in early stages of tumorigenesis, and Fes deficiency may amplify the already extremely high inflammation caused by PyMT oncogene to an even greater extent. This high level of inflammation induced by PyMT plus Fes deficiency might exceed a physiological threshold such that it becomes mutagenic to accelerate tumorigenesis. Therefore, inflammation is a double-edged sword with both anti-tumorigenic and pro-tumorigenic roles in tumor development.

Here, we explored the role of Fes kinase in a transgenic mouse model of the HER2 subtype of breast cancer, and demonstrated that Fes deficiency correlated with delayed tumor onset in these transgenic mice. This novel finding provides a rationale for exploring Fes inhibition as a strategy to attenuate the carcinogenic process associated with HER2 overexpressing breast cancer.

Chapter 4

Tumor cell-derived IL-4 suppresses tumorigenesis in mouse orthotopic mammary engraftment models of breast cancer

4.1 Abstract

Interleukin 4 (IL-4) is a cytokine that, among other actions, can induce macrophages to undergo alternative activation and polarize to M2 macrophages which have been reported to promote tumorigenesis and metastasis. IL-4 also promotes the formation of multinucleated giant cells from macrophages *in vitro* and participates in the development of the foreign body reaction *in vivo*. AC2M2 cells, a highly metastatic mouse carcinoma cell line, were transduced with retroviruses expressing IL-4 (IL4-AC2M2) or empty vector control (EV-AC2M2). Stimulation experiments showed that AC2M2-derived IL-4 polarized macrophages to express the M2 marker, arginase 1. EV- and IL4-AC2M2 cells grew at the same rate *in vitro*. However, mice orthotopically engrafted with IL4-AC2M2 cells grew tumors at a significantly reduced rate as compared to mice engrafted with control EV-AC2M2 cells. IL-4 expression also correlated with elimination of lung metastasis. Reduced primary tumor growth and complete abolishment of lung metastasis in the IL-4 group correlated with a 30-fold increase of tumor associated macrophage populations and macrophage phagocytosis of tumor cells as well as *in vivo* expression of arginase I..

Thus, tumor-derived IL-4 suppressed tumorigenesis and lung metastasis by activating macrophage phagocytosis in the tumor microenvironment; suggesting that IL-4 could be a good candidate for immunotherapy.

4.2 Introduction

IL-4 is a pleiotropic type I cytokine that plays a critical role in the regulation of immune responses [173, 174]. IL-4 is produced and secreted by many immune cells, including, $CD4^+$ Th2 helper T cells [177], $CD4^+NK1.1^+$ NKT cells [178, 179], basophils [180-182], mast cells [183, 184], and activated eosinophils [185]. IL-4 was first described as B-cell growth factor [186], and has been shown to promote immunoglobulin class switching of B cells [190-192].

Besides being a B-cell differentiation and stimulatory factor, IL-4 has broad functions in multiple cell types of hematopoitic and non-hematopoietic origin. Upon exposure to IL-4, naïve T (Th0) cells differentiate into Th2 helper T cells while differentiation toward the Th1 cell phenotype is inhibited. IL-4 stimulated Th2 cells are also capable of producing additional IL-4 and a series of other cytokines including IL-5, IL-10 and IL-13 [193, 194]. IL-4 induces vascular endothelial cells to express vascular cell adhesion molecule-1 (VCAM-1) [195-197], which leads to the selective recruitment of T cells, eosinophils and basophils to sites of inflammation [196, 198, 199].

IL-4 is a potent macrophage fusion factor, capable of inducing macrophages to form large multinucleated giant cells that are central players in the inflammatory response to foreign materials and in adverse responses to implants [330-333]. IL-4 is also a survival factor, protecting lymphocytes and myeloid progenitors from apoptosis [201-205]. In contrast to M1-like classical macrophage activation by LPS and IFN-γ, IL-4 is capable of inducing macrophages to undergo alternative M2 macrophage activation [66, 206-208, 210, 211]. Instead of killing tumor cells, M2 activated macrophages are believed to promote tumor cell growth, invasion and metastasis by secreting paracrine acting factors and extracellular matrix remodeling factors including EGF, MMP and VEGF [209].

IL-4 initiates signal transduction through one of two different receptor complexes, a type I or type II receptor. The type I receptor comprises a 140kDa IL-4Rα chain and a common gamma chain (γc), which is a signal-transducing unit shared by receptors for members of the IL-2 subfamily of hematopoietins [217-219]. The type II receptor also consists of the IL-4Rα chain but the γc is substituted by the IL-13 low affinity receptor 1 (IL-13Rα1) [220]. The type I receptor is specific for IL-4, whereas the type II receptor can be activated by either IL-4 or IL-13. Hematopoietic cells such as T and B cells express only the type I receptor, whereas cells of the myeloid lineage such as monocytes, macrophages, and fibroblasts express both type I and type II IL-4Rs [223]. Upon IL-4 binding, IL-4R recruits and activates Jak1 and Jak3 kinases; these in turn activate Stat6, promoting its translocation into the

nucleus to initiate the transcription of IL-4 target genes [174, 231-237]. In addition, IL-4R recruits and activates IRS molecules [244, 245]. Phosphorylated IRS-1/2 interacts with the p85 regulatory subunit of PI3K and the adaptor molecule Grb2, which leads to the activation of the PI3K—Akt and Ras—MAPK signaling pathways, respectively.

The role of IL-4 in cancer has long been investigated. Studies have suggested contradictory findings that IL-4 could either enhance or inhibit cancer cell proliferation *in vitro* depending on the cancer cell type [279-285]. Being a survival factor, IL-4 has been shown to protect cells from apoptosis in prostate, breast, thyroid, and bladder tumor cell lines [286, 287]. Several studies have shown that malignant tumor cells genetically engineered to produce IL-4 displayed potent anti-tumor effects *in vivo*, suggesting the potential use of IL-4 secreting tumor cells as tumor vaccines for treating patients with advanced cancers [291-293]. However, almost no positive responses have occurred in clinical trials of recombinant human IL-4 in patients with renal cell carcinoma, chronic lymphocytic leukemia, and non-Hodgkin's lymphoma [295-297].

In order to explore the role of IL-4 in breast cancer tumorigenesis and metastasis, we engineering AC2M2 mouse carcinoma cells to express either empty vector control or IL-4. Using an orthotopic engraftment model, we found mice engrafted with IL4-AC2M2 cells grew tumors at a significantly reduced rate as

compared to control mice engrafted with EV-AC2M2 cells. Most strikingly, mice bearing IL4-AC2M2 tumors had no lung metastasis while EV-AC2M2 tumors consistently produced extensive lung metastasis. Reduced primary tumor growth and complete abolishment of metastasis in mice engrafted with IL4-AC2M2 cells correlated with increased numbers of tumor associated macrophages and macrophage phagocytosis of tumor cells. These observations suggest that tumor-derived IL-4 expression could enhance the efficacy of oncolytic viruses or tumor vaccine strategies in the treatment of breast cancer.

4.3 Materials and methods

4.3.1 Cell lines

AC2M2, a highly metastatic basal-like murine mammary carcinoma cell line [102] and HEK-293T cells were routinely cultured in DMEM (Invitrogen) containing 10% FBS (Sigma), 2mM L-glutamine, and 2mM antibiotic-antimycotics (AA; Invitrogen) in a 5% CO_2 humidified incubator at 37℃. Retroviruses or lentiviruses were produced by co-transfection of HEK-293T cells with retroviral packaging plasmid (ϕ-NX-ECOpac for retroviruses and pCMV-ΔR8.91 and pMD.2G for lentiviruses) along with the proviral pMSCVpuro retroviral plasmid (Clontech) or the pWPI lentiviral plasmid (kindly provided by Didier Trono). AC2M2 cells were transduced with lentiviruses expressing green fluorescence protein (GFP) and a high

GFP expressing subpopulation was selected by cell sorting. GFP-expressing AC2M2 cells were transduced with pMSCVpuro retroviruses encoding recombinant murine IL-4 (IL4) or the empty vector control (EV).

BMA3.1A7 (BMA) cells, a macrophage cell line derived from C57BL/6 mice [334], were grown in complete Roswell Park Memorial Institute (RPMI) culture medium containing 5% FBS, 2mM L-glutamine, and 2mM AA.

4.3.2 ELISA

The Mouse IL-4 ELISA Ready-SET-Go! ® kit (eBioscience) was used according to the manufacture's recommended protocol. Samples included culture medium collected from HEK-293T cells transfected with retroviral packaging plasmids and EV- or IL4-proviral pMSCV plasmids or non-transfected cells, as well as parental, EV- or IL4-retrovirus transduced AC2M2 cells. 10×, 100×, and 1000× fold dilutions were assayed in triplicate.

4.3.3 Cell proliferation assay

Four $\times 10^4$ EV- or IL4-AC2M2 cells were plated in triplicate on 6-well plates. At 4 hours post plating, and at 24 hour intervals thereafter for 5 days, cells were collected with trypsin/EDTA, and counted using a Z1 Coulter Particle Counter

(Beckman).

4.3.4 Dose-response stimulation experiment

To study paracrine effects of tumor cell-derived IL-4 on macrophages, conditioned media collected from EV-AC2M2 or IL4-AC2M2 cell cultures were added to 50% confluent BMA cell monolayers in a gradient of 5, 20, 50 or 100% of total culture medium. BMA cells were treated with 2.5, 5 or 10μg/mL recombinant mouse IL-4 (rIL-4) as positive controls, or media alone as a negative control. Cell lysates were prepared at 24 hours and used for immunoblotting analysis.

4.3.5 Immunoblotting analysis

Lysates from control mammary glands or tumor-bearing glands were prepared in RIPA lysis buffer (10mM Tris pH 7.2, 158mM NaCl, 1mM EDTA, 0.1% SDS, 1% sodium deoxycholate, 1% Triton 100 with 10μg/mL aprotinin, 10μg/mL leupeptin, 100μM sodium orthovanadate, 100μM phenylmethylsulfonyl fluoride) using a Ultra-Turrax T25 homogenizer (Terochem Scientific). For cell cultures, cells were washed with ice-cold PBS containing 100μM vanadate, and then lysed with RIPA lysis buffer for 20min. The remaining procedures have been described in detail previously [158, 302]. Briefly, lysates were centrifuged at 13,000 $\times g$ for 15 min at 4 ℃ to obtain the soluble fractions. After protein quantification, samples were diluted with

SDS sample buffer and heated for 5 min at 95℃. Proteins were then resolved by SDS-PAGE and transferred to membranes using a semi-dry transfer apparatus (Bio-Rad). Membranes were blocked with either 5% skimmed milk or 5% BSA for 1 hr, and incubated overnight with primary antibody at 4℃. After washing in TBST, membranes were incubated with the appropriate secondary antibody for 1 hr at room temperature, and proteins were detected by using enhanced chemiluminescence reagents (NEN Life Science Products). Antibodies used in immunoblotting included anti-arginase 1 (BD Bioscience), anti-Stat6 (Upstate), anti-tubulin (Sigma), anti-phospho-Stat6, anti-phospho-Jak1, anti-Jak1 and anti-phospho-Jak3, which were all purchased from Cell Signaling.

4.3.6 Mice

Mice used in this study included nude (NCr-*Foxn1*$^{nu/nu}$; Taconic), CBA/CaJ (Jackson Labs) and BALB/c Rag2$^{-/-}$; IL2Rγc$^{-/-}$ double-knockout (kindly provided by Dr. M. Ito, Central Institute for Experimental Animals, Kawasaki, Japan). Mice were housed in the Queen's University Animal Care Facility and procedures were carried out according to the guidelines of the Canadian Council on Animal Care, with the approval of the institutional animal care committee.

4.3.7 Orthotopic mouse engraftment model

After subcutaneous injection of meloxicam (2mg/kg), female age-matched mice were anesthetized by isoflurane inhalation and injected with 7,500 GFP expressing EV- or IL4-AC2M2 cells into the fourth inguinal mammary gland. In nude mice, tumors were allowed to grow to 16 days, when tumor size was assessed by caliper measurements and recovery tumor resection surgery was performed. Mice were kept alive for additional 12 days post tumor resection. On day 28, mice were euthanized, lungs were dissected and GFP expressing metastatic nodules were imaged as described previously [302]. In CBA and $Rag2^{-/-}$; $IL2R\gamma c^{-/-}$ mice, primary tumor growth was monitored over a period of 36 days or 19 days, respectively. Primary tumors were removed by recovery surgery after the last tumor measurement and mice were kept alive for 12 days post tumor resection prior to assessment of lung metastasis as described above.

For some $Rag2^{-/-}$; $IL2R\gamma c^{-/-}$ engraftment experiments, primary tumors were resected at the same size (tumor volume = $500mm^3$), on day 14 post-engraftment of EV-AC2M2 cells or day 19 post-engraftment of IL4-AC2M2 cells. After tumor resection surgery, mice were kept alive for the same amount of time (i.e. 12 days) before lung metastasis was assessed. Four fresh tumor samples from each cohort were processed immediately for flow cytometry analysis. The remaining three tumors from each cohort were bisected and one half was snap frozen and saved for immunoblotting

analysis, while the other half was fixed in 4% paraformaldehyde, paraffin embedded and sectioned for histopathological and immunohistochemical staining.

4.3.8 Peritoneal lavage

After mice were euthanized by deep isoflurane inhalation and cervical dislocation, 5mL of prewarmed lavage media [RPMI1640 (Invitrogen), 10mM HEPES, 5mM EDTA, 10U/mL heparin, 1% AA and 50μM α-monothioglycerol] were injected into the peritoneum, followed by gentle message of the abdomen and collection of the lavage media. Cells were isolated by centrifugation and resuspended in 5mL of erythrocyte lysis buffer (154mM NH_4Cl, 10mM $KHCO_3$, 100μM EDTA) for 5 min on ice to lyse red blood cells. The remaining cells were then resuspended in peritoneal macrophage medium [RPMI1640 (Invitrogen), 5% FBS, 1mM HEPES, 1% AA, 2mM glutamine and 50μM α-monothioglycerol], plated and incubated in a 5% CO_2 humidified incubator at 37℃. After 2 hours, non-adherent cells were washed off with PBS, and adherent cells (i.e. peritoneal macrophages) were used for subsequent experiments.

4.3.9 Immunofluorescent microscopy

Peritoneal macrophages were labeled with CellTracker^{TM} Orange CMRA according to manufacture protocol (Invitrogen), and then trypsinized and seeded onto

a 6-well plate containing gelatin-coated coverslips. After 24 hours of co-cultivation with either EV-AC2M2 or IL4-AC2M2 cells, coverslips were mounted onto glass slides with Mowiol (Calbiochem) and imaged using spinning-disc microscopy.

4.3.10 Overnight video time-lapse

CellTracker^{TM} Orange CMRA labeled peritoneal macrophages were co-cultured with GFP-expressing AC2M2 cells on 8 well μ-slide (Idbi) for 24 hours, and then images were taken every 5 minutes using spinning-disc microscopy for 18 hours. Movies were made by integrating all the images together using MetaMorph® microscopy automation & Image analysis software. Further quantitative analysis were done using ImagePro software.

4.3.11 Flow cytometry analysis

Control EV- and IL4-AC2M2 tumor-bearing mammary glands were harvested from Rag2$^{-/-}$; IL2Rγc$^{-/-}$ mice when tumors reached the same size as described above. These glands were digested in tissue digestion buffer and single cell suspensions were prepared as described in detail previously [302]. Samples were stained with 0.1μg/mL PE-conjugated rat anti-mouse F4/80 antibody (Caltag) for macrophages, washed with ice-cold 1% BSA/PBS, and analyzed by flow cytometry.

4.3.12 Immunohistochemical staining

Five μm sections of formalin fixed paraffin embedded control EV- and IL4-AC2M2 tumor-bearing mammary glands were stained with arginase 1 (1:5000 dilution with extended staining protocol #125; Sigma) for macrophages by automated Ventana staining system Discovery XT, and stainings were scanned with Aperio scanner. Images were taken and further quantitations were done using Aperio ImageScope.

4.3.13 Statistics

All statistical analysis was done by using GraphPad Prism software. All error bars represent standard error of the mean. P values were calculated by Student's *t* test analysis. Data sets with $P \leq 0.05$ were considered significant.

4.4 Results

4.4.1 Tumor cell-derived IL-4 has biological effects on macrophages *in vitro*

GFP-expressing AC2M2 mouse breast carcinoma cells were transduced with empty vector control (EV-) or mouse IL-4 expressing (IL4-) retroviruses. To confirm ectopic IL-4 expression, conditioned medium from parental, EV-, and IL4-AC2M2 cell cultures were analyzed for IL-4 by ELISA. IL-4 concentrations of 3.21 ng/mL

were measured in IL4-AC2M2 cell culture medium, while no detectable levels of IL-4 were apparent in parental and EV-AC2M2 culture medium.

IL-4 is a Th2 type cytokine reported to be capable of inducing an alternative pathway of macrophages activation and polarization to an M2 or wound healing phenotype [210, 335, 336]. We therefore investigated whether IL-4 secreted by IL4-AC2M2 cells had any biological effects on the polarization of macrophages. BMA macrophage cells were cultured with increasing doses of conditioned medium from either EV-AC2M2 or IL4-AC2M2 cells for 24 hours. For a positive control, BMA cells were stimulated with recombinant mouse IL-4 (rIL-4) at concentrations of 2.5, 5 or 10 ng/mL for the same length of time. Non-stimulated BMA cells were used as negative control. Immunoblotting analysis showed that BMA cells treated with either recombinant IL-4 or IL-4 conditioned medium expressed arginase 1 (Arg1), a marker for M2 macrophage polarization (Figure 4.1). As low as 2.5ng/ml of recombinant IL-4 was able to stimulate BMA cells to express Arg 1, whereas IL-4 conditioned medium showed a dose response effect of increasing Arg 1 expression levels with increasing doses of IL-4 conditioned medium. However, Arg1 expression was not detectable in either non-stimulated BMA cells or BMA cells cultured with conditioned medium from EV-AC2M2 cells. In addition, IL-4 conditioned medium was able to induce the same levels of Stat6 and Jak3 activation as recombinant IL-4. These observations confirmed that recombinant IL-4 produced by IL4-AC2M2 cells had biological effects *in vitro*, including polarizing macrophages to a M2 phenotype as well as activating the

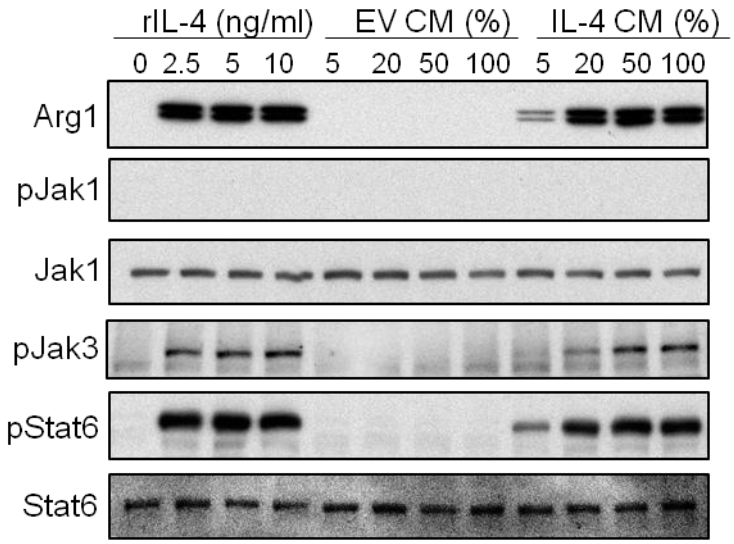

Figure 4.1 M2 macrophage activation and Jak3-Stat6 activation induced by tumor cell-derived IL-4. To test whether recombinant IL-4 ectopically expressed from AC2M2 had any biological activity, conditioned medium collected from EV-AC2M2 (EV CM) or IL4-AC2M2 (IL-4 CM) cells was added to 50% confluent BMA cell cultures at increasing CM concentrations of 5%, 20%, 50% or 100%, and cultured for 24 hours. BMA cells were treated with 2.5, 5 or 10ng/ml recombinant mouse IL-4 (rIL-4) for positive controls, whereas untreated BMA cells were used as a negative control. Lysates were analyzed by immunoblotting for macrophage polarization using anti-arginase 1 (Arg1) antibody, and Jak/Stat activation using anti-phospho-Jak1 (pJak1), anti-phospho-Jak3 (pJak3) and anti-phospho-Stat6 (pStat6) antibodies. Arg1 expression as well as Jak3 and Stat6 activation were detected in BMA cells cultured with IL-4 conditioned medium in a dose-dependent manner. In contrast, neither EV-AC2M2 CM treated nor untreated BMA cells showed any detectable Arg1 expression or Jak1/Jak3/Stat6 activation. However, recombinant IL-4 was unable to activate Jak1 activity although BMA cells have stable Jak1 expression.

JAK-STAT signaling pathway.

Before exploring the *in vivo* effect of cancer cell derived IL-4 expression on tumor growth in animal models, we first wanted to see whether ectopic IL-4 expression would have an autocrine effect on tumor cell proliferation *in vitro*. We found that EV-AC2M2 and IL4-AC2M2 cells grew at indistinguishable rates (P= 0.3654; Figure 4.2).

4.4.2 IL-4-expressing tumor cells do not develop tumors in immune competent mice

Most tumor-associated macrophages (TAMs) are considered to be M2 macrophages which have pro-tumoral functions that facilitate tissue remodeling through secretion of matrix-metalloproteases and growth factors that promote angiogenesis and tumor cell motility, as well as suppressing adaptive immunity [207, 323, 337]. Since IL-4 can induce M2 macrophage activation *in vitro*, we expected to see enhanced primary tumor growth and lung metastasis in mice that were engrafted with IL4-AC2M2 tumor cells as compared to those engrafted with control EV-AC2M2 tumor cells.

GFP-expressing EV-AC2M2 or IL4-AC2M2 mouse breast carcinoma cells were engrafted into the mammary glands of immune competent syngeneic CBA mice, and tumor growth was monitored for a period of 36 days. Primary tumors were then

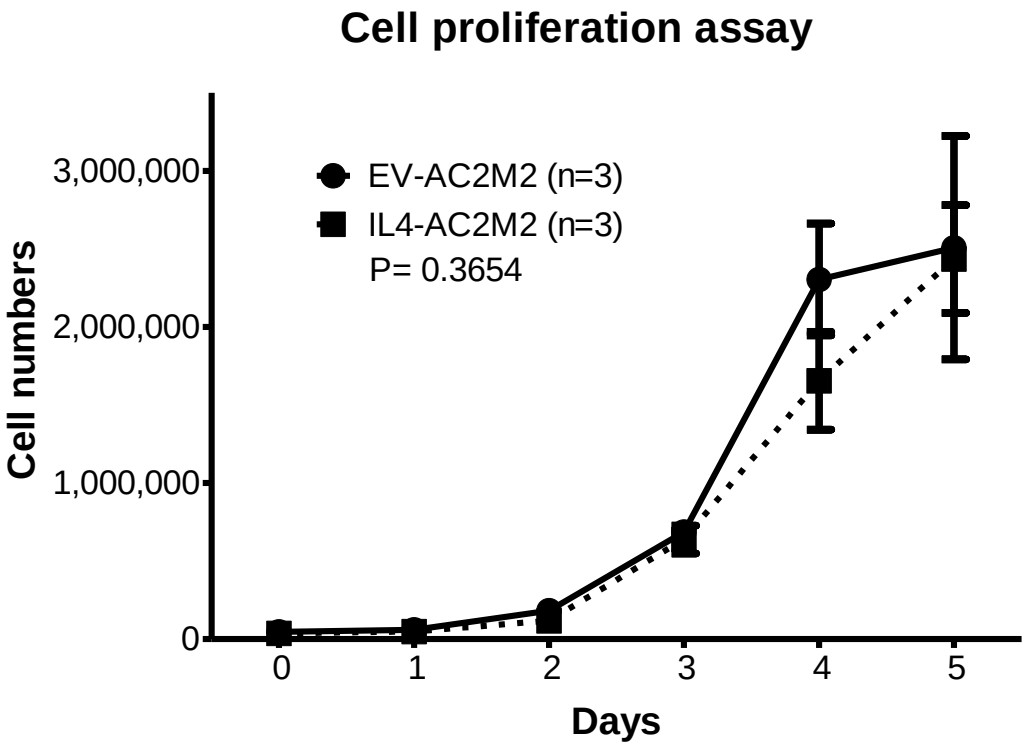

Figure 4.2 Ectopic IL-4 expression does not affect tumor cell proliferation *in vitro*. On day 0, 40,000 EV-AC2M2 or IL4-AC2M2 cells were seeded in triplicate (n=3) on 6-well plates. Four hours later or at the indicated days post plating, cells were trypsinized, and cell numbers were counted using Z1 Coulter Particle Counter. No significant difference was observed in growth rates *in vitro* between EV-AC2M2 and IL4-AC2M2 cells (P= 0.3654).

removed to promote metastatic growth and lung metastasis which was examined 12 days later. In CBA mice, IL4-AC2M2 cells did not grow at all during the entire period of tumor assessment, whereas tumors did develop in mice injected with EV-AC2M2 cells (Figure 4.3). However, these tumors grew to approximately 100mm^3 on 13 days after initial engraftment, and they maintained the same size until day 17 when they started to regress. By day 36, tumors that arose from EV-AC2M2 cells had completed disappeared in CBA mice. Lung metastasis was observed in one of six mice in the control group versus none in the IL-4 group (Figure 4.4).

4.4.3 IL-4 suppresses tumor growth and eliminates lung metastasis in nude mice

The tumor growth behavior observed in immune competent CBA mice suggested some sort of immune responses happening in these mice. We next repeated the engraftment study in athymic nude mice that lack T cells, and tested whether IL-4 would influence tumorigenesis and metastasis in this immune compromised model.

Similarly, GFP-expressing EV-AC2M2 or IL4-AC2M2 cells were orthotopically engrafted into the mammary glands of nude mice. Tumor volumes were measured on day 16 post-engraftment and lung metastasis was assessed as described above. Tumors grew to a greater extent in nude mice compared with in CBA mice, and those which arose from IL4-AC2M2 tumor cells were significantly smaller than those from control EV-AC2M2 cells (P= 0.0239; Figure 4.5). Lung metastatic nodules were

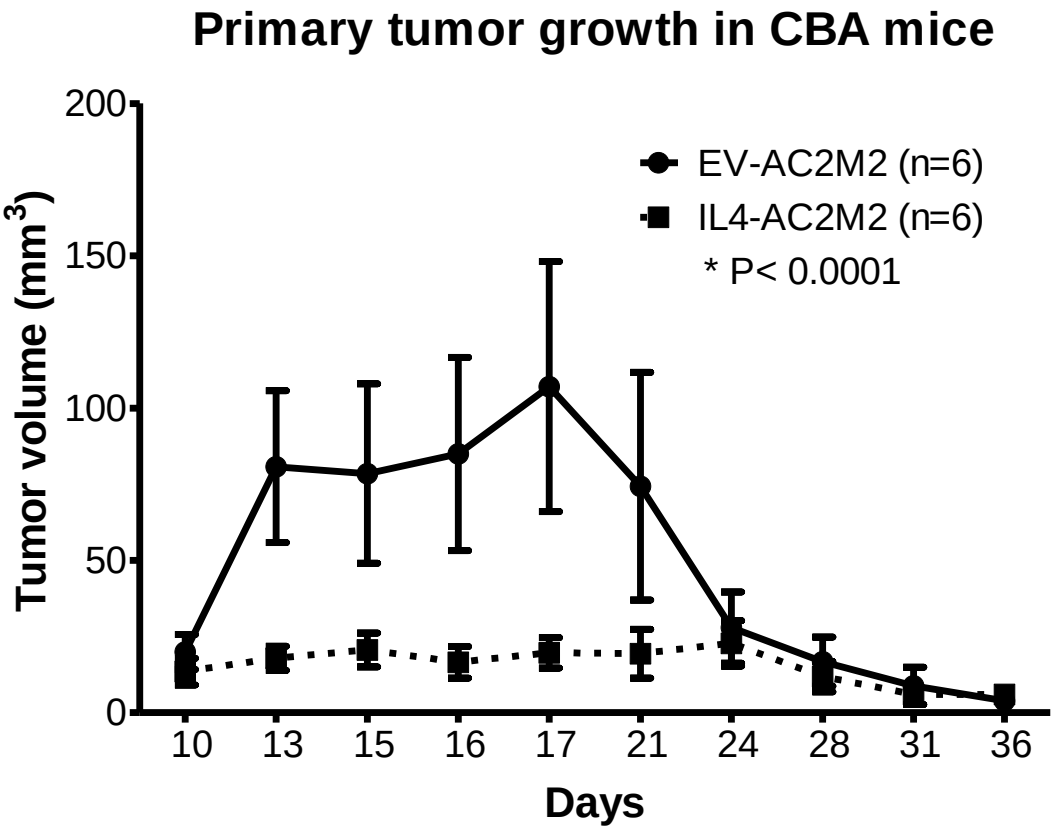

Figure 4.3 IL-4 expressing tumor cells did not develop tumors in CBA mice. 7,500 EV-AC2M2 or IL4-AC2M2 cells were engrafted into the fourth mammary glands of immune competent CBA mice and tumorigenesis was assessed over a period of 36 days. Control tumors grew to approximately 100mm^3 on day 13 post-engraftment. These tumors maintained the same size until day 17 when they started to regress. By day 36, control tumors had almost completely disappeared. In contrast, IL-4 expressing tumors did not grow at all over the entire period of tumor assessment. (P< 0.0001; n=6 for each group)

A

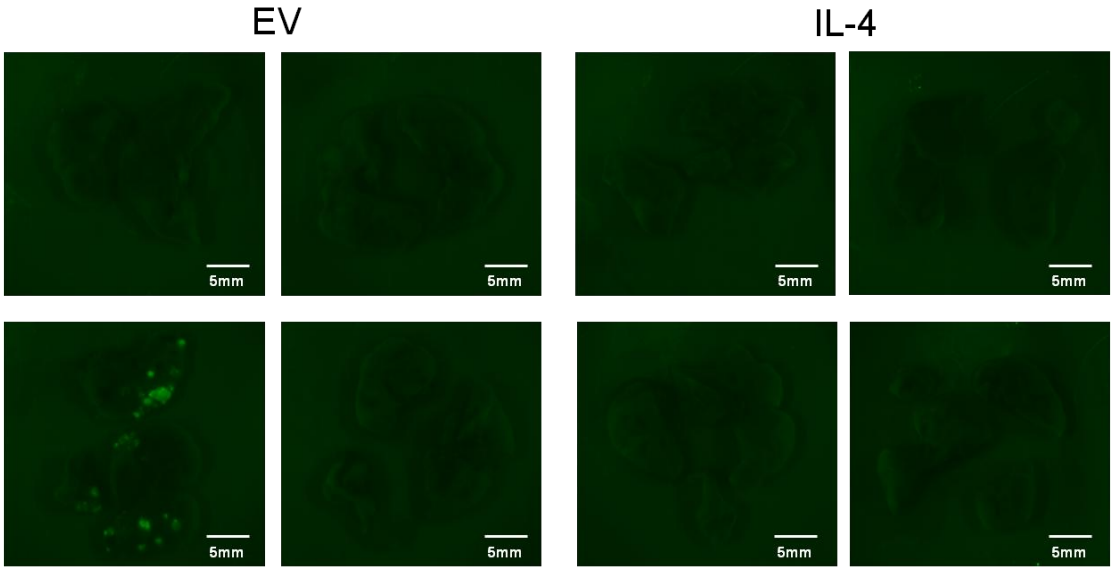
EV
IL-4
5mm
5mm
5mm
5mm
5mm
5mm
5mm
5mm

B

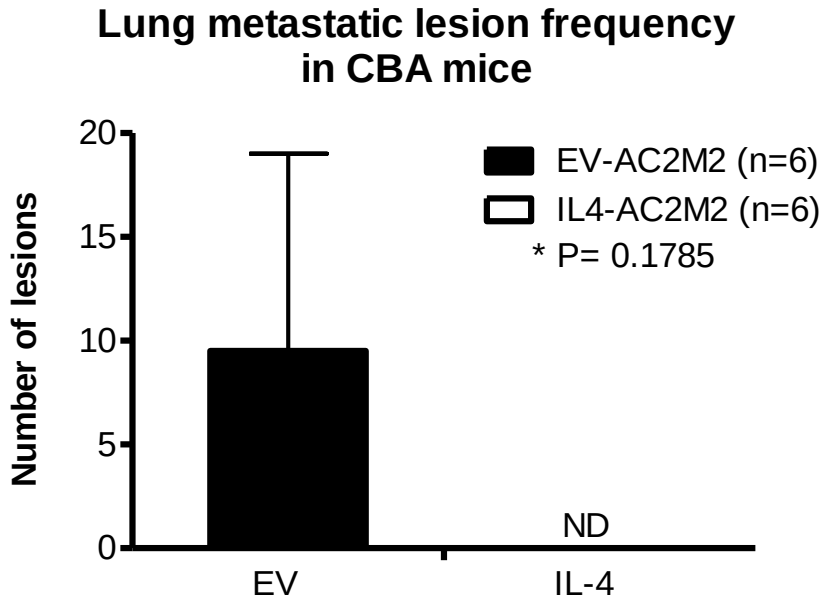
Lung metastatic lesion frequency in CBA mice
Number of lesions
20
15
10
5
0
EV-AC2M2 (n=6)
IL4-AC2M2 (n=6)
* P= 0.1785
ND
EV
IL-4

Figure 4.4 Reduced lung metastasis in CBA mice bearing IL-4 expressing tumors. 7,500 GFP-expressing EV-AC2M2 (EV) and IL4-AC2M2 (IL-4) cells were engrafted into the fourth mammary glands of immune competent CBA mice and allowed to grow for 36 days. Tumors were then resected and mice were kept alive for additional 12 days. Lungs were dissected to assess metastatic lesions by biophotonic imaging. 17% (1 of 6) of the lungs harvested from control tumor-bearing mice (EV-AC2M2) harbored detectable metastasis while none (0 of 6) of the lungs from IL-4 expressing tumor-bearing mice (IL4-AC2M2) displayed lung metastasis (P= 0.1785; n=6 for each group). Panel A are photographs that indicate representative images of lungs from four different mice of each group. (ND stands for not detectable)

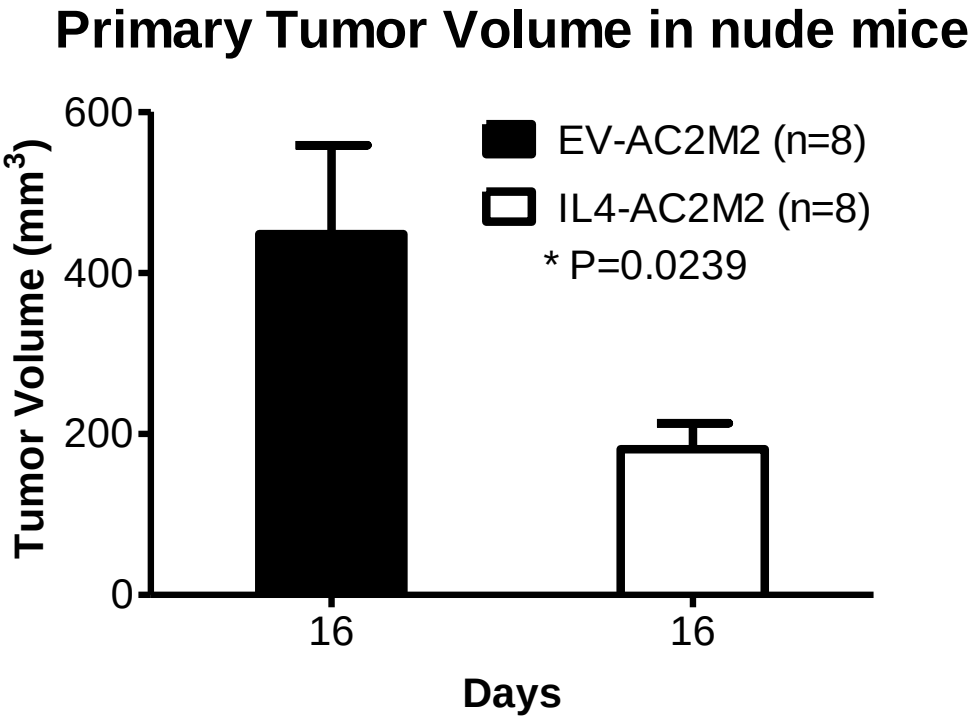

Figure 4.5 Tumor growth at the orthotopic site in nude mice was reduced when IL-4 was present. 7,500 EV-AC2M2 or IL4-AC2M2 cells were engrafted into the fourth mammary glands of nude mice and tumor volume was measured with calipers on day 16 post-engraftment. Tumors were significantly smaller in mice engrafted with IL-4 expressing AC2M2 tumor cells (IL4-AC2M2) compared to those with control tumor cells (EV-AC2M2) (P= 0.0239; n=8 for both groups).

detected in 3 of 8 mice engrafted with EV-AC2M2 cells (P= 0.0238; Figure 4.6). In contrast, no lung metastasis was observed in 8 mice that were engrafted with IL4-AC2M2 cells.

4.4.4 Tumor derived IL-4 significantly inhibits primary tumor growth and completely abolishes lung metastasis in Rag2$^{-/-}$; IL2Rγc$^{-/-}$ mice

In nude mice, we observed better tumor growth relative to CBA mice, and the higher frequency of lung metastasis in nude mice underscored the difference between IL4-AC2M2 and EV-AC2M2 behaviour. We next asked how tumors behave in a more immune compromised strain – Rag2$^{-/-}$; IL2Rγc$^{-/-}$ double-knockout mice that are deficient in T cells, B cells and natural killer (NK) cells.

GFP-expressing EV-AC2M2 or IL4-AC2M2 cells were engrafted into the mammary glands of age-matched, female Rag2$^{-/-}$; IL2Rγc$^{-/-}$ double-knockout mice. Tumor growth at the orthotopic site was monitored for a period of 19 days. In general, tumors grew much faster in Rag2$^{-/-}$; IL2Rγc$^{-/-}$ double-knockout mice as compared to those in CBA or nude mice described earlier. Tumor growth at the orthotopic site was significantly slower with IL4-AC2M2 relative to EV-AC2M2 cells (P< 0.001; Figure 4.7). On day 19 post-engraftment, tumors that arose from EV-AC2M2 cells reached approximately 1300 mm^3 versus 400 mm^3 from IL4-AC2M2 cells. Primary tumors were resected on day 19 and mice were kept alive for additional 12 days. Mice were

A

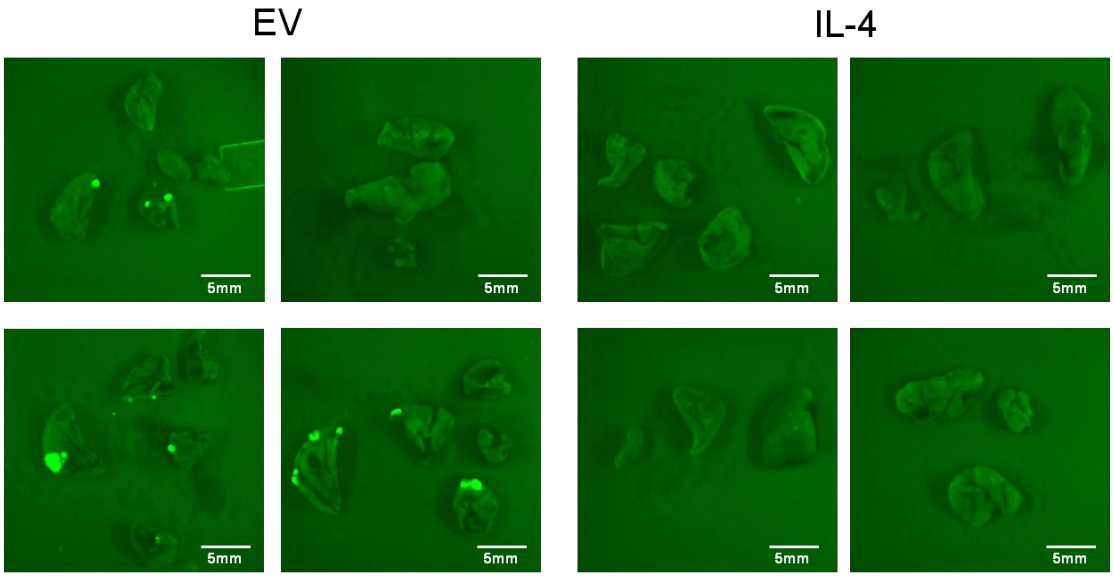
EV
IL-4
5mm
5mm
5mm
5mm
5mm
5mm
5mm
5mm

B

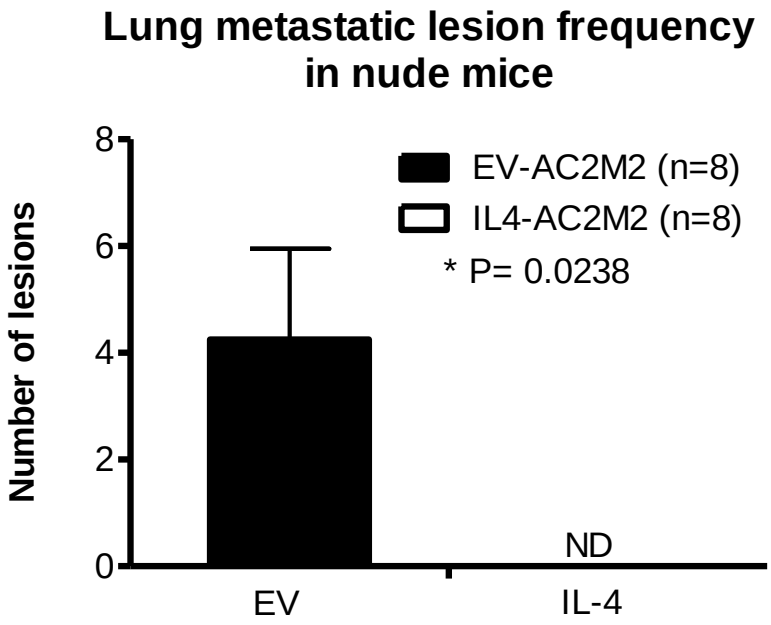
Lung metastatic lesion frequency in nude mice
Number of lesions
8
6
4
2
0
EV-AC2M2 (n=8)
IL4-AC2M2 (n=8)
* P= 0.0238
ND
EV
IL-4

Figure 4.6 Reduced lung metastasis in nude mice bearing IL-4 expressing tumors. 7,500 GFP-expressing EV-AC2M2 (EV) or IL4-AC2M2 (IL-4) cells were engrafted into the fourth mammary glands of wild type nude mice and allowed to grow for 16 days. Tumors were then removed to promote tumor growth at metastatic sites and lungs were removed for biophotonic imaging of metastatic lesions 12 days later. 38% (3 of 8) of the lungs harvested from control tumor-bearing mice (EV-AC2M2) harbored detectable metastasis while none (0 of 8) of the lungs from IL-4 expressing tumor-bearing mice (IL4-AC2M2) displayed lung metastasis (P= 0.0238; n=8 for each group). Panel A are photographs that indicate representative images of lungs from four different mice of each group. (ND stands for not detectable)

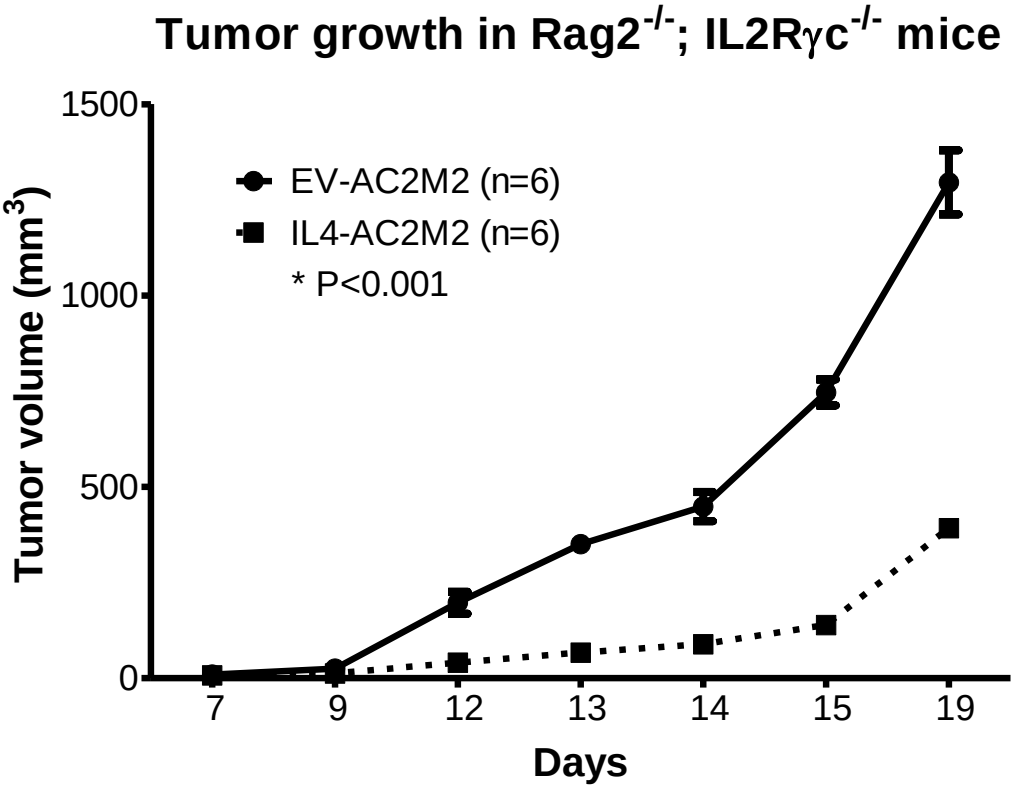

Figure 4.7 Orthotopic tumor growth rates were reduced in Rag2$^{-/-}$; IL2Rγc$^{-/-}$ mice bearing IL-4 expressing tumors. 7,500 EV-AC2M2 or IL4-AC2M2 cells were engrafted into the fourth mammary glands of Rag2$^{-/-}$; IL2Rγc$^{-/-}$ mice and tumorigenesis was assessed over a period of 19 days. Tumor growth rate of IL-4 expressing tumors (IL4-AC2M2) was significantly slower as compared to control tumors (EV-AC2M2) ($P < 0.001$; n=6 for each group).

then euthanized and lungs were dissected to examine for metastatic lesions using biophotonic imaging. Lungs from all mice that were injected with EV-AC2M2 cells contained multiple metastatic lesions. In contrast, no lung metastasis was observed in tumor-bearing mice engrafted with IL4-AC2M2 cells ($P < 0.0001$; Figure 4.8).

Finally, we tested whether the striking metastasis difference seen in $Rag2^{-/-}$; $IL2R\gamma c^{-/-}$ mice might be due to the significant differences in tumor size at the time of tumor resection surgery. To address this concern, we repeated the engraftment experiment with $Rag2^{-/-}$; $IL2R\gamma c^{-/-}$ mice. Instead of resecting tumors at equal times post engraftment, primary tumors were resected when they reached the same size (approximately 500 mm^3) in both groups. Five additional days were required for IL4-AC2M2 tumors to achieve this size. Both groups of mice were kept alive for the same length of time (12 days) after tumor resection surgery, and lung metastasis was assessed as described above. Again, lungs harvested from all mice injected with EV-AC2M2 cells were filled with metastatic nodules, whereas no lesions were observed in the lungs of the IL4-AC2M2 cohort ($P < 0.0001$; Figure 4.9). These observations argue that tumor size is not responsible for the difference in metastatic potential.

A

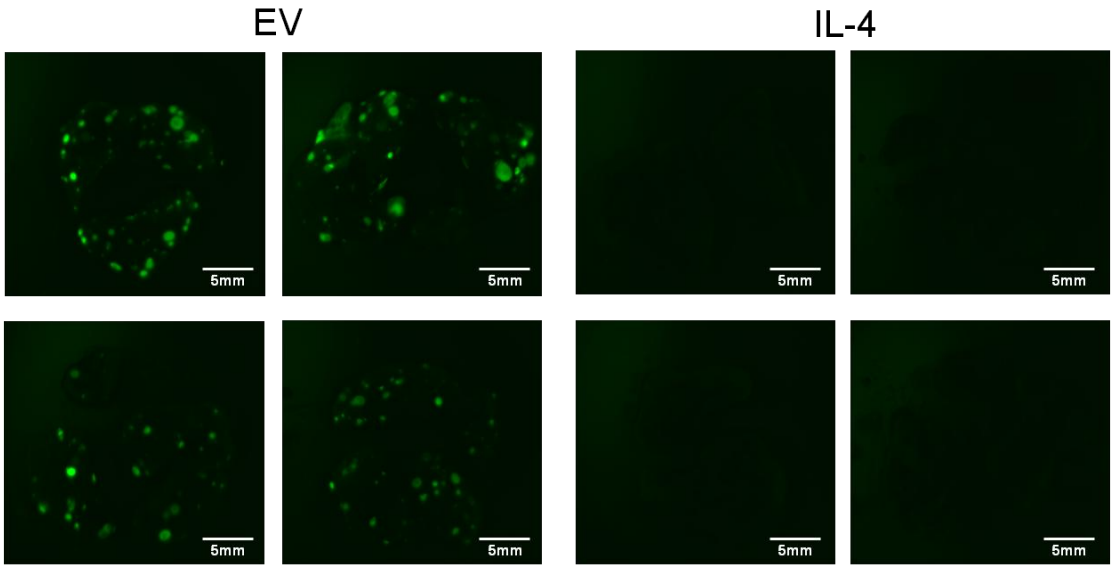
EV
IL-4
5mm
5mm
5mm
5mm
5mm
5mm
5mm
5mm

B

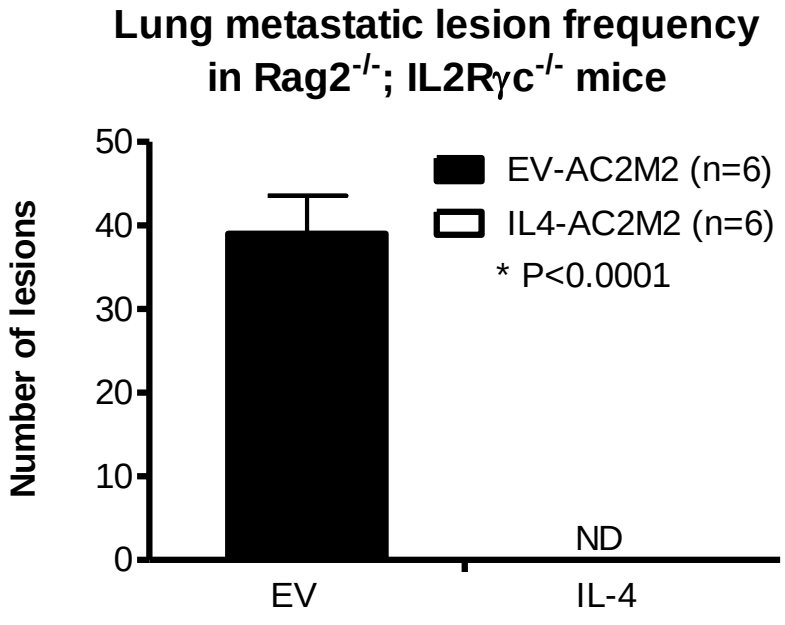
Lung metastatic lesion frequency
in Rag2-/-; IL2Rγc-/- mice
Number of lesions
50
40
30
20
10
0
EV-AC2M2 (n=6)
IL4-AC2M2 (n=6)
* P<0.0001
ND
EV
IL-4

Figure 4.8 Complete elimination of lung metastasis in Rag2$^{-/-}$; IL2Rγc$^{-/-}$ mice bearing IL-4 expressing tumors. 7,500 GFP-expressing EV-AC2M2 (EV) and IL4-AC2M2 (IL-4) cells were engrafted into the fourth mammary glands of Rag2$^{-/-}$; IL2Rγc$^{-/-}$ mice and allowed to grow for 19 days. Tumors were then removed to promote tumor growth at metastatic sites and lungs were removed for biophotonic imaging of metastatic lesions 12 days later. 100% (6 of 6) of the lungs harvested from control tumor-bearing mice (EV-AC2M2) harbored detectable metastasis while none (0 of 6) of the lungs from IL-4 expressing tumor-bearing mice (IL4-AC2M2) displayed lung metastasis ($P < 0.0001$; n=6 for each group). Panel A are photographs that indicate representative images of lungs from four different mice of each group. (ND stands for not detectable)

A

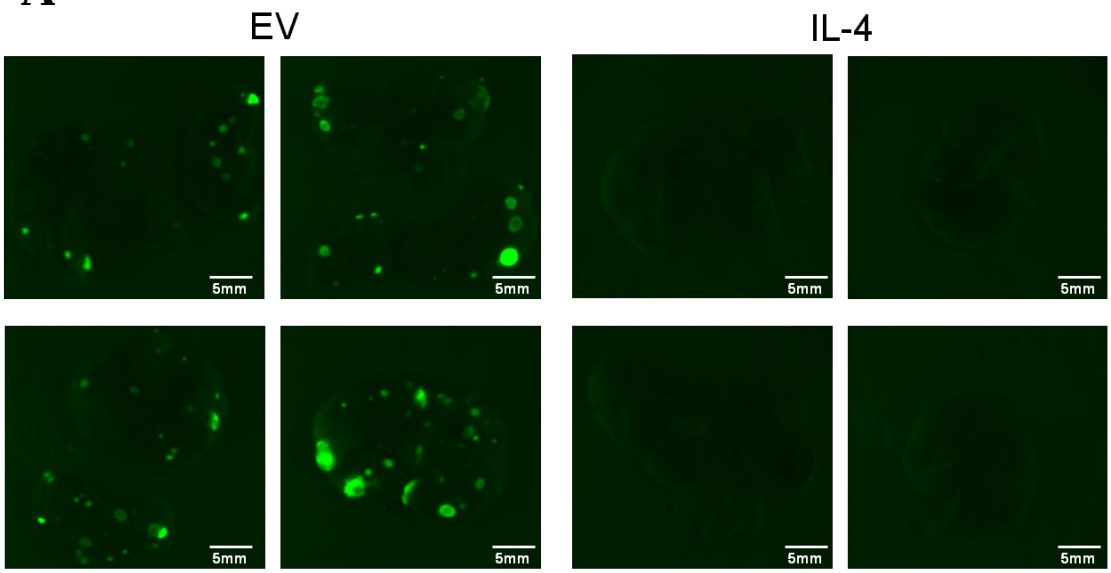
EV
IL-4
5mm
5mm
5mm
5mm
5mm
5mm
5mm
5mm

B

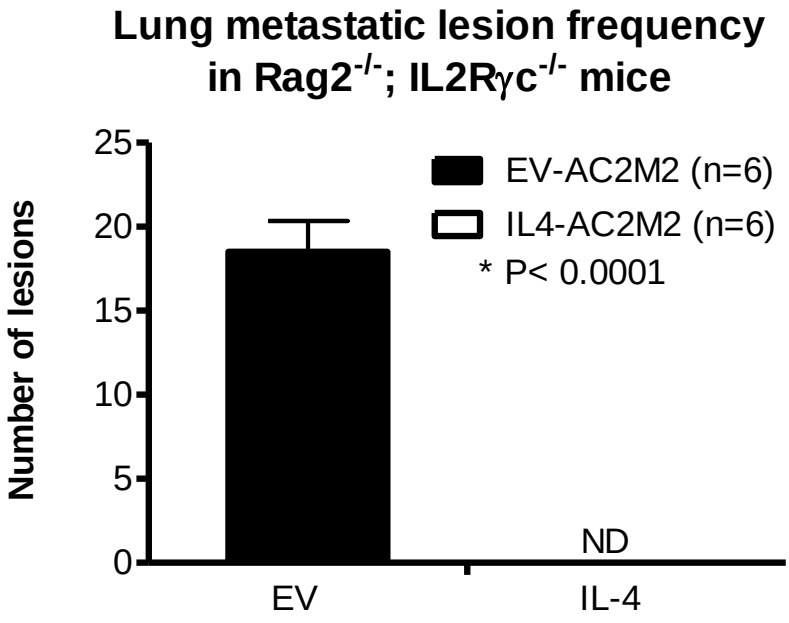
Lung metastatic lesion frequency
in Rag2-/-; IL2Rγc-/- mice
Number of lesions
25
20
15
10
5
0
EV-AC2M2 (n=6)
IL4-AC2M2 (n=6)
* P< 0.0001
ND
EV
IL-4

Figure 4.9 Complete elimination of lung metastasis in Rag2$^{-/-}$; IL2Rγc$^{-/-}$ mice bearing IL-4 expressing tumors when control and IL-4 expressing tumors were removed at the same size. 7,500 GFP-expressing EV-AC2M2 (EV) and IL4-AC2M2 (IL-4) cells were engrafted into the fourth mammary glands of Rag2$^{-/-}$; IL2Rγc$^{-/-}$ mice. Tumors were removed at the same size (approximately 500mm^3) from both groups. Mice were kept alive for 12 days after tumor resection surgery. Mice were then euthanized and lungs were dissected for biophotonic imaging of metastatic lesions. 100% (6 of 6) of the lungs harvested from control tumor-bearing mice (EV-AC2M2) harbored detectable metastasis while none (0 of 6) of the lungs from IL-4 expressing tumor-bearing mice (IL4-AC2M2) displayed lung metastasis ($P < 0.0001$; n=6 for each group). Panel A are photographs that indicate representative images of lungs from four different mice of each group. (ND stands for not detectable)

4.4.5 Increased numbers of tumor-associated macrophages and macrophage phagocytosis of tumor cells in IL4-expressing tumor stroma

We next explored how IL-4 affects the tumor microenvironment to slow tumor growth rate and to constrain tumors cells from developing metastases in distant organs. Since $Rag2^{-/-}$; $IL2R\gamma c^{-/-}$ mice lack T cells, B cells and NK cells in the tumor microenvironment, we focused on cells of the myeloid lineage for possible explanations. We therefore harvested mammary glands containing control or IL-4 expressing tumors and quantified macrophages using surface antigen labeling with F4/80 antibody and flow cytometry. We found a significant increase (approximately 20-fold) in the $F4/80^{+}$ tumor-associated macrophage content in IL-4 expressing tumor-bearing mammary glands ($P< 0.0001$; Figure 4.10 A). By taking advantage of GFP expression of tumor cells, we were also able to quantify the populations that were both GFP^{+} and $F4/80^{+}$, indicative of either tumor cells phagocytosed by macrophages or tumor cells interacting with macrophages. GFP^{+} tumor cells present in mammary glands containing control tumors seemed shifted to the PE channel and became $F4/80^{+}GFP^{+}$ double positive in the presence of IL-4, suggesting a greater degree of macrophage phagocytosis occurring in these IL-4 expressing tumor-containing mammary glands (Figure 4.10 B).

We also detected high levels of arginase 1 expression, as an indicator of presence of M2 polarized macrophages in IL-4 expressing tumor containing

A

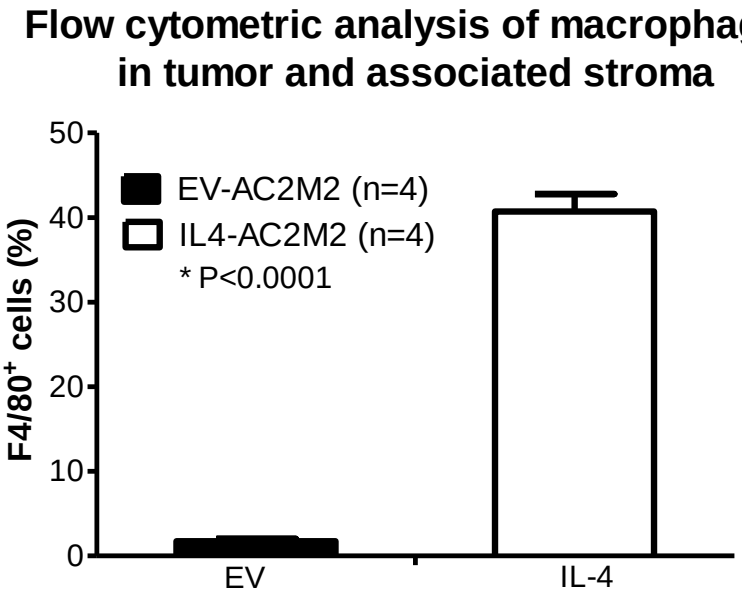
Flow cytometric analysis of macrophages in tumor and associated stroma
F4/80+ cells (%)
50
40
30
20
10
0
EV-AC2M2 (n=4)
IL4-AC2M2 (n=4)
* P<0.0001
EV
IL-4

B

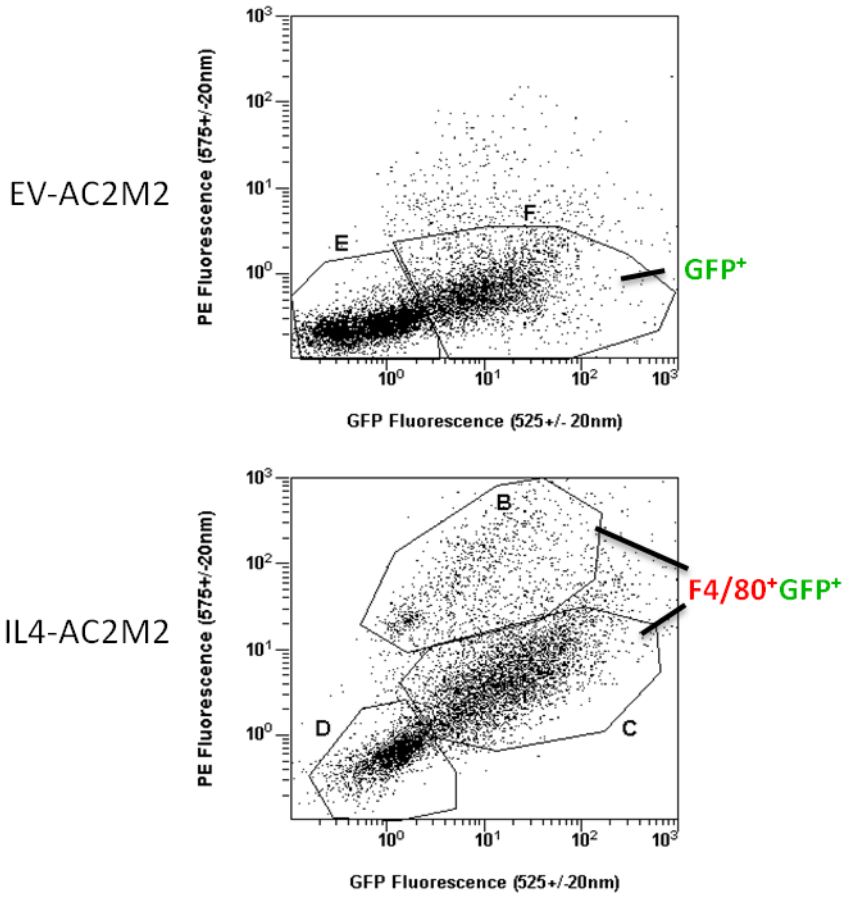
EV-AC2M2
PE Fluorescence (575+/-20nm)
GFP Fluorescence (525+/- 20nm)
E
F
GFP+
IL4-AC2M2
PE Fluorescence (575+/-20nm)
GFP Fluorescence (525+/-20nm)
B
C
D
F4/80+GFP+

Figure 4.10 Elevated macrophages and macrophage phagocytosis of tumor cells in IL-4 expressing tumor-bearing mammary glands. 7,500 GFP-expressing EV-AC2M2 or IL4-AC2M2 cells were engrafted into the fourth mammary glands of $Rag2^{-/-}$; $IL2R\gamma c^{-/-}$ mice and tumorigenesis was monitored. Control and IL-4 expressing tumor-bearing mammary glands were harvested on day 13 and 16 respectively when tumors reached the same size. Single cell suspensions were prepared and stained with PE-conjugated F4/80 antibody to identify macrophages and the relative percentages of stained cells were determined by flow cytometry. A) There were significantly more macrophages in IL-4 expressing tumors and associated stroma relative to control ($P< 0.001$; n=4 for both groups). B) In the scatter plots, GFP^- populations were labeled as population E and D in mammary gland samples containing EV-AC2M2 and IL4-AC2M2 tumors, respectively. GFP^+ tumor cells (population F) present in control tumor-bearing mammary glands were shifted upwards into the PE channel and become $F4/80^+$ GFP^+ double positive in the presence of IL-4, suggesting possible higher levels of macrophage phagocytosis of tumors cells or more macrophage and tumor cell interactions when IL-4 was present in the tumor microenvironment.

mammary glands, both by immunoblotting analysis (Figure 4.11) and by immunohistochemical staining (Figure 4.12). Arginase 1 was not detected by immunoblotting in mammary glands containing control tumors. Although we were able to observe some arginase 1 positive stained macrophages in control tumor sections by immunohistochemistry, their frequency was approximately 10-fold less compared to that in IL-4 expressing tumors.

4.4.6 More prominent macrophage phagocytosis of tumor cells in IL-4 expressing co-culture

IL-4 has been shown to induce macrophage fusion to form multinucleate giant cells which have more phagocytic capability [330-333]. After detecting more macrophages by various methods, we next investigated whether IL-4 secreted by IL4-AC2M2 would induce giant cell formation and provoke more prominent phagocytosis of tumor cells.

We therefore *in vitro* co-cultured orange cell tracker dye labeled peritoneal macrophages with either EV-AC2M2 or IL4-AC2M2 for 24 hours, and then imaged by spinning disc microscopy. We observed enlarged macrophages in the IL4-AC2M2 co-cultures as well as some yellow cells, indicating that GFP tumor cells may have been phagocytosed by enlarged macrophages (Figure 4.13). In an attempt to directly

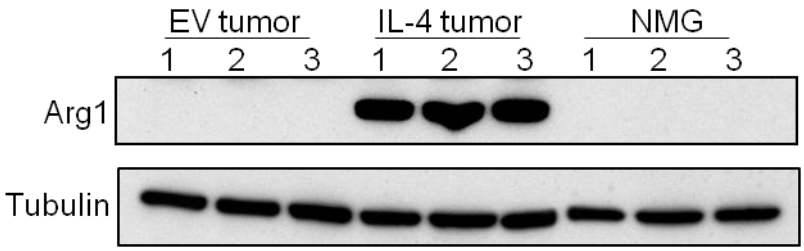

Figure 4.11 High levels of arginase 1 expression in mammary glands bearing IL-4 expressing tumors. 7,500 GFP-expressing EV-AC2M2 or IL4-AC2M2 cells were engrafted into the fourth mammary glands of $Rag2^{-/-}$; $IL2R\gamma c^{-/-}$ mice and tumorigenesis was monitored. Control (EV tumor) and IL-4 (IL-4 tumor) expressing tumor-bearing mammary glands were harvested on day 13 and 16 respectively when tumors reached the same size, and bisected for either immunoblotting analysis or immunohistochemical tissue staining. Lysates were made from 3 EV tumors, 3 IL-4 tumors and 3 normal mammary glands (NMG), and blotted with anti-arginase 1 (Arg1) antibody. High levels of Arg1 expression were detected in all three IL-4 expressing tumor-bearing mammary gland samples, whereas control tumor-containing mammary glands and normal mammary glands had no detectable Arg1 expression. Anti-tubulin blot was used as protein loading control.

A

EV

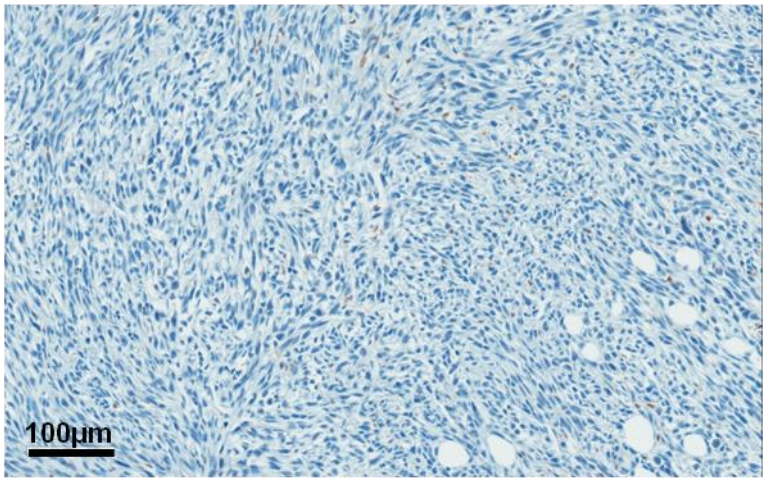

IL-4

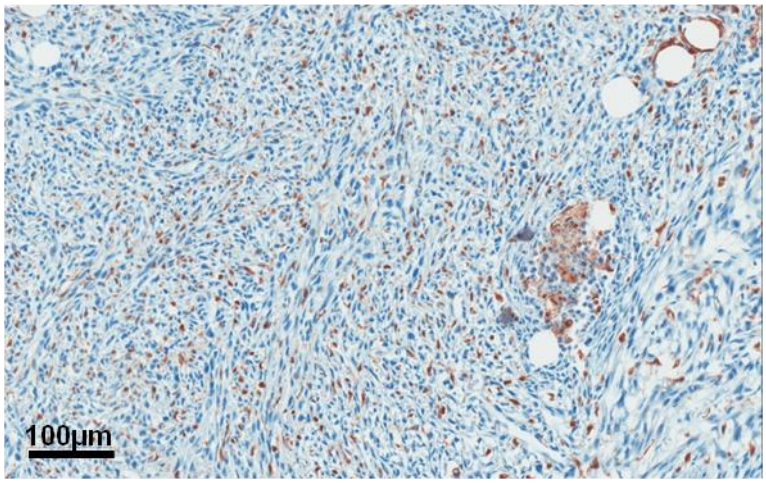

B

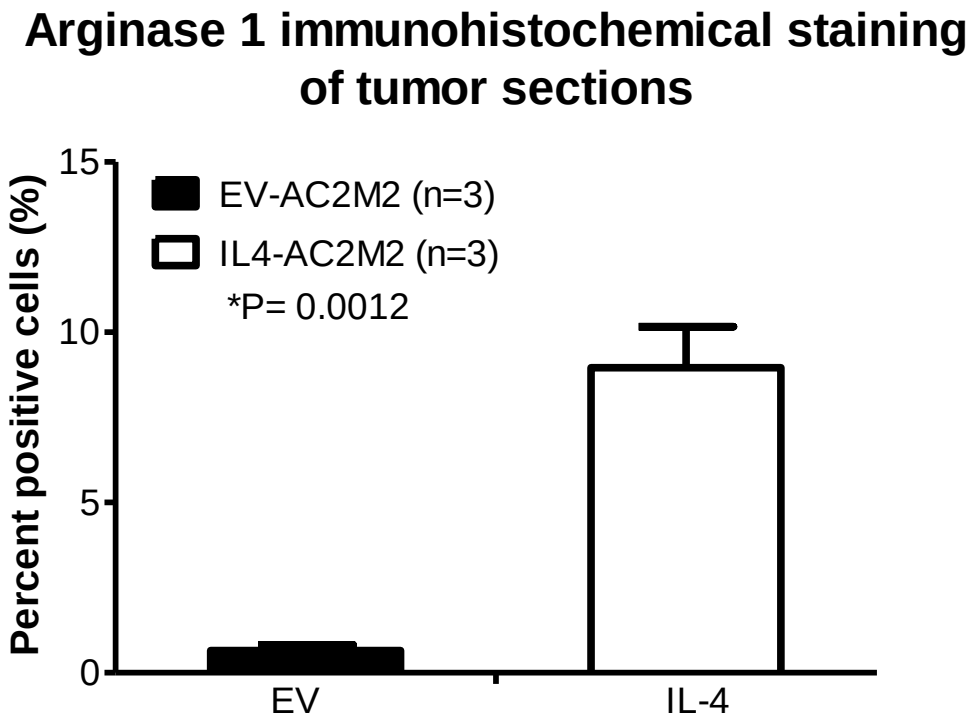

Figure 4.12 Increased numbers of arginase 1 positively stained macrophages in IL-4 expressing tumor sections. 7,500 GFP-expressing EV-AC2M2 or IL4-AC2M2 cells were engrafted into the fourth mammary glands of $Rag2^{-/-}$; $IL2R\gamma c^{-/-}$ mice and tumorigenesis was monitored. Control (EV-AC2M2) and IL-4 (IL4-AC2M2) expressing tumor-bearing mammary glands were harvested on day 13 and 16 respectively when tumors reached the same size, and bisected for either immunoblotting analysis or immunohistochemical tissue staining. Tumor tissues were fixed in 4% paraformaldehyde and paraffin embedded, and 5μm tissue sections were stained with arginase 1 for macrophages by Ventana staining system. A) Representative images were taken from both control and IL-4 expressing tumor sections. Brown positive staining cells were abundantly observed in IL-4 expressing tumor section, but rarely seen in control tumor section. B) Positive stainings were quantified using Aperio software. Arginase 1 positively stained macrophages were almost 10-fold more in IL-4 expressing tumors as compared to control tumors (P= 0.0012; n=3 for both groups).

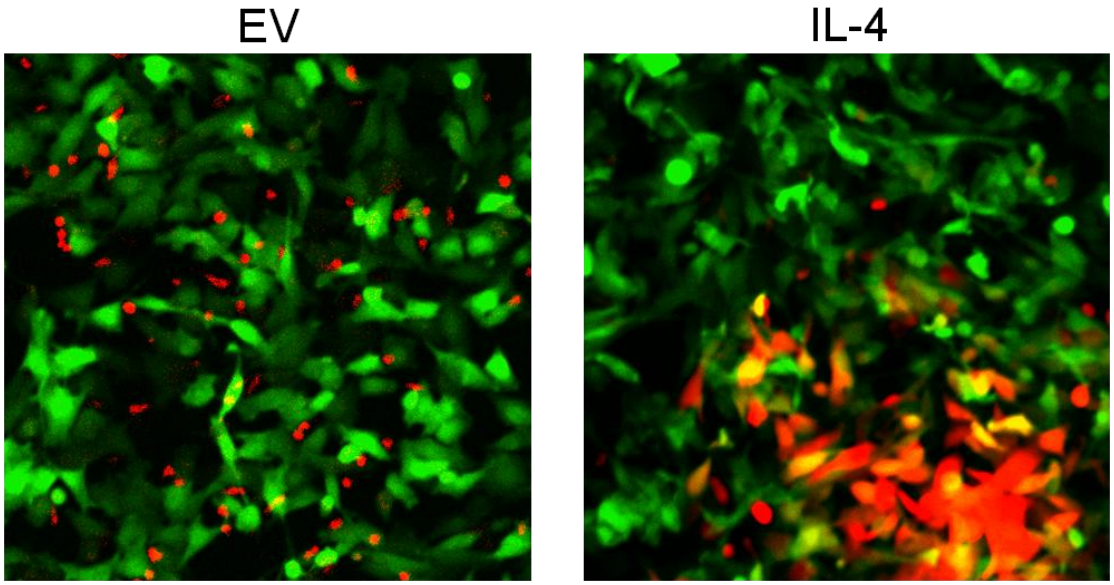

Figure 4.13 Enlarged macrophages and more macrophage phagocytosis of tumor cells in IL-4 expressing co-culture. Peritoneal macrophages were labeled with orange cell tracker dye (red), and then co-cultured with GFP-expressing EV-AC2M2 (EV) or IL4-AC2M2 (IL-4) tumor cells (green). Images were taken by spinning-disc microscopy after 24 hours of co-cultivation. Larger size macrophages as well as clusters of macrophages were observed in IL4-AC2M2 co-cultures. Yellow cells were also seen in IL4-AC2M2 co-cultures, indicative of macrophage-tumor cell fusion or phagocytosis events.

observe macrophage fusion and phagocytosis events in real time, we repeated these co-cultures and captured images for 18 hours by video time lapse microscopy. During the entire imaging period, we consistently observed more dynamic macrophage tumor cell interactions when macrophages were co-cultured with IL4-AC2M2 tumor cells as compared to EV-AC2M2 cells. Larger macrophages, possibly giant cells, were also seen in IL4-AC2M2 co-cultures but not in the EV-AC2M2 co-cultures. Statistical analysis showed that there are significantly more yellow cells (indicative of fused macrophage-tumor cells) relative to the number of macrophages throughout the entire 18 hours in the IL4-AC2M2 co-cultures ($P < 0.0001$; Figure 4.14).

4.5 Discussions

Previous reports have suggested that IL-4 could either promote or inhibit cancer cell proliferation *in vitro* by exerting effects through binding to IL-4R expressed on cancer cells [279-285]. We observed no difference in cell growth rates between AC2M2 breast carcinoma cells transduced with either empty vector control or IL-4. This observation led us to speculate that AC2M2 cells may not express IL-4R, or at least not to sufficient levels to promote autocrine effects with ectopic IL-4 expression. Rather than affecting tumor growth in an autocrine fashion, tumor-cell derived IL-4 may have effects on tumorigenesis and metastasis by modulating cells in the tumor niche in a paracrine manner. IL-4 has been reported to have broad functions

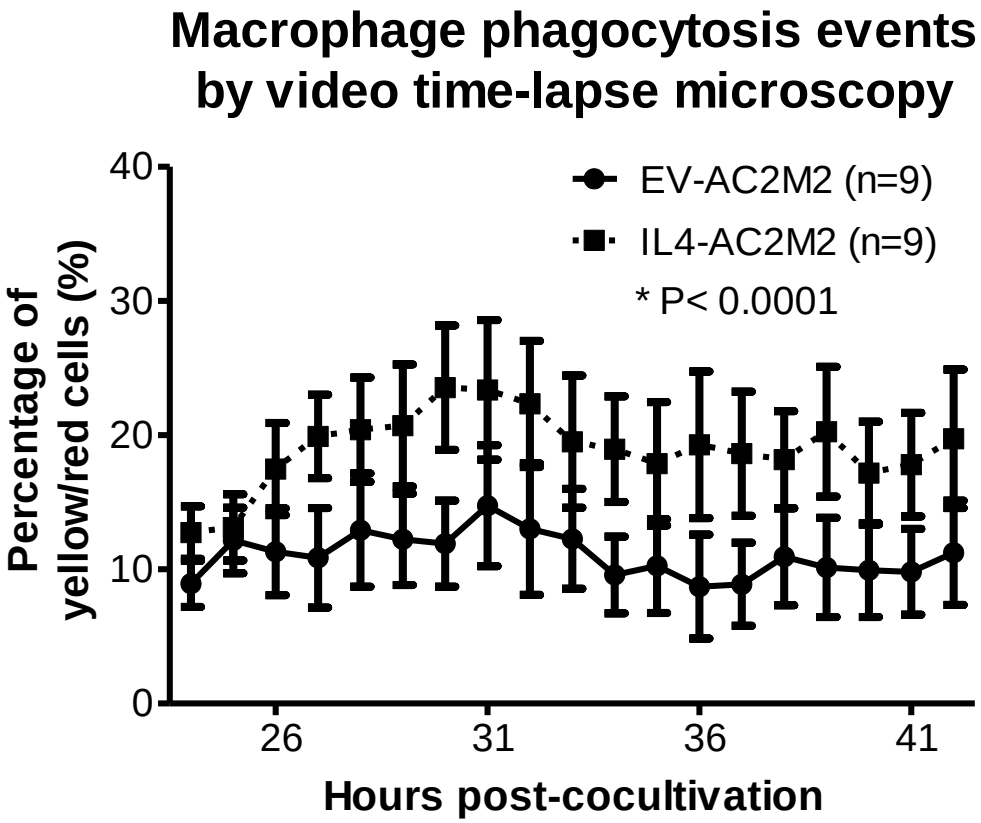

Figure 4.14 Higher degree of macrophage phagocytosis of tumor cells in the presence of IL-4. Orange cell tracker dye labeled peritoneal macrophages (red) were co-cultured with either GFP-expressing EV-AC2M2 or GFP-expressing IL4-AC2M2 cells for initial 24 hours. Nine random fields were then selected from each co-culture and imaged every 5 minutes for 18 hours by video time-lapse microscopy. Numbers of yellow cells and red macrophages were quantified using ImagePro software. Higher percentages of yellow cells were found in IL4-AC2M2 co-cultures ($P < 0.0001$; n=9 for both groups)

in multiple cell types of hematopoietic origin [66, 186-194, 200-205, 210, 211, 330-333]. When we performed mouse orthotopic engraftment experiments with AC2M2 breast carcinoma cells expressing empty vector control or IL-4 in three different mouse strains, including immune-competent CBA mice, athymic nude mice, and $Rag2^{-/-}$; $IL2R\gamma c^{-/-}$ double-knockout mice, we observed the most pronounced differences in tumorigenesis and metastasis in $Rag2^{-/-}$; $IL2R\gamma c^{-/-}$ double-knockout mice. Since these mice have no T cells, NK cells and B cells, we speculate that the differences may be attributed to cells of the myeloid lineage in the tumor microenvironment.

The concept of classic versus alternative macrophage activation as well as the role of IL-4 on alternative macrophage activation has been extensively described in recent years [95, 208, 209]. Classically, activated inflammatory M1-like macrophages are induced by IFN-γ, LPS, TNF-α, and GM-CSF; and they mediate resistance to microbial infections as well as antitumorigenic properties [208]. Alternatively, IL-4 induces the activation of M2-like macrophages; and in response to other cytokines, including TGF-β, IL-10, and CSF-1, they acquire tumor-promoting properties to enhance tumor cell growth, invasion and metastasis [95, 209]. When BMA macrophage cells were stimulated *in vitro* with mouse recombinant IL-4 or IL-4 containing conditioned medium, they expressed arginase 1, a common M2 macrophage marker, in a dose-dependent manner. This observation agreed with the current literature that IL-4 is able to induce M2 macrophage activation. Also, *in vivo*,

when AC2M2 breast carcinoma cells transduced with either empty vector control or IL-4 were engrafted into mouse mammary glands, we observed significantly higher levels of arginase 1 expression in IL-4 expressing tumor-containing mammary glands detected both *in situ* and by immunoblotting. Taken together, these observations suggest that IL-4 induced M2 macrophage activation *in vitro* as well as in the tumor microenvironment in the orthotopic engraftment model.

Since alternatively activated M2 macrophages induced by IL-4 are believed to promote tumorigenesis and distant metastasis [209], we expected to see more aggressive tumor growth and more frequent lung metastasis in mice engrafted with IL-4 expressing AC2M2 cells. However, we observed the opposite; specifically, tumors arising from IL-4 expressing AC2M2 cells grew significantly slower than empty vector control, and lung metastasis was completely abolished in mice bearing IL-4 expressing tumors. IL-4 has been reported to act as a potent macrophage fusion factor, inducing macrophages to form large multinucleated giant cells which have enhanced phagocytic capability [330-333]. Thus, we speculated that tumor cell-derived IL-4 induced tumor-associated macrophages to be more phagocytic. Indeed, flow cytometry analysis detected almost 20 times more $F4/80^+$ macrophage populations in IL-4 expressing tumor stroma. More importantly, these $F4/80^+$ macrophages were also GFP^+, indicative of macrophage phagocytosis of tumor cells. This suggests that not only did tumor-derived IL-4 promote the recruitment of more $F4/80^+$ macrophages into the tumor microenvironment, but also that these

macrophages are more phagocytic.

We also speculate that highly migratory tumor cells which are the sources of distant metastasis may be more likely to be the targets of phagocytic macrophages induced by IL-4. This is one possible explanation for why IL-4 expressing tumors grew slower and mice bearing these tumors developed no detectable metastasis. Observations from *in vitro* experiments further supported this speculation. Peritoneal macrophages became enlarged after 24 hours of co-culture with IL-4 expressing AC2M2 tumor cells. In these co-culture experiments, we also observed many yellow cells, suggesting GFP-expressing tumor cells have been fused with red cell tracker dye labeled macrophages. These were not seen in co-cultures of peritoneal macrophages with control AC2M2 tumor cells. We also performed video time-lapse experiments to monitor macrophage and tumor cell fusion events. Throughout the 18 hours time course, we constantly observed significantly more yellow cells, indicative of more fusion events in co-cultures of peritoneal macrophages with IL-4 expressing AC2M2 cells.

Several studies have used malignant tumor cells genetically engineered to produce IL-4 and shown potent anti-tumor effects *in vivo* associated with inhibiting primary tumor burden [291-293]. Our studies support an inhibitory effect of tumor-derived IL-4 on primary tumor growth, but perhaps even more significantly, they showed a dramatic effect of IL-4 in eliminating distant metastasis. Additional

experiments suggest that this reduced primary tumor growth and complete elimination of lung metastasis might be due to the recruitment of phagocytic macrophages induced by tumor cell-derived IL-4 in the tumor microenvironment. These findings support the use of IL-4 as a potential therapeutic agent for patients with metastatic cancers. Clinical trials have shown that administration of IL-4 plus GM-CSF was able to enhance dendritic cell number and their functions in cancer patients [298]. Therefore, further studies are required to assess the effect of other immune cells, as well as the possibility of using IL-4 and GM-CSF as adjuvants for cancer treatments.

Previous studies reported that non-receptor tyrosine kinase Fes interacts with the IL-4Rα chain in B cells, and potentiates recruitment of PI3K to IRS2 [260-262]. However, we are unaware of reports linking Fes to IL-4/IL-13 signaling in macrophages. Since Fes-knockout mice displayed similar phenotypes of reduced tumor growth and lung metastasis in the AC2M2 engraftment model [302], it will be important to study whether Fes participates in IL-4 signaling, and whether engineering tumor cells with IL-4 expression and disrupting Fes in the tumor stroma might have additive or synergistic effects in suppressing tumor growth and distant metastasis. Ultimately, this could provide additional treatment options for advanced breast cancer patients.

Chapter 5

General Discussion

5.1 Summary of findings and significance of results

The *fes* gene was originally identified as an oncogene from retrovirally induced avian and feline tumors [122-126], and viral *fes* was able to induce tumors in transgenic mice [166]. This early work suggested that activating mutations or inappropriate expression of the *fes* proto-oncogene might contribute to human cancer. Previous work in our lab demonstrated that *fes-null* mice displayed a hyperinflammatory phenotype in response to LPS challenge due to the release of increased amounts of the proinflammatory cytokine TNF-α and hyperactive NFκB signaling pathway in *fes-null* macrophages [162, 165], which suggested a role of Fes in regulating innate immunity and inflammation. Considering the link between inflammation and cancer [60, 338-340], it seems reasonable to speculate a possible role of Fes in cancer progression through regulation of inflammation. In addition, colon cancer studies from Smithgall's group have also implicated Fes as a tumor suppressor in colorectal cancer [171, 172]; and studies using MMTV-PyMT transgenic mice suggested Fes could also play a tumor suppressor role in breast cancer [170]. All of these studies beg the question of what role Fes may have in the progression of human epithelial cancers, and whether Fes would be a good therapeutic

target for treating cancer patients. Therefore, this project was aimed at elucidating the role of the Fes protein tyrosine kinase in human breast cancer using genetic manipulation of *fes* in mouse models.

5.1.1 Stromal tumor promoting roles for Fes in regulating tumorigenesis

Considering the tissue-specific Fes expression in myeloid and vascular endothelial cells [157], as well as increased Fes expression in epithelial cells during lactation [158], the role of Fes in tumorigenesis needs to be addressed from two different angles: tumor cell intrinsic roles and stromal cell specific roles.

In the second chapter, we took advantage of a highly lung metastatic AC2M2 mouse breast carcinoma cell line [102, 341] and established an orthotopic mammary gland engraftment model in nude mice. To study the tumor cell autonomous role of Fes, we first manipulated Fes expression in AC2M2 cells by overexpressing wild-type, kinase-dead or kinase-activated Fes, and there was no apparent effect on tumor growth at the orthotopic injection site or metastasis to the lungs. However, when the role of Fes in the tumor stroma was explored by comparing tumorigenesis after AC2M2 tumor cell engraftment into wild-type or *fes-null* mice, significant reductions in tumor growth rates and metastasis were observed in *fes-null* mice. This correlated with reductions in tumor angiogenesis, tumor-associated macrophages and circulating tumor cells. Furthermore, *fes-null* macrophages did not promote the *in vitro* invasive

properties of co-cultured tumor cells to the same extend as wild-type macrophages did, and *fes-null* macrophages were also deficient in their ability to become invasive in the presence of co-cultured tumor cells. These observations argue that Fes plays a tumor promoting role through stromal cells within the tumor niche, but this study did not reveal any tumor cell intrinsic effects of Fes, at least in this particular basal-cell line breast tumor model.

We also employed a transgenic model of spontaneous breast cancer, the MMTV-Neu mouse model [105], to investigate the role of Fes in mammary tumorigenesis. *fes*-deficient mice showed a significantly longer tumor latency than wild-type controls in this HER2 model. We argue that delayed tumor onset might be, in part, due to the hyperinflammatory status of *fes*-deficient normal mammary glands at the pre-malignant stage. This was associated with increased numbers of $CD3^+$ T cells and $CD11b^+$ myeloid cells which could lead to enhanced tumor immunity at this early stage in tumorigenesis. The work in this chapter also suggested a tumor promoting role of Fes kinase in human breast cancer, possibly by acting through stromal cells, such as T cells and myeloid cells, in the tumor microenvironment.

5.1.2 Possible tumor cell intrinsic roles of Fes in tumorigenesis

Although we did not detect a tumor cell intrinsic role for Fes in the AC2M2 orthotopic engraftment model, it does not exclude this possibility. In the

MMTV-PyMT transgenic mouse model of breast cancer, Fes plays a tumor suppressor role by delaying tumor onset. However, in a transgenic mouse model of breast cancer driven by an activated Neu transgene, Fes promotes tumor initiation since *fes*-deficient mice showed longer tumor latency. These apparent contradictory observations may be partly due to distinct roles of Fes in PyMT- and Neu-induced cellular transformation, but we have not done any experiments to address this question. Further experiments could include soft agar colony formation assay to study whether PyMT or activated HER2/Neu could transform either wild-type or *fes*-knockout embryonic fibroblasts. Anchorage-independent growth is one of the hallmarks of cell transformation, and provides a convenient quantitative *in vitro* assay for assessing transformation of cells. If PyMT transforms *fes*-knockout fibroblasts more efficiently than wild-type fibroblasts (or vice versa for activated HER2/Neu), it could provide evidence for tumor cell intrinsic roles for Fes which might explain the opposite effects of Fes-disruption on tumor initiation in these two transgenic models.

Fes expression is low or undetectable in most breast cancer cell lines we have examined, including SKBR3 and BT474 (data not shown). This is why we chose to explore the possibility of tumor cell intrinsic roles for Fes by ectopically expressing either wild type or mutant alleles of Fes in the AC2M2 model. Alternatively, if Fes expression were detected in a breast tumor cell line, we could use RNA interference approaches to knock it down and then explore the effect of this on tumorigenesis in xenograft or syngeneic engraftment models. One recent study suggested that both the

protein expression level and the enzymatic activity of Fes were upregulated in transformed, highly proliferative MDA-MB-231 breast cancer cells [301]. Perhaps, future studies of this type with MDA-MB-231 cells can be used to study the tumor cell intrinsic role of Fes in regulating tumorigenesis in a triple-negative breast cancer model.

5.1.3 Possible roles of Fes on different phenotypes of macrophages

Ever since Virchow hypothesized that the origin of cancer was at sites of chronic inflammation [59], the idea of inflammation being associated with cancer has persisted [60, 338-340]. In tumor development, inflammation appears to be a double-edged sword. Acute inflammation tends to be anti-tumorigenic, whereas chronic inflammation tends to be pro-tumorigenic. Related to the work in this thesis, Fes is abundantly expressed in macrophages, which is a major type of innate immune cell. A better understanding of the roles of Fes in different phenotypes of macrophages may help explain the effect of Fes disruption on tumor progression (Figure 5.1).

Classically activated M1 macrophages exert anti-microbial and anti-tumorigenic effects, including direct killing of microorganisms and tumor cells [209]. In contrast to inflammatory M1 macrophage activation, macrophages have been shown to undergo alternative M2 activation in the context of wound healing or

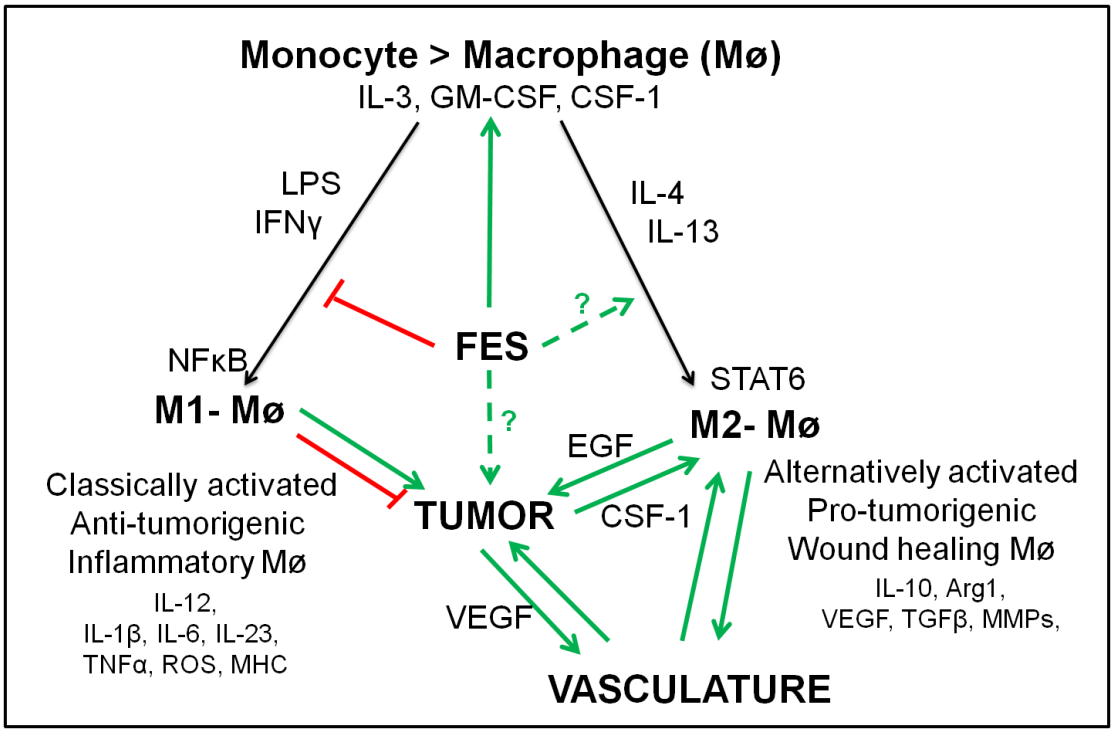

Figure 5.1 Fes influences on macrophages in tumorigenesis. In response to different stimuli, macrophages (Mø) can undergo either M1 or M2 polarization [66, 210]. M1 classical macrophages (M1-Mø) induced by LPS and IFN-γ play an anti-tumorigenic role by secreting a number of factors, whereas alternatively activated M2 macrophages play pro-tumorigenic roles by promoting tumor cell growth, invasion and metastasis by secreting paracrine acting factors including EGF and VEGF. Fes appears to attenuate NFκB activation downstream of LPS during classical activation of M1 macrophages. The pro-inflammatory functions of M1-Mø, including ROS production, may initially contribute to initiation of tumorigenesis (indicated in green). This may explain why tumor onset time was reduced in *fes-null* mice in MMTV-PyMT breast cancer model. However, expression of TNF-α and other pro-inflammatory cytokines may endow M1-Mø with anti-tumorigenic functions at early stages of tumor progression by promoting the recruitment and activation of cytotoxic T cells. This may explain why *fes*-deficient mice had longer tumor latency in the MMTV-Neu transgenic model of breast cancer. Furthermore, at later stages of tumorigenesis, Fes may promote polarization toward M2 macrophages, which facilitate tumor growth, invasion and metastasis. This may explain why *fes-null* mice developed significantly smaller tumors and less lung metastasis in AC2M2 orthotopic engraftment studies. Positive or negative effects on signaling or tumorigenesis are indicated with green or red lines, respectively. Solid lines indicate roles that are supported by published studies, while dotted lines indicate speculative roles. (Adapted from [342])

within the tumor microenvironment [66, 210, 211]. Instead of killing tumor cells, M2 macrophages promote tumor cell growth, invasion and metastasis by secreting many factors [209]. Inflammatory M1 macrophages and wound-healing M2 macrophages coexist throughout all stages of tumor development; however, inflammatory M1 macrophages are predominant in early stages of tumor progression, i.e. tumor initiation, whereas the balance skews toward alternatively activated M2 macrophages which become predominant and thereby facilitate tumor growth and metastasis in later stages of tumor development.

In the MMTV-Neu transgenic model, increased NFκB activation and more $CD11b^+$ myeloid cells were observed in *fes*-deficient pre-malignant mammary glands, which suggested a hyperinflammatory status of these mammary tissues. We speculate that this hyperinflammatory phenotype correlates with more inflammatory M1-like macrophages in *fes*-deficient normal mammary glands. We also speculate that this increase in inflammatory M1-like macrophages is still within the physiological threshold, so that these macrophages play their normal functions as antigen-presenting cells and facilitate the recruitment of cytotoxic T cells to eliminate neoplastic cells and thereby delay tumor onset. Indeed, we detected higher numbers of $CD3^+$ T cells in *fes*-deficient normal mammary glands, which might have contributed to delayed tumor initiation in *fes*-deficient transgenic mice. From this perspective, Fes may play an oncogenic role in tumor initiation by suppressing the anti-tumorigenic activity of classically activated M1 inflammatory macrophages.

Interestingly, Fes disruption in the MMTV-PyMT induced breast cancer model correlated with a very different effect. In that model, Fes appears to play a tumor suppressor role at the level of tumor initiation, since tumor onset time was reduced in *fes-null* mice as compared to wild-type mice [170]. To explain the apparent conflicting roles of Fes in the MMTV-Neu and MMTV-PyMT models, we speculate that the PyMT oncogene may induce a much greater degree of inflammation than activated HER2/Neu in early stages of tumorigenesis. In support of this, MMTV-PyMT induces spontaneous mammary tumors as early as 35 days [103], in contrast to several months of tumor latency in the MMTV-Neu model [105]. PyMT transforms cells by interacting with and activating a number of key signaling proteins, including Src, Shc, PI3K, 14-3-3 and PLC-γ [116]. The Neu oncoprotein engages many of the same signaling proteins, including Shc, Grb2, DOK-R and two unidentified proteins, P34 and p150 [343], but is a less powerful oncoprotein in comparison with PyMT. We speculate that Fes deficiency may amplify the already extremely high inflammation caused by PyMT oncogene to an even greater extent. We also speculate that the level of inflammation induced by PyMT plus Fes deficiency might exceed some physiological threshold such that inflammatory M1-like macrophages switch gear and start to produce reactive oxygen species (ROS) and other potential mutagens which would serve as a second hit to accelerate tumorigenesis. Thus, increased levels of inflammation and ROS production in the mammary tissues of *fes-null* mice might contribute to earlier tumor initiation in the

MMTV-PyMT transgenic model. Therefore, Fes could be acting as a tumor suppressor by restraining the production of ROS and other mutagenic mediators produced by inflammatory M1-like macrophages.

Switching to explore the later stages of tumorigenesis which the AC2M2 orthotopic engraftment model focused on, tumor-associated macrophages tend to be more M2-like, which are associated with increased angiogenesis and metastasis through paracrine interactions with both tumor cells and vascular endothelial cells. In the AC2M2 orthotopic engraftment study, reduced numbers of tumor-associated macrophages were observed in more developed tumors in *fes-null* mice. We speculate that Fes might promote the polarization of macrophages toward M2 phenotype once tumors are established and start to grow. This might explain the correlation between reduced numbers of $F4/80^{+}$ tumor-associated macrophages and reduced tumor growth and metastasis in *fes-null* mice. In the context of tumor growth and metastasis, Fes may promote tumorigenesis through roles in wound-healing M2 like macrophages.

Clearly, the proposed model (Figure 5.1) illustrating roles of Fes in M1 versus M2 macrophages in tumorigenesis is over simplified, and further experiments are required to more fully elucidate Fes functions in macrophages and determine if Fes inhibition will provide therapeutic benefits in specific types of cancer.

5.1.4 Possible roles of IL-4 on macrophages in tumorigenesis

Upon stimulation by IL-4 secreted from $CD4^+$ Th2 cells, mast cells and basophils, macrophages may undergo alternative M2 activation. Alternatively activated M2 macrophages are capable of promoting tumor cell growth, invasion and metastasis by secreting many factors including EGF, MMPs and VEGF [209]. When IL-4 expressing AC2M2 breast carcinoma cells were engrafted into $Rag2^{-/-}$; $IL2R\gamma c^{-/-}$ double-knockout mice, we observed significantly smaller tumors and complete abolishment of lung metastasis in the presence of IL-4. This apparently contradictory observation may relate to the nature of IL-4 action when produced by tumor cells rather than by its normal physiologic sources.

When secreted by immune cells in the tumor microenvironment, the IL-4 concentration experienced by monocytes might be much lower, resulting in polarization towards the M2 phenotype, thereby promoting tumorigenesis and metastasis. However, in the case of ectopic expression by tumor cells, IL-4 levels might be much higher resulting in a different macrophage phenotype including formation large multinucleated giant cells with enhanced phagocytic capability [330-333]. This speculation is supported by subsequent *in vitro* experiments where we observed more phagocytic macrophages in the presence of IL-4.

5.2 Future directions

5.2.1 Inhibition of Fes in human breast cancer

A majority of cancer studies have focused on examining the functions of oncogenes and tumor suppressor genes and the signaling pathways regulating tumor cell proliferation and/or tumor cell death. However, more and more researchers have realized that tumors live in a dynamic microenvironment which is critical for tumor development, and inhibition of the tumor microenvironment could indirectly suppress tumorigenesis and metastasis. This thesis provides strong evidence that inhibition of Fes in the tumor stroma might be therapeutically beneficial for treating cancer patients.

Since the clinical success of the Bcr-Abl inhibitor imatinib in chronic myeloid leukemia, considerable efforts have been dedicated to developing selective small molecule inhibitors for kinases that are implicated in cancer and other diseases [344]. In addition to an oncogenic role of Fes through regulating inflammation demonstrated in this thesis, Kanda and Miyata have also implicated Fes as a potential target for anti-angiogenic therapy to treat patients with anti-VEGF refractory cancer [345]. To date, TAE684 has been characterized as a potent Fes tyrosine kinase inhibitor both *in vitro* and *in vivo* by Smithgall's group [346]. In work not described in this thesis, I began to explore inhibition of Fes and Fer kinases using the drug TAE684 in our AC2M2 cell culture system (Appendix 2). While TAE684 was capable of inhibiting

Fes expressed in AC2M2 cells, preliminary studies testing TAE684 in the AC2M2 engraftment model did not reveal any anti-tumorigenic effects (data not shown). Before we draw any conclusions about the ability of TAE684 to inhibit tumorigenesis *in vivo*, this drug-treatment experiment needs to be repeated with different dosing schedules and longer periods of tumor assessment, as well as large cohorts of animals.

TAE684 was originally discovered as a potent inhibitor of the anaplastic lymphoma kinase (Alk) [347]; although it inhibits Fes kinase activity *in vitro* and in cell culture [346], it may also act on other targets *in vivo*. Based on the work described in this thesis, there appears to be strong rationale for targeting Fes in the tumor stroma. However, targeting Fes kinase alone may not be sufficient to reduce primary tumor burden and metastasis in cancer patients. Thus, combinations of Fes inhibitors with other therapies should also be considered for breast cancer patients. A better understanding of Fes functions in cells of the tumor niche may help in the design of such combinatory treatment strategies.

5.2.2 IL-4 as a good candidate for tumor vaccines

The development of tumor vaccines has been a major thrust of immunotherapy [348-351]. Regardless of what constitutes the vaccine, the desired result is to provide antigen in a stimulatory manner which allows the *in vivo* generation of a potent anti-tumor immune response. In general, cancer vaccines can be divided into three

categories. These include the use of lymphocyte-defined tumor antigen (LDTA), whole autologous or allogeneic tumor cell vaccines, and LDTA-pulsed dendritic cells. One of the approaches to tumor cell vaccines has been to genetically modify the autologous or allogeneic tumor cells to express agents designed to enhance the anti-tumor immune response [352]. For example, cytokines TNF-α, GM-CSF, IFN-γ or IL-2 have been used as immune stimulating molecules for the generation of tumor vaccines [353-358]. In 1997, the first use of GM-CSF-transduced, lethally irradiated, autologous melanoma cells was reported as a therapeutic vaccine and produced antitumor immune responses associated with partial, albeit temporary clinical benefit [359]. A phase I clinical trial investigating the biologic activity of these vaccines found infiltrations of T cells, dendritic cells, macrophages and eosinophils at the immunization sites in all 21 patients evaluated [360, 361]. In addition, autologous tumor-reactive CTLs were detected following vaccination. GM-CSF-secreting autologous tumor vaccines have also been utilized in clinical trials for renal cell carcinoma and prostate cancer [354, 362-364].

In this thesis, we have shown that tumor cell-secreted IL-4 resulted in a significant reduction in primary tumor growth; but more strikingly, a complete abolishment of lung metastasis was observed using AC2M2 orthotopic engraftment model. This may be partly due to enhanced phagocytic ability of macrophages in the presence of IL-4. These observations provided strong evidence that IL-4 may be a good candidate for a gene-modified tumor vaccine. Although several other studies

have already reported the potent anti-tumor effect of genetically engineered IL-4 producing tumor cells in animal models [291, 293], they failed to demonstrate the more powerful effect of tumor cell-derived IL-4 on inhibiting distant metastasis. For future experiments, we could retrovirally transduce other cytokines such as IFN-γ into AC2M2 cells and determine the role of tumor cell-derived IFN-γ on tumorigenesis and metastasis. Since IFN-γ exerts an opposing role on macrophage polarization relative to IL-4, it would be interesting to test whether IFN-γ would have an opposite effect in the tumor vaccine setting using the AC2M2 orthotopic engraftment model. A clinical trial has suggested that systemic administration of IL-4 in combination with GM-CSF led to the differentiation of dendritic cells and enhanced their number and function in cancer patients [298]. It would therefore be important to explore the feasibility of using IL-4 in combination with GM-CSF in a tumor vaccine approach.

5.2.3 Molecular mechanisms related to Fes

In this thesis, we made empirical observations that Fes kinase plays an oncogenic role in tumor initiation, growth and metastasis using the MMTV-Neu transgenic mouse model and the AC2M2 orthotopic engraftment model, and also provided evidence suggesting the tumor promoting role of Fes may act through regulation of inflammation and angiogenesis. However, this thesis has not explored functions of Fes at the molecular or cellular levels.

A recent study has found that constitutively expressed MHC I molecules attenuated TLR-triggered innate inflammatory responses via a Fes-SHP2 pathway, which protected mice from sepsis [365]. Upon TLR activation by ligands such as LPS, the intracellular domain of MHC class I molecules in cultured macrophages was phosphorylated by a Src family kinase, then Fes was recruited to phosphorylated MHC I via its SH2 domain. This led to enhanced Fes activity and recruitment of the protein tyrosine phosphatase SHP2, which inhibited TLR-triggered innate inflammatory responses, such as secretion of pro-inflammatory cytokine TNF-α. This finding was consistent with our previous observations that *fes-null* macrophages displayed a hyperactivation of NFκB signaling with higher secretion of TNF-α. Knockdown of SHP2 in HER2 positive and triple-negative breast cancer cell lines has been shown to eradicate breast-tumor-initiating cells, and resulted in reduced tumor growth and metastasis in xenograft models [366]. Since Fes is capable of activating SHP2 phosphatase, future work should include elucidating the cooperation between Fes and SHP2 and exploring how this crosstalk influences inflammation and tumor development.

In summary, this thesis work provides strong evidences that Fes plays a tumor promoting role in human breast cancer using both orthotopic mouse engraftment model and transgenic mouse model; and hence, Fes is a potential therapeutic target for treating breast cancer patients.

References

1. Canadian Cancer Society's Advisory Committee on Cancer Statistics. Canadian Cancer Statistics 2013. Toronto, ON: Canadian Cancer Society; 2013
2. American Cancer Society. What is Breast Cancer? http://www.cancer.org/cancer/breastcancer/detailedguide/breast-cancer-what-is-breast-cancer
3. Harvey, J.A., *Unusual breast cancers: useful clues to expanding the differential diagnosis.* Radiology, 2007. **242**(3): p. 683-94.
4. Chen, S. and G. Parmigiani, *Meta-analysis of BRCA1 and BRCA2 penetrance.* J Clin Oncol, 2007. **25**(11): p. 1329-33.
5. Howlader, N., Noone, A.M., Krapcho, M. et al. (eds.). (2013) SEER Cancer Statistics Review, 1975-2010. Bethesda, MD: National Cancer Institute. Retrieved June 24, 2013.
6. Earlier detection and diagnosis of breast cancer: A report from It's About Time! Canadian Breast Cancer Foundation- Ontario Region. (2010).
7. Brenton, J.D., et al., *Molecular classification and molecular forecasting of breast cancer: ready for clinical application?* J Clin Oncol, 2005. **23**(29): p. 7350-60.
8. Parker, J.S., et al., *Supervised risk predictor of breast cancer based on intrinsic subtypes.* J Clin Oncol, 2009. **27**(8): p. 1160-7.
9. Rakha, E.A., et al., *Expression profiling technology: its contribution to our understanding of breast cancer.* Histopathology, 2008. **52**(1): p. 67-81.
10. Schnitt, S.J., *Classification and prognosis of invasive breast cancer: from morphology to molecular taxonomy.* Mod Pathol, 2010. **23 Suppl 2**: p. S60-4.
11. Sorlie, T., et al., *Gene expression patterns of breast carcinomas distinguish tumor subclasses with clinical implications.* Proc Natl Acad Sci U S A, 2001. **98**(19): p. 10869-74.
12. Sorlie, T., et al., *Repeated observation of breast tumor subtypes in independent gene expression data sets.* Proc Natl Acad Sci U S A, 2003. **100**(14): p. 8418-23.
13. Sotiriou, C. and L. Pusztai, *Gene-expression signatures in breast cancer.* N Engl J Med, 2009. **360**(8): p. 790-800.
14. Perou, C.M., et al., *Molecular portraits of human breast tumours.* Nature,

2000. **406**(6797): p. 747-52.

15. Arvold, N.D., et al., *Age, breast cancer subtype approximation, and local recurrence after breast-conserving therapy.* J Clin Oncol. **29**(29): p. 3885-91.

16. Dawood, S., et al., *Defining breast cancer prognosis based on molecular phenotypes: results from a large cohort study.* Breast Cancer Res Treat. **126**(1): p. 185-92.

17. Voduc, K.D., et al., *Breast cancer subtypes and the risk of local and regional relapse.* J Clin Oncol, 2010. **28**(10): p. 1684-91.

18. Reis-Filho, J.S. and A.N. Tutt, *Triple negative tumours: a critical review.* Histopathology, 2008. **52**(1): p. 108-18.

19. National Cancer Institute. Breast Cancer Treatment (PDQ®). http://www.cancer.gov/cancertopics/pdq/treatment/breast/Patient/page5

20. American Cancer Society. Chemotherapy for breast cancer. http://www.cancer.org/cancer/breastcancer/detailedguide/breast-cancer-treating-chemotherapy

21. Jordan, V.C., *Fourteenth Gaddum Memorial Lecture. A current view of tamoxifen for the treatment and prevention of breast cancer.* Br J Pharmacol, 1993. **110**(2): p. 507-17.

22. Pegram, M.D., et al., *Rational combinations of trastuzumab with chemotherapeutic drugs used in the treatment of breast cancer.* J Natl Cancer Inst, 2004. **96**(10): p. 739-49.

23. Rusnak, D.W., et al., *Assessment of epidermal growth factor receptor (EGFR, ErbB1) and HER2 (ErbB2) protein expression levels and response to lapatinib (Tykerb, GW572016) in an expanded panel of human normal and tumour cell lines.* Cell Prolif, 2007. **40**(4): p. 580-94.

24. Slamon, D.J., et al., *Studies of the HER-2/neu proto-oncogene in human breast and ovarian cancer.* Science, 1989. **244**(4905): p. 707-12.

25. Jones, S.E., et al., *Adjuvant docetaxel and cyclophosphamide plus trastuzumab in patients with HER2-amplified early stage breast cancer: a single-group, open-label, phase 2 study.* Lancet Oncol, 2013. **14**(11): p. 1121-1128.

26. Swain, S.M., et al., *Pertuzumab, trastuzumab, and docetaxel for HER2-positive metastatic breast cancer (CLEOPATRA study): overall survival results from a randomised, double-blind, placebo-controlled, phase 3 study.* Lancet Oncol, 2013.**14**(6): p. 461-71.

27. Bachelot, T., et al., *Lapatinib plus capecitabine in patients with previously untreated brain metastases from HER2-positive metastatic breast cancer (LANDSCAPE): a single-group phase 2 study.* Lancet Oncol, 2012. **14**(1): p.

64-71.

28. Goss, P.E., et al., *Adjuvant lapatinib for women with early-stage HER2-positive breast cancer: a randomised, controlled, phase 3 trial.* Lancet Oncol, 2012.**14**(1): p. 88-96.

29. Althuis, M.D., et al., *Global trends in breast cancer incidence and mortality 1973-1997.* Int J Epidemiol, 2005. **34**(2): p. 405-12.

30. Geiger, T.R. and D.S. Peeper, *Metastasis mechanisms.* Biochim Biophys Acta, 2009. **1796**(2): p. 293-308.

31. Parmar, H. and G.R. Cunha, *Epithelial-stromal interactions in the mouse and human mammary gland in vivo.* Endocr Relat Cancer, 2004. **11**(3): p. 437-58.

32. Richert, M.M., et al., *An atlas of mouse mammary gland development.* J Mammary Gland Biol Neoplasia, 2000. **5**(2): p. 227-41.

33. Thiery, J.P., *Epithelial-mesenchymal transitions in tumour progression.* Nat Rev Cancer, 2002. **2**(6): p. 442-54.

34. Jechlinger, M., et al., *Expression profiling of epithelial plasticity in tumor progression.* Oncogene, 2003. **22**(46): p. 7155-69.

35. Egeblad, M. and Z. Werb, *New functions for the matrix metalloproteinases in cancer progression.* Nat Rev Cancer, 2002. **2**(3): p. 161-74.

36. Friedl, P. and K. Wolf, *Tumour-cell invasion and migration: diversity and escape mechanisms.* Nat Rev Cancer, 2003. **3**(5): p. 362-74.

37. Wicki, A., et al., *Tumor invasion in the absence of epithelial-mesenchymal transition: podoplanin-mediated remodeling of the actin cytoskeleton.* Cancer Cell, 2006. **9**(4): p. 261-72.

38. Gimbrone, M.A., Jr., et al., *Tumor dormancy in vivo by prevention of neovascularization.* J Exp Med, 1972. **136**(2): p. 261-76.

39. Bergers, G. and L.E. Benjamin, *Tumorigenesis and the angiogenic switch.* Nat Rev Cancer, 2003. **3**(6): p. 401-10.

40. Hanahan, D. and R.A. Weinberg, *Hallmarks of cancer: the next generation.* Cell, 2011. **144**(5): p. 646-74.

41. Hanahan, D. and R.A. Weinberg, *The hallmarks of cancer.* Cell, 2000. **100**(1): p. 57-70.

42. Hanahan, D. and J. Folkman, *Patterns and emerging mechanisms of the angiogenic switch during tumorigenesis.* Cell, 1996. **86**(3): p. 353-64.

43. Fidler, I.J., *Metastasis: guantitative analysis of distribution and fate of tumor embolilabeled with 125 I-5-iodo-2'-deoxyuridine.* J Natl Cancer Inst, 1970. **45**(4): p. 773-82.

44. Chambers, A.F., A.C. Groom, and I.C. MacDonald, *Dissemination and growth of cancer cells in metastatic sites.* Nat Rev Cancer, 2002. **2**(8): p. 563-72.

45. Fidler, I.J., *The pathogenesis of cancer metastasis: the 'seed and soil' hypothesis revisited.* Nat Rev Cancer, 2003. **3**(6): p. 453-8.

46. Paget, S., *The distribution of secondary growths in cancer of the breast. 1889.* Cancer Metastasis Rev, 1989. **8**(2): p. 98-101.

47. Mueller, M.M. and N.E. Fusenig, *Friends or foes - bipolar effects of the tumour stroma in cancer.* Nat Rev Cancer, 2004. **4**(11): p. 839-49.

48. Wels, J., et al., *Migratory neighbors and distant invaders: tumor-associated niche cells.* Genes Dev, 2008. **22**(5): p. 559-74.

49. Dvorak, H.F., *Tumors: wounds that do not heal. Similarities between tumor stroma generation and wound healing.* N Engl J Med, 1986. **315**(26): p. 1650-9.

50. Schafer, M. and S. Werner, *Cancer as an overhealing wound: an old hypothesis revisited.* Nat Rev Mol Cell Biol, 2008. **9**(8): p. 628-38.

51. Iwano, M., et al., *Evidence that fibroblasts derive from epithelium during tissue fibrosis.* J Clin Invest, 2002. **110**(3): p. 341-50.

52. Petersen, O.W., et al., *Epithelial to mesenchymal transition in human breast cancer can provide a nonmalignant stroma.* Am J Pathol, 2003. **162**(2): p. 391-402.

53. Ronnov-Jessen, L. and O.W. Petersen, *Induction of alpha-smooth muscle actin by transforming growth factor-beta 1 in quiescent human breast gland fibroblasts. Implications for myofibroblast generation in breast neoplasia.* Lab Invest, 1993. **68**(6): p. 696-707.

54. Trimboli, A.J., et al., *Direct evidence for epithelial-mesenchymal transitions in breast cancer.* Cancer Res, 2008. **68**(3): p. 937-45.

55. Kojima, Y., et al., *Autocrine TGF-beta and stromal cell-derived factor-1 (SDF-1) signaling drives the evolution of tumor-promoting mammary stromal myofibroblasts.* Proc Natl Acad Sci U S A, 2010. **107**(46): p. 20009-14.

56. Orimo, A., et al., *Stromal fibroblasts present in invasive human breast carcinomas promote tumor growth and angiogenesis through elevated SDF-1/CXCL12 secretion.* Cell, 2005. **121**(3): p. 335-48.

57. Hu, M., et al., *Role of COX-2 in epithelial-stromal cell interactions and progression of ductal carcinoma in situ of the breast.* Proc Natl Acad Sci U S A, 2009. **106**(9): p. 3372-7.

58. Stuelten, C.H., et al., *Transient tumor-fibroblast interactions increase tumor*

cell malignancy by a TGF-Beta mediated mechanism in a mouse xenograft model of breast cancer. PLoS One, 2010.**5**(3): p. e9832.

59. Balkwill, F. and A. Mantovani, *Inflammation and cancer: back to Virchow?* Lancet, 2001. **357**(9255): p. 539-45.

60. Coussens, L.M. and Z. Werb, *Inflammation and cancer.* Nature, 2002. **420**(6917): p. 860-7.

61. Kornfeld, D., A. Ekbom, and T. Ihre, *Is there an excess risk for colorectal cancer in patients with ulcerative colitis and concomitant primary sclerosing cholangitis? A population based study.* Gut, 1997. **41**(4): p. 522-5.

62. Leek, R.D. and A.L. Harris, *Tumor-associated macrophages in breast cancer.* J Mammary Gland Biol Neoplasia, 2002. **7**(2): p. 177-89.

63. Brigati, C., et al., *Tumors and inflammatory infiltrates: friends or foes?* Clin Exp Metastasis, 2002. **19**(3): p. 247-58.

64. Bingle, L., N.J. Brown, and C.E. Lewis, *The role of tumour-associated macrophages in tumour progression: implications for new anticancer therapies.* J Pathol, 2002. **196**(3): p. 254-65.

65. Martinez, F.O., L. Helming, and S. Gordon, *Alternative activation of macrophages: an immunologic functional perspective.* Annu Rev Immunol, 2009. **27**: p. 451-83.

66. Martinez, F.O., et al., *Macrophage activation and polarization.* Front Biosci, 2008. **13**: p. 453-61.

67. Leek, R.D., et al., *Macrophage infiltration is associated with VEGF and EGFR expression in breast cancer.* J Pathol, 2000. **190**(4): p. 430-6.

68. Lewis, J.S., et al., *Expression of vascular endothelial growth factor by macrophages is up-regulated in poorly vascularized areas of breast carcinomas.* J Pathol, 2000. **192**(2): p. 150-8.

69. O'Sullivan, C., et al., *Secretion of epidermal growth factor by macrophages associated with breast carcinoma.* Lancet, 1993. **342**(8864): p. 148-9.

70. Wyckoff, J.B., et al., *Direct visualization of macrophage-assisted tumor cell intravasation in mammary tumors.* Cancer Res, 2007. **67**(6): p. 2649-56.

71. Gregory, A.D. and A.M. Houghton, *Tumor-associated neutrophils: new targets for cancer therapy.* Cancer Res, 2011.**71**(7): p. 2411-6.

72. Hadrup, S., M. Donia, and P. Thor Straten, *Effector CD4 and CD8 T cells and their role in the tumor microenvironment.* Cancer Microenviron, 2012. **6**(2): p. 123-33.

73. Catalfamo, M. and P.A. Henkart, *Perforin and the granule exocytosis*

cytotoxicity pathway. Curr Opin Immunol, 2003. **15**(5): p. 522-7.

74. Clark, R. and G.M. Griffiths, *Lytic granules, secretory lysosomes and disease.* Curr Opin Immunol, 2003. **15**(5): p. 516-21.

75. Lieberman, J., *The ABCs of granule-mediated cytotoxicity: new weapons in the arsenal.* Nat Rev Immunol, 2003. **3**(5): p. 361-70.

76. Gooden, M.J., et al., *The prognostic influence of tumour-infiltrating lymphocytes in cancer: a systematic review with meta-analysis.* Br J Cancer, 2011. **105**(1): p. 93-103.

77. Hori, S., T. Nomura, and S. Sakaguchi, *Control of regulatory T cell development by the transcription factor Foxp3.* Science, 2003. **299**(5609): p. 1057-61.

78. Sakaguchi, S., *Naturally arising Foxp3-expressing CD25+CD4+ regulatory T cells in immunological tolerance to self and non-self.* Nat Immunol, 2005. **6**(4): p. 345-52.

79. Shimizu, J., S. Yamazaki, and S. Sakaguchi, *Induction of tumor immunity by removing CD25+CD4+ T cells: a common basis between tumor immunity and autoimmunity.* J Immunol, 1999. **163**(10): p. 5211-8.

80. Casares, N., et al., *CD4+/CD25+ regulatory cells inhibit activation of tumor-primed CD4+ T cells with IFN-gamma-dependent antiangiogenic activity, as well as long-lasting tumor immunity elicited by peptide vaccination.* J Immunol, 2003. **171**(11): p. 5931-9.

81. Woo, E.Y., et al., *Regulatory CD4(+)CD25(+) T cells in tumors from patients with early-stage non-small cell lung cancer and late-stage ovarian cancer.* Cancer Res, 2001. **61**(12): p. 4766-72.

82. Vargo-Gogola, T. and J.M. Rosen, *Modelling breast cancer: one size does not fit all.* Nat Rev Cancer, 2007. **7**(9): p. 659-72.

83. Lacroix, M. and G. Leclercq, *Relevance of breast cancer cell lines as models for breast tumours: an update.* Breast Cancer Res Treat, 2004. **83**(3): p. 249-89.

84. Neve, R.M., et al., *A collection of breast cancer cell lines for the study of functionally distinct cancer subtypes.* Cancer Cell, 2006. **10**(6): p. 515-27.

85. Kenny, P.A., et al., *The morphologies of breast cancer cell lines in three-dimensional assays correlate with their profiles of gene expression.* Mol Oncol, 2007. **1**(1): p. 84-96.

86. Debnath, J. and J.S. Brugge, *Modelling glandular epithelial cancers in three-dimensional cultures.* Nat Rev Cancer, 2005. **5**(9): p. 675-88.

87. Lee, G.Y., et al., *Three-dimensional culture models of normal and malignant breast epithelial cells.* Nat Methods, 2007. **4**(4): p. 359-65.

88. Paszek, M.J. and V.M. Weaver, *The tension mounts: mechanics meets morphogenesis and malignancy.* J Mammary Gland Biol Neoplasia, 2004. **9**(4): p. 325-42.

89. Shaw, K.R., C.N. Wrobel, and J.S. Brugge, *Use of three-dimensional basement membrane cultures to model oncogene-induced changes in mammary epithelial morphogenesis.* J Mammary Gland Biol Neoplasia, 2004. **9**(4): p. 297-310.

90. Chan, S.K., M.E. Hill, and W.J. Gullick, *The role of the epidermal growth factor receptor in breast cancer.* J Mammary Gland Biol Neoplasia, 2006. **11**(1): p. 3-11.

91. Dillon, R.L., D.E. White, and W.J. Muller, *The phosphatidyl inositol 3-kinase signaling network: implications for human breast cancer.* Oncogene, 2007. **26**(9): p. 1338-45.

92. Kenny, P.A. and M.J. Bissell, *Targeting TACE-dependent EGFR ligand shedding in breast cancer.* J Clin Invest, 2007. **117**(2): p. 337-45.

93. Paszek, M.J., et al., *Tensional homeostasis and the malignant phenotype.* Cancer Cell, 2005. **8**(3): p. 241-54.

94. van Golen, K.L., *Inflammatory breast cancer: relationship between growth factor signaling and motility in aggressive cancers.* Breast Cancer Res, 2003. **5**(3): p. 174-9.

95. Balkwill, F., K.A. Charles, and A. Mantovani, *Smoldering and polarized inflammation in the initiation and promotion of malignant disease.* Cancer Cell, 2005. **7**(3): p. 211-7.

96. Haagensen, C.D., *The physiology of the breast as it concerns the clinician.* Am J Obstet Gynecol, 1971. **109**(2): p. 206-9.

97. Hovey, R.C., T.B. McFadden, and R.M. Akers, *Regulation of mammary gland growth and morphogenesis by the mammary fat pad: a species comparison.* J Mammary Gland Biol Neoplasia, 1999. **4**(1): p. 53-68.

98. Kuperwasser, C., et al., *Reconstruction of functionally normal and malignant human breast tissues in mice.* Proc Natl Acad Sci U S A, 2004. **101**(14): p. 4966-71.

99. Wyckoff, J.B., et al., *A critical step in metastasis: in vivo analysis of intravasation at the primary tumor.* Cancer Res, 2000. **60**(9): p. 2504-11.

100. Chambers, A.F., et al., *Molecular biology of breast cancer metastasis. Clinical implications of experimental studies on metastatic inefficiency.* Breast Cancer

Res, 2000. **2**(6): p. 400-7.

101. Elliott, B.E., et al., *The membrane cytoskeletal crosslinker ezrin is required for metastasis of breast carcinoma cells.* Breast Cancer Res, 2005. **7**(3): p. R365-73.

102. Elliott, B.E., et al., *Capacity of adipose tissue to promote growth and metastasis of a murine mammary carcinoma: effect of estrogen and progesterone.* Int J Cancer, 1992. **51**(3): p. 416-24.

103. Guy, C.T., R.D. Cardiff, and W.J. Muller, *Induction of mammary tumors by expression of polyomavirus middle T oncogene: a transgenic mouse model for metastatic disease.* Mol Cell Biol, 1992. **12**(3): p. 954-61.

104. Guy, C.T., et al., *Expression of the neu protooncogene in the mammary epithelium of transgenic mice induces metastatic disease.* Proc Natl Acad Sci U S A, 1992. **89**(22): p. 10578-82.

105. Muller, W.J., et al., *Single-step induction of mammary adenocarcinoma in transgenic mice bearing the activated c-neu oncogene.* Cell, 1988. **54**(1): p. 105-15.

106. Sinn, E., et al., *Coexpression of MMTV/v-Ha-ras and MMTV/c-myc genes in transgenic mice: synergistic action of oncogenes in vivo.* Cell, 1987. **49**(4): p. 465-75.

107. Hynes, N.E. and D.F. Stern, *The biology of erbB-2/neu/HER-2 and its role in cancer.* Biochim Biophys Acta, 1994. **1198**(2-3): p. 165-84.

108. Olayioye, M.A., et al., *The ErbB signaling network: receptor heterodimerization in development and cancer.* EMBO J, 2000. **19**(13): p. 3159-67.

109. Slamon, D.J., et al., *Human breast cancer: correlation of relapse and survival with amplification of the HER-2/neu oncogene.* Science, 1987. **235**(4785): p. 177-82.

110. Mansour, E.G., P.M. Ravdin, and L. Dressler, *Prognostic factors in early breast carcinoma.* Cancer, 1994. **74**(1 Suppl): p. 381-400.

111. Ravdin, P.M. and G.C. Chamness, *The c-erbB-2 proto-oncogene as a prognostic and predictive marker in breast cancer: a paradigm for the development of other macromolecular markers--a review.* Gene, 1995. **159**(1): p. 19-27.

112. Andrulis, I.L., et al., *neu/erbB-2 amplification identifies a poor-prognosis group of women with node-negative breast cancer. Toronto Breast Cancer Study Group.* J Clin Oncol, 1998. **16**(4): p. 1340-9.

113. Lemoine, N.R., et al., *Absence of activating transmembrane mutations in the*

c-erbB-2 proto-oncogene in human breast cancer. Oncogene, 1990. **5**(2): p. 237-9.

114. Zoll, B., et al., *Alterations of the c-erbB2 gene in human breast cancer.* J Cancer Res Clin Oncol, 1992. **118**(6): p. 468-73.

115. Lin, E.Y., et al., *Progression to malignancy in the polyoma middle T oncoprotein mouse breast cancer model provides a reliable model for human diseases.* Am J Pathol, 2003. **163**(5): p. 2113-26.

116. Fluck, M.M. and B.S. Schaffhausen, *Lessons in signaling and tumorigenesis from polyomavirus middle T antigen.* Microbiol Mol Biol Rev, 2009. **73**(3): p. 542-63.

117. Marshall, C.J., *Specificity of receptor tyrosine kinase signaling: transient versus sustained extracellular signal-regulated kinase activation.* Cell, 1995. **80**(2): p. 179-85.

118. van der Geer, P., T. Hunter, and R.A. Lindberg, *Receptor protein-tyrosine kinases and their signal transduction pathways.* Annu Rev Cell Biol, 1994. **10**: p. 251-337.

119. Kolibaba, K.S. and B.J. Druker, *Protein tyrosine kinases and cancer.* Biochim Biophys Acta, 1997. **1333**(3): p. F217-48.

120. Roskoski, R., Jr., *The ErbB/HER receptor protein-tyrosine kinases and cancer.* Biochem Biophys Res Commun, 2004. **319**(1): p. 1-11.

121. Robinson, D.R., Y.M. Wu, and S.F. Lin, *The protein tyrosine kinase family of the human genome.* Oncogene, 2000. **19**(49): p. 5548-57.

122. Franchini, G., et al., *onc sequences (v-fes) of Snyder-Theilen feline sarcoma virus are derived from noncontiguous regions of a cat cellular gene (c-fes).* Nature, 1981. **290**(5802): p. 154-7.

123. Hampe, A., et al., *Nucleotide sequences of feline retroviral oncogenes (v-fes) provide evidence for a family of tyrosine-specific protein kinase genes.* Cell, 1982. **30**(3): p. 775-85.

124. Sherr, C.J., et al., *Molecular cloning of Snyder-Theilen feline leukemia and sarcoma viruses: comparative studies of feline sarcoma virus with its natural helper virus and with Moloney murine sarcoma virus.* J Virol, 1980. **34**(1): p. 200-12.

125. Shibuya, M. and H. Hanafusa, *Nucleotide sequence of Fujinami sarcoma virus: evolutionary relationship of its transforming gene with transforming genes of other sarcoma viruses.* Cell, 1982. **30**(3): p. 787-95.

126. Shibuya, M., et al., *Homology exists among the transforming sequences of avian and feline sarcoma viruses.* Proc Natl Acad Sci U S A, 1980. **77**(11): p.

6536-40.

127. Groffen, J., et al., *Isolation of human oncogene sequences (v-fes homolog) from a cosmid library.* Science, 1982. **216**(4550): p. 1136-8.

128. Groffen, J., et al., *Transforming genes of avian (v-fps) and mammalian (v-fes) retroviruses correspond to a common cellular locus.* Virology, 1983. **125**(2): p. 480-6.

129. Huang, C.C., C. Hammond, and J.M. Bishop, *Nucleotide sequence and topography of chicken c-fps. Genesis of a retroviral oncogene encoding a tyrosine-specific protein kinase.* J Mol Biol, 1985. **181**(2): p. 175-86.

130. Roebroek, A.J., et al., *The structure of the human c-fes/fps proto-oncogene.* EMBO J, 1985. **4**(11): p. 2897-903.

131. Stehelin, D., et al., *DNA related to the transforming gene(s) of avian sarcoma viruses is present in normal avian DNA.* Nature, 1976. **260**(5547): p. 170-3.

132. Greer, P., *Closing in on the biological functions of Fps/Fes and Fer.* Nat Rev Mol Cell Biol, 2002. **3**(4): p. 278-89.

133. Carmier, J.F. and J. Samarut, *Chicken myeloid stem cells infected by retroviruses carrying the v-fps oncogene do not require exogenous growth factors to differentiate in vitro.* Cell, 1986. **44**(1): p. 159-65.

134. Sadowski, I., T. Pawson, and A. Lagarde, *v-fps protein-tyrosine kinase coordinately enhances the malignancy and growth factor responsiveness of pre-neoplastic lung fibroblasts.* Oncogene, 1988. **2**(3): p. 241-7.

135. Ellis, C., et al., *Phosphorylation of GAP and GAP-associated proteins by transforming and mitogenic tyrosine kinases.* Nature, 1990. **343**(6256): p. 377-81.

136. Koch, C.A., et al., *The common src homology region 2 domain of cytoplasmic signaling proteins is a positive effector of v-fps tyrosine kinase function.* Mol Cell Biol, 1989. **9**(10): p. 4131-40.

137. Moran, M.F., et al., *Protein-tyrosine kinases regulate the phosphorylation, protein interactions, subcellular distribution, and activity of p21ras GTPase-activating protein.* Mol Cell Biol, 1991. **11**(4): p. 1804-12.

138. Fukui, Y., A.R. Saltiel, and H. Hanafusa, *Phosphatidylinositol-3 kinase is activated in v-src, v-yes, and v-fps transformed chicken embryo fibroblasts.* Oncogene, 1991. **6**(3): p. 407-11.

139. Maru, Y., et al., *Tyrosine phosphorylation of BCR by FPS/FES protein-tyrosine kinases induces association of BCR with GRB-2/SOS.* Mol Cell Biol, 1995. **15**(2): p. 835-42.

140. McGlade, J., et al., *Shc proteins are phosphorylated and regulated by the v-Src and v-Fps protein-tyrosine kinases.* Proc Natl Acad Sci U S A, 1992. **89**(19): p. 8869-73.

141. Garcia, R., et al., *Constitutive activation of Stat3 in fibroblasts transformed by diverse oncoproteins and in breast carcinoma cells.* Cell Growth Differ, 1997. **8**(12): p. 1267-76.

142. Kurata, W.E. and A.F. Lau, *p130gag-fps disrupts gap junctional communication and induces phosphorylation of connexin43 in a manner similar to that of pp60v-src.* Oncogene, 1994. **9**(1): p. 329-35.

143. Sangrar, W., A.W. Craig, and P.A. Greer, *FES and FER: The F-BAR domain-containing protein-tyrosine kinases*, in *The Pombe Cdc15 Homology Proteins*, P. Aspentrom, Editor. 2009, Landes Bioscience.

144. Fischman, K., et al., *A murine fer testis-specific transcript (ferT) encodes a truncated Fer protein.* Mol Cell Biol, 1990. **10**(1): p. 146-53.

145. Chitu, V. and E.R. Stanley, *Pombe Cdc15 homology (PCH) proteins: coordinators of membrane-cytoskeletal interactions.* Trends Cell Biol, 2007. **17**(3): p. 145-56.

146. Frost, A., et al., *Structural basis of membrane invagination by F-BAR domains.* Cell, 2008. **132**(5): p. 807-17.

147. Songyang, Z., et al., *Catalytic specificity of protein-tyrosine kinases is critical for selective signalling.* Nature, 1995. **373**(6514): p. 536-9.

148. Songyang, Z., et al., *Specific motifs recognized by the SH2 domains of Csk, 3BP2, fps/fes, GRB-2, HCP, SHC, Syk, and Vav.* Mol Cell Biol, 1994. **14**(4): p. 2777-85.

149. Craig, A.W., R. Zirngibl, and P. Greer, *Disruption of coiled-coil domains in Fer protein-tyrosine kinase abolishes trimerization but not kinase activation.* J Biol Chem, 1999. **274**(28): p. 19934-42.

150. Kim, L. and T.W. Wong, *Growth factor-dependent phosphorylation of the actin-binding protein cortactin is mediated by the cytoplasmic tyrosine kinase FER.* J Biol Chem, 1998. **273**(36): p. 23542-8.

151. Weinmaster, G., E. Hinze, and T. Pawson, *Mapping of multiple phosphorylation sites within the structural and catalytic domains of the Fujinami avian sarcoma virus transforming protein.* J Virol, 1983. **46**(1): p. 29-41.

152. Rogers, J.A., et al., *Autophosphorylation of the Fes tyrosine kinase. Evidence for an intermolecular mechanism involving two kinase domain tyrosine residues.* J Biol Chem, 1996. **271**(29): p. 17519-25.

153. Tong, J., et al., *Tandem immunoprecipitation of phosphotyrosine-mass spectrometry (TIPY-MS) indicates C19ORF19 becomes tyrosine-phosphorylated and associated with activated epidermal growth factor receptor.* J Proteome Res, 2008. **7**(3): p. 1067-77.

154. Mertins, P., et al., *Investigation of protein-tyrosine phosphatase 1B function by quantitative proteomics.* Mol Cell Proteomics, 2008. **7**(9): p. 1763-77.

155. Hjermstad, S.J., et al., *Regulation of the human c-fes protein tyrosine kinase (p93c-fes) by its src homology 2 domain and major autophosphorylation site (Tyr-713).* Oncogene, 1993. **8**(8): p. 2283-92.

156. Filippakopoulos, P., et al., *Structural coupling of SH2-kinase domains links Fes and Abl substrate recognition and kinase activation.* Cell, 2008. **134**(5): p. 793-803.

157. Haigh, J., J. McVeigh, and P. Greer, *The fps/fes tyrosine kinase is expressed in myeloid, vascular endothelial, epithelial, and neuronal cells and is localized in the trans-golgi network.* Cell Growth Differ, 1996. **7**(7): p. 931-44.

158. Truesdell, P.F., et al., *fps/fes knockout mice display a lactation defect and the fps/fes tyrosine kinase is a component of E-cadherin-based adherens junctions in breast epithelial cells during lactation.* Exp Cell Res, 2009. **315**(17): p. 2929-40.

159. Pawson, T., et al., *The FER gene is evolutionarily conserved and encodes a widely expressed member of the FPS/FES protein-tyrosine kinase family.* Mol Cell Biol, 1989. **9**(12): p. 5722-5.

160. Greer, P., et al., *Myeloid expression of the human c-fps/fes proto-oncogene in transgenic mice.* Mol Cell Biol, 1990. **10**(6): p. 2521-7.

161. Greer, P., et al., *The Fps/Fes protein-tyrosine kinase promotes angiogenesis in transgenic mice.* Mol Cell Biol, 1994. **14**(10): p. 6755-63.

162. Zirngibl, R.A., Y. Senis, and P.A. Greer, *Enhanced endotoxin sensitivity in fps/fes-null mice with minimal defects in hematopoietic homeostasis.* Mol Cell Biol, 2002. **22**(8): p. 2472-86.

163. Senis, Y., et al., *Targeted disruption of the murine fps/fes proto-oncogene reveals that Fps/Fes kinase activity is dispensable for hematopoiesis.* Mol Cell Biol, 1999. **19**(11): p. 7436-46.

164. Hackenmiller, R., et al., *Abnormal Stat activation, hematopoietic homeostasis, and innate immunity in c-fes-/- mice.* Immunity, 2000. **13**(3): p. 397-407.

165. Parsons, S.A. and P.A. Greer, *The Fps/Fes kinase regulates the inflammatory response to endotoxin through down-regulation of TLR4, NF-kappaB activation, and TNF-alpha secretion in macrophages.* J Leukoc Biol, 2006.

80(6): p. 1522-8.

166. Yee, S.P., et al., *Lymphoid and mesenchymal tumors in transgenic mice expressing the v-fps protein-tyrosine kinase.* Mol Cell Biol, 1989. **9**(12): p. 5491-9.

167. Karthaus, H.F., et al., *Expression of the human fes cellular oncogene in renal cell tumors.* Urol Res, 1986. **14**(3): p. 123-7.

168. Kanda, S., et al., *Downregulation of the c-Fes protein-tyrosine kinase inhibits the proliferation of human renal carcinoma cells.* Int J Oncol, 2009. **34**(1): p. 89-96.

169. Bardelli, A., et al., *Mutational analysis of the tyrosine kinome in colorectal cancers.* Science, 2003. **300**(5621): p. 949.

170. Sangrar, W., et al., *An identity crisis for fps/fes: oncogene or tumor suppressor?* Cancer Res, 2005. **65**(9): p. 3518-22.

171. Delfino, F.J., H. Stevenson, and T.E. Smithgall, *A growth-suppressive function for the c-fes protein-tyrosine kinase in colorectal cancer.* J Biol Chem, 2006. **281**(13): p. 8829-35.

172. Shaffer, J.M. and T.E. Smithgall, *Promoter methylation blocks FES protein-tyrosine kinase gene expression in colorectal cancer.* Genes Chromosomes Cancer, 2009. **48** (3): p272-84.

173. Paul, W.E., *Interleukin-4: a prototypic immunoregulatory lymphokine.* Blood, 1991. **77**(9): p. 1859-70.

174. Nelms, K., et al., *The IL-4 receptor: signaling mechanisms and biologic functions.* Annu Rev Immunol, 1999. **17**: p. 701-38.

175. Walter, M.R., et al., *Crystal structure of recombinant human interleukin-4.* J Biol Chem, 1992. **267**(28): p. 20371-6.

176. Carr, C., et al., *Disulfide assignments in recombinant mouse and human interleukin 4.* Biochemistry, 1991. **30**(6): p. 1515-23.

177. Seder, R.A., *Acquisition of lymphokine-producing phenotype by CD4+ T cells.* J Allergy Clin Immunol, 1994. **94**(6 Pt 2): p. 1195-202.

178. Yoshimoto, T. and W.E. Paul, *CD4pos, NK1.1pos T cells promptly produce interleukin 4 in response to in vivo challenge with anti-CD3.* J Exp Med, 1994. **179**(4): p. 1285-95.

179. Chen, H. and W.E. Paul, *Cultured NK1.1+ CD4+ T cells produce large amounts of IL-4 and IFN-gamma upon activation by anti-CD3 or CD1.* J Immunol, 1997. **159**(5): p. 2240-9.

180. Min, B., et al., *Basophils produce IL-4 and accumulate in tissues after*

infection with a Th2-inducing parasite. J Exp Med, 2004. **200**(4): p. 507-17.

181. Mitre, E., et al., *Parasite antigen-driven basophils are a major source of IL-4 in human filarial infections.* J Immunol, 2004. **172**(4): p. 2439-45.

182. MacGlashan, D., Jr., et al., *Secretion of IL-4 from human basophils. The relationship between IL-4 mRNA and protein in resting and stimulated basophils.* J Immunol, 1994. **152**(6): p. 3006-16.

183. Plaut, M., et al., *Mast cell lines produce lymphokines in response to cross-linkage of Fc epsilon RI or to calcium ionophores.* Nature, 1989. **339**(6219): p. 64-7.

184. Weiss, D.L. and M.A. Brown, *Regulation of IL-4 production in mast cells: a paradigm for cell-type-specific gene expression.* Immunol Rev, 2001. **179**: p. 35-47.

185. Dubucquoi, S., et al., *Interleukin 5 synthesis by eosinophils: association with granules and immunoglobulin-dependent secretion.* J Exp Med, 1994. **179**(2): p. 703-8.

186. Howard, M., et al., *Identification of a T cell-derived b cell growth factor distinct from interleukin 2.* J Exp Med, 1982. **155**(3): p. 914-23.

187. Noelle, R., et al., *Increased expression of Ia antigens on resting B cells: an additional role for B-cell growth factor.* Proc Natl Acad Sci U S A, 1984. **81**(19): p. 6149-53.

188. Rabin, E.M., J. Ohara, and W.E. Paul, *B-cell stimulatory factor 1 activates resting B cells.* Proc Natl Acad Sci U S A, 1985. **82**(9): p. 2935-9.

189. Oliver, K., et al., *B-cell growth factor (B-cell growth factor I or B-cell-stimulating factor, provisional 1) is a differentiation factor for resting B cells and may not induce cell growth.* Proc Natl Acad Sci U S A, 1985. **82**(8): p. 2465-7.

190. Gascan, H., et al., *Human B cell clones can be induced to proliferate and to switch to IgE and IgG4 synthesis by interleukin 4 and a signal provided by activated CD4+ T cell clones.* J Exp Med, 1991. **173**(3): p. 747-50.

191. Coffman, R.L., et al., *B cell stimulatory factor-1 enhances the IgE response of lipopolysaccharide-activated B cells.* J Immunol, 1986. **136**(12): p. 4538-41.

192. Vitetta, E.S., et al., *Serological, biochemical, and functional identity of B cell-stimulatory factor 1 and B cell differentiation factor for IgG1.* J Exp Med, 1985. **162**(5): p. 1726-31.

193. Seder, R.A., et al., *The presence of interleukin 4 during in vitro priming determines the lymphokine-producing potential of CD4+ T cells from T cell receptor transgenic mice.* J Exp Med, 1992. **176**(4): p. 1091-8.

194. Hsieh, C.S., et al., *Differential regulation of T helper phenotype development by interleukins 4 and 10 in an alpha beta T-cell-receptor transgenic system.* Proc Natl Acad Sci U S A, 1992. **89**(13): p. 6065-9.

195. Thornhill, M.H., et al., *Tumor necrosis factor combines with IL-4 or IFN-gamma to selectively enhance endothelial cell adhesiveness for T cells. The contribution of vascular cell adhesion molecule-1-dependent and -independent binding mechanisms.* J Immunol, 1991. **146**(2): p. 592-8.

196. Fukuda, T., et al., *Role of interleukin-4 and vascular cell adhesion molecule-1 in selective eosinophil migration into the airways in allergic asthma.* Am J Respir Cell Mol Biol, 1996. **14**(1): p. 84-94.

197. Bennett, B.L., et al., *Interleukin-4 suppression of tumor necrosis factor alpha-stimulated E-selectin gene transcription is mediated by STAT6 antagonism of NF-kappaB.* J Biol Chem, 1997. **272**(15): p. 10212-9.

198. Nakajima, H., et al., *Role of vascular cell adhesion molecule 1/very late activation antigen 4 and intercellular adhesion molecule 1/lymphocyte function-associated antigen 1 interactions in antigen-induced eosinophil and T cell recruitment into the tissue.* J Exp Med, 1994. **179**(4): p. 1145-54.

199. Schleimer, R.P., et al., *IL-4 induces adherence of human eosinophils and basophils but not neutrophils to endothelium. Association with expression of VCAM-1.* J Immunol, 1992. **148**(4): p. 1086-92.

200. Helming, L. and S. Gordon, *Macrophage fusion induced by IL-4 alternative activation is a multistage process involving multiple target molecules.* Eur J Immunol, 2007. **37**(1): p. 33-42.

201. Zubiaga, A.M., E. Munoz, and B.T. Huber, *IL-4 and IL-2 selectively rescue Th cell subsets from glucocorticoid-induced apoptosis.* J Immunol, 1992. **149**(1): p. 107-12.

202. Illera, V.A., et al., *Apoptosis in splenic B lymphocytes. Regulation by protein kinase C and IL-4.* J Immunol, 1993. **151**(6): p. 2965-73.

203. Dancescu, M., et al., *Interleukin 4 protects chronic lymphocytic leukemic B cells from death by apoptosis and upregulates Bcl-2 expression.* J Exp Med, 1992. **176**(5): p. 1319-26.

204. Zamorano, J., et al., *IL-4 protects cells from apoptosis via the insulin receptor substrate pathway and a second independent signaling pathway.* J Immunol, 1996. **157**(11): p. 4926-34.

205. Minshall, C., et al., *IL-4 and insulin-like growth factor-I inhibit the decline in Bcl-2 and promote the survival of IL-3-deprived myeloid progenitors.* J Immunol, 1997. **159**(3): p. 1225-32.

206. Mills, C.D., et al., *M-1/M-2 macrophages and the Th1/Th2 paradigm.* J Immunol, 2000. **164**(12): p. 6166-73.

207. Sica, A., et al., *Macrophage polarization in tumour progression.* Semin Cancer Biol, 2008. **18**(5): p. 349-55.

208. Martinez, F.O., et al., *Transcriptional profiling of the human monocyte-to-macrophage differentiation and polarization: new molecules and patterns of gene expression.* J Immunol, 2006. **177**(10): p. 7303-11.

209. Mantovani, A., et al., *Cancer-related inflammation.* Nature, 2008. **454**(7203): p. 436-44.

210. Gordon, S., *Alternative activation of macrophages.* Nat Rev Immunol, 2003. **3**(1): p. 23-35.

211. Mosser, D.M. and J.P. Edwards, *Exploring the full spectrum of macrophage activation.* Nat Rev Immunol, 2008. **8**(12): p. 958-69.

212. Mantovani, A., A. Sica, and M. Locati, *New vistas on macrophage differentiation and activation.* Eur J Immunol, 2007. **37**(1): p. 14-6.

213. Goerdt, S. and C.E. Orfanos, *Other functions, other genes: alternative activation of antigen-presenting cells.* Immunity, 1999. **10**(2): p. 137-42.

214. Stein, M., et al., *Interleukin 4 potently enhances murine macrophage mannose receptor activity: a marker of alternative immunologic macrophage activation.* J Exp Med, 1992. **176**(1): p. 287-92.

215. Lowenthal, J.W., et al., *Expression of high affinity receptors for murine interleukin 4 (BSF-1) on hemopoietic and nonhemopoietic cells.* J Immunol, 1988. **140**(2): p. 456-64.

216. Ohara, J. and W.E. Paul, *Receptors for B-cell stimulatory factor-1 expressed on cells of haematopoietic lineage.* Nature, 1987. **325**(6104): p. 537-40.

217. Mosley, B., et al., *The murine interleukin-4 receptor: molecular cloning and characterization of secreted and membrane bound forms.* Cell, 1989. **59**(2): p. 335-48.

218. Russell, S.M., et al., *Interleukin-2 receptor gamma chain: a functional component of the interleukin-4 receptor.* Science, 1993. **262**(5141): p. 1880-3.

219. Park, L.S., et al., *Characterization of the high-affinity cell-surface receptor for murine B-cell-stimulating factor 1.* Proc Natl Acad Sci U S A, 1987. **84**(6): p. 1669-73.

220. Orchansky, P.L., et al., *Characterization of the cytoplasmic domain of interleukin-13 receptor-alpha.* J Biol Chem, 1999. **274**(30): p. 20818-25.

221. Callard, R.E., D.J. Matthews, and L. Hibbert, *IL-4 and IL-13 receptors: are*

they one and the same? Immunol Today, 1996. **17**(3): p. 108-10.

222. Chomarat, P. and J. Banchereau, *Interleukin-4 and interleukin-13: their similarities and discrepancies.* Int Rev Immunol, 1998. **17**(1-4): p. 1-52.

223. Wills-Karp, M. and F.D. Finkelman, *Untangling the complex web of IL-4- and IL-13-mediated signaling pathways.* Sci Signal, 2008. **1**(51): p. pe55.

224. Keegan, A.D., et al., *An IL-4 receptor region containing an insulin receptor motif is important for IL-4-mediated IRS-1 phosphorylation and cell growth.* Cell, 1994. **76**(5): p. 811-20.

225. Seldin, D.C. and P. Leder, *Mutational analysis of a critical signaling domain of the human interleukin 4 receptor.* Proc Natl Acad Sci U S A, 1994. **91**(6): p. 2140-4.

226. Koettnitz, K. and F.S. Kalthoff, *Human interleukin-4 receptor signaling requires sequences contained within two cytoplasmic regions.* Eur J Immunol, 1993. **23**(4): p. 988-91.

227. Deutsch, H.H., et al., *Distinct sequence motifs within the cytoplasmic domain of the human IL-4 receptor differentially regulate apoptosis inhibition and cell growth.* J Immunol, 1995. **154**(8): p. 3696-703.

228. Ryan, J.J., et al., *Growth and gene expression are predominantly controlled by distinct regions of the human IL-4 receptor.* Immunity, 1996. **4**(2): p. 123-32.

229. Hanson, E.M., et al., *Regulation of the dephosphorylation of Stat6. Participation of Tyr-713 in the interleukin-4 receptor alpha, the tyrosine phosphatase SHP-1, and the proteasome.* J Biol Chem, 2003. **278**(6): p. 3903-11.

230. Reichel, M., et al., *The IL-4 receptor alpha-chain cytoplasmic domain is sufficient for activation of JAK-1 and STAT6 and the induction of IL-4-specific gene expression.* J Immunol, 1997. **158**(12): p. 5860-7.

231. Russell, S.M., et al., *Interaction of IL-2R beta and gamma c chains with Jak1 and Jak3: implications for XSCID and XCID.* Science, 1994. **266**(5187): p. 1042-5.

232. Miyazaki, T., et al., *Functional activation of Jak1 and Jak3 by selective association with IL-2 receptor subunits.* Science, 1994. **266**(5187): p. 1045-7.

233. Ryan, J.J., et al., *Characterization of a mobile Stat6 activation motif in the human IL-4 receptor.* J Immunol, 1998. **161**(4): p. 1811-21.

234. Quelle, F.W., et al., *Cloning of murine Stat6 and human Stat6, Stat proteins that are tyrosine phosphorylated in responses to IL-4 and IL-3 but are not required for mitogenesis.* Mol Cell Biol, 1995. **15**(6): p. 3336-43.

235. Mikita, T., et al., *Requirements for interleukin-4-induced gene expression and functional characterization of Stat6.* Mol Cell Biol, 1996. **16**(10): p. 5811-20.

236. Chen, X.H., et al., *Jak1 expression is required for mediating interleukin-4-induced tyrosine phosphorylation of insulin receptor substrate and Stat6 signaling molecules.* J Biol Chem, 1997. **272**(10): p. 6556-60.

237. Chen, H.C. and N.C. Reich, *Live cell imaging reveals continuous STAT6 nuclear trafficking.* J Immunol. **185**(1): p. 64-70.

238. Ihle, J.N., *STATs: signal transducers and activators of transcription.* Cell, 1996. **84**(3): p. 331-4.

239. Tinnell, S.B., et al., *STAT6, NF-kappaB and C/EBP in CD23 expression and IgE production.* Int Immunol, 1998. **10**(10): p. 1529-38.

240. Barks, J.L., J.J. McQuillan, and M.F. Iademarco, *TNF-alpha and IL-4 synergistically increase vascular cell adhesion molecule-1 expression in cultured vascular smooth muscle cells.* J Immunol, 1997. **159**(9): p. 4532-8.

241. Takeda, K., et al., *Essential role of Stat6 in IL-4 signalling.* Nature, 1996. **380**(6575): p. 627-30.

242. Shimoda, K., et al., *Lack of IL-4-induced Th2 response and IgE class switching in mice with disrupted Stat6 gene.* Nature, 1996. **380**(6575): p. 630-3.

243. Noben-Trauth, N., et al., *An interleukin 4 (IL-4)-independent pathway for CD4+ T cell IL-4 production is revealed in IL-4 receptor-deficient mice.* Proc Natl Acad Sci U S A, 1997. **94**(20): p. 10838-43.

244. Gustafson, T.A., et al., *Phosphotyrosine-dependent interaction of SHC and insulin receptor substrate 1 with the NPEY motif of the insulin receptor via a novel non-SH2 domain.* Mol Cell Biol, 1995. **15**(5): p. 2500-8.

245. O'Neill, T.J., A. Craparo, and T.A. Gustafson, *Characterization of an interaction between insulin receptor substrate 1 and the insulin receptor by using the two-hybrid system.* Mol Cell Biol, 1994. **14**(10): p. 6433-42.

246. Wang, H.Y., J. Zamorano, and A.D. Keegan, *A role for the insulin-interleukin (IL)-4 receptor motif of the IL-4 receptor alpha-chain in regulating activation of the insulin receptor substrate 2 and signal transducer and activator of transcription 6 pathways. Analysis by mutagenesis.* J Biol Chem, 1998. **273**(16): p. 9898-905.

247. Sun, X.J., et al., *Role of IRS-2 in insulin and cytokine signalling.* Nature, 1995. **377**(6545): p. 173-7.

248. Sun, X.J., et al., *Structure of the insulin receptor substrate IRS-1 defines a unique signal transduction protein.* Nature, 1991. **352**(6330): p. 73-7.

249. Sun, X.J., et al., *Pleiotropic insulin signals are engaged by multisite phosphorylation of IRS-1.* Mol Cell Biol, 1993. **13**(12): p. 7418-28.

250. Chardin, P., et al., *Human Sos1: a guanine nucleotide exchange factor for Ras that binds to GRB2.* Science, 1993. **260**(5112): p. 1338-43.

251. Downward, J., *Control of ras activation.* Cancer Surv, 1996. **27**: p. 87-100.

252. Marais, R., et al., *Ras recruits Raf-1 to the plasma membrane for activation by tyrosine phosphorylation.* EMBO J, 1995. **14**(13): p. 3136-45.

253. Marais, R. and C.J. Marshall, *Control of the ERK MAP kinase cascade by Ras and Raf.* Cancer Surv, 1996. **27**: p. 101-25.

254. Welham, M.J., V. Duronio, and J.W. Schrader, *Interleukin-4-dependent proliferation dissociates p44erk-1, p42erk-2, and p21ras activation from cell growth.* J Biol Chem, 1994. **269**(8): p. 5865-73.

255. Welham, M.J., et al., *Multiple hemopoietins, with the exception of interleukin-4, induce modification of Shc and mSos1, but not their translocation.* J Biol Chem, 1994. **269**(33): p. 21165-76.

256. Duronio, V., et al., *p21ras activation via hemopoietin receptors and c-kit requires tyrosine kinase activity but not tyrosine phosphorylation of p21ras GTPase-activating protein.* Proc Natl Acad Sci U S A, 1992. **89**(5): p. 1587-91.

257. Crowley, M.T., S.L. Harmer, and A.L. DeFranco, *Activation-induced association of a 145-kDa tyrosine-phosphorylated protein with Shc and Syk in B lymphocytes and macrophages.* J Biol Chem, 1996. **271**(2): p. 1145-52.

258. Wery, S., et al., *Interleukin-4 induces activation of mitogen-activated protein kinase and phosphorylation of shc in human keratinocytes.* J Biol Chem, 1996. **271**(15): p. 8529-32.

259. Zamorano, J. and A.D. Keegan, *Regulation of apoptosis by tyrosine-containing domains of IL-4R alpha: Y497 and Y713, but not the STAT6-docking tyrosines, signal protection from apoptosis.* J Immunol, 1998. **161**(2): p. 859-67.

260. Izuhara, K., et al., *Interaction of the c-fes proto-oncogene product with the interleukin-4 receptor.* J Biol Chem, 1994. **269**(28): p. 18623-9.

261. Izuhara, K., et al., *Interleukin-4 induces association of the c-fes proto-oncogene product with phosphatidylinositol-3 kinase.* Blood, 1996. **88**(10): p. 3910-8.

262. Jiang, H., et al., *Fes mediates the IL-4 activation of insulin receptor substrate-2 and cellular proliferation.* J Immunol, 2001. **166**(4): p. 2627-34.

263. Kay, A.B., *Allergy and allergic diseases. First of two parts.* N Engl J Med, 2001. **344**(1): p. 30-7.

264. Kay, A.B., *Allergy and allergic diseases. Second of two parts.* N Engl J Med, 2001. **344**(2): p. 109-13.

265. Wills-Karp, M., et al., *Interleukin-13: central mediator of allergic asthma.* Science, 1998. **282**(5397): p. 2258-61.

266. Grunig, G., et al., *Requirement for IL-13 independently of IL-4 in experimental asthma.* Science, 1998. **282**(5397): p. 2261-3.

267. Grunewald, S.M., et al., *An antagonistic IL-4 mutant prevents type I allergy in the mouse: inhibition of the IL-4/IL-13 receptor system completely abrogates humoral immune response to allergen and development of allergic symptoms in vivo.* J Immunol, 1998. **160**(8): p. 4004-9.

268. Tomkinson, A., et al., *A murine IL-4 receptor antagonist that inhibits IL-4- and IL-13-induced responses prevents antigen-induced airway eosinophilia and airway hyperresponsiveness.* J Immunol, 2001. **166**(9): p. 5792-800.

269. Borish, L.C., et al., *Efficacy of soluble IL-4 receptor for the treatment of adults with asthma.* J Allergy Clin Immunol, 2001. **107**(6): p. 963-70.

270. Steinke, J.W. and L. Borish, *Th2 cytokines and asthma. Interleukin-4: its role in the pathogenesis of asthma, and targeting it for asthma treatment with interleukin-4 receptor antagonists.* Respir Res, 2001. **2**(2): p. 66-70.

271. Maes, T., G.F. Joos, and G.G. Brusselle, *Targeting interleukin-4 in asthma: lost in translation?* Am J Respir Cell Mol Biol, 2012. **47**(3): p. 261-70.

272. Feldmann, M., F.M. Brennan, and R.N. Maini, *Role of cytokines in rheumatoid arthritis.* Annu Rev Immunol, 1996. **14**: p. 397-440.

273. Mosmann, T.R. and R.L. Coffman, *TH1 and TH2 cells: different patterns of lymphokine secretion lead to different functional properties.* Annu Rev Immunol, 1989. **7**: p. 145-73.

274. Lorenz, H.M. and J.R. Kalden, *Biologic agents in the treatment of inflammatory rheumatic diseases.* Curr Opin Rheumatol, 1999. **11**(3): p. 179-84.

275. Finnegan, A., et al., *IL-4 and IL-12 regulate proteoglycan-induced arthritis through Stat-dependent mechanisms.* J Immunol, 2002. **169**(6): p. 3345-52.

276. Finnegan, A., et al., *Proteoglycan (aggrecan)-induced arthritis in BALB/c mice is a Th1-type disease regulated by Th2 cytokines.* J Immunol, 1999. **163**(10): p. 5383-90.

277. Woods, J.M., et al., *IL-4 adenoviral gene therapy reduces inflammation,*

proinflammatory cytokines, vascularization, and bony destruction in rat adjuvant-induced arthritis. J Immunol, 2001. **166**(2): p. 1214-22.

278. Morita, Y., et al., *Dendritic cells genetically engineered to express IL-4 inhibit murine collagen-induced arthritis.* J Clin Invest, 2001. **107**(10): p. 1275-84.

279. Obiri, N.I., et al., *Expression of high affinity interleukin-4 receptors on human renal cell carcinoma cells and inhibition of tumor cell growth in vitro by interleukin-4.* J Clin Invest, 1993. **91**(1): p. 88-93.

280. Hoon, D.S., et al., *Interleukin 4 alone and with gamma-interferon or alpha-tumor necrosis factor inhibits cell growth and modulates cell surface antigens on human renal cell carcinomas.* Cancer Res, 1991. **51**(20): p. 5687-93.

281. Gooch, J.L., A.V. Lee, and D. Yee, *Interleukin 4 inhibits growth and induces apoptosis in human breast cancer cells.* Cancer Res, 1998. **58**(18): p. 4199-205.

282. Blais, Y., et al., *Interleukin-4 and interleukin-13 inhibit estrogen-induced breast cancer cell proliferation and stimulate GCDFP-15 expression in human breast cancer cells.* Mol Cell Endocrinol, 1996. **121**(1): p. 11-8.

283. Obiri, N.I., et al., *Expression of high-affinity IL-4 receptors on human melanoma, ovarian and breast carcinoma cells.* Clin Exp Immunol, 1994. **95**(1): p. 148-55.

284. Toi, M., R. Bicknell, and A.L. Harris, *Inhibition of colon and breast carcinoma cell growth by interleukin-4.* Cancer Res, 1992. **52**(2): p. 275-9.

285. Prokopchuk, O., et al., *Interleukin-4 enhances proliferation of human pancreatic cancer cells: evidence for autocrine and paracrine actions.* Br J Cancer, 2005. **92**(5): p. 921-8.

286. Conticello, C., et al., *IL-4 protects tumor cells from anti-CD95 and chemotherapeutic agents via up-regulation of antiapoptotic proteins.* J Immunol, 2004. **172**(9): p. 5467-77.

287. Todaro, M., et al., *Autocrine production of interleukin-4 and interleukin-10 is required for survival and growth of thyroid cancer cells.* Cancer Res, 2006. **66**(3): p. 1491-9.

288. Shurin, M.R., et al., *Th1/Th2 balance in cancer, transplantation and pregnancy.* Springer Semin Immunopathol, 1999. **21**(3): p. 339-59.

289. Puri, R.K., et al., *Human neurological cancer cells express interleukin-4 (IL-4) receptors which are targets for the toxic effects of IL4-Pseudomonas exotoxin chimeric protein.* Int J Cancer, 1994. **58**(4): p. 574-81.

290. Kawakami, K., P. Leland, and R.K. Puri, *Structure, function, and targeting of*

interleukin 4 receptors on human head and neck cancer cells. Cancer Res, 2000. **60**(11): p. 2981-7.

291. Golumbek, P.T., et al., *Treatment of established renal cancer by tumor cells engineered to secrete interleukin-4.* Science, 1991. **254**(5032): p. 713-6.

292. Santin, A.D., et al., *Development and characterization of an IL-4-secreting human ovarian carcinoma cell line.* Gynecol Oncol, 1995. **58**(2): p. 230-9.

293. Tepper, R.I., P.K. Pattengale, and P. Leder, *Murine interleukin-4 displays potent anti-tumor activity in vivo.* Cell, 1989. **57**(3): p. 503-12.

294. Benedetti, S., et al., *Gene therapy of experimental brain tumors using neural progenitor cells.* Nat Med, 2000. **6**(4): p. 447-50.

295. Lundin, J., et al., *Interleukin 4 therapy for patients with chronic lymphocytic leukaemia: a phase I/II study.* Br J Haematol, 2001. **112**(1): p. 155-60.

296. Taylor, C.W., et al., *Phase II evaluation of interleukin-4 in patients with non-Hodgkin's lymphoma: a Southwest Oncology Group trial.* Anticancer Drugs, 2000. **11**(9): p. 695-700.

297. Whitehead, R.P., et al., *Phase II trial of recombinant human interleukin-4 in patients with advanced renal cell carcinoma: a southwest oncology group study.* J Immunother, 2002. **25**(4): p. 352-8.

298. Gitlitz, B.J., et al., *Phase I trial of granulocyte macrophage-colony stimulating factor and interleukin-4 as a combined immunotherapy for patients with cancer.* J Immunother, 2003. **26**(2): p. 171-8.

299. Smithgall, T.E., et al., *The c-Fes family of protein-tyrosine kinases.* Crit Rev Oncog, 1998. **9**(1): p. 43-62.

300. Haigh, J.J., et al., *Activated Fps/Fes partially rescues the in vivo developmental potential of Flk1-deficient vascular progenitor cells.* Blood, 2004. **103**(3): p. 912-20.

301. Ye, Q., et al., *A new signaling pathway (JAK-Fes-phospholipase D) that is enhanced in highly proliferative breast cancer cells.* J Biol Chem, 2013. **288**(14): p. 9881-91.

302. Zhang, S., et al., *Fes tyrosine kinase expression in the tumor niche correlates with enhanced tumor growth, angiogenesis, circulating tumor cells, metastasis, and infiltrating macrophages.* Cancer Res, 2011. **71**(4): p. 1465-73.

303. Udell, C.M., et al., *Fer and Fps/Fes participate in a Lyn-dependent pathway from FcepsilonRI to platelet-endothelial cell adhesion molecule 1 to limit mast cell activation.* J Biol Chem, 2006. **281**(30): p. 20949-57.

304. Stanley, E.R., *Murine bone marrow-derived macrophages.* Methods Mol Biol,

1997. **75**: p. 301-4.

305. Goswami, S., et al., *Macrophages promote the invasion of breast carcinoma cells via a colony-stimulating factor-1/epidermal growth factor paracrine loop.* Cancer Res, 2005. **65**(12): p. 5278-83.

306. Kanda, S., et al., *Non-receptor protein-tyrosine kinases as molecular targets for antiangiogenic therapy (Review).* Int J Mol Med, 2007. **20**(1): p. 113-21.

307. Sangrar, W., et al., *Hemostatic and hematological abnormalities in gain-of-function fps/fes transgenic mice are associated with the angiogenic phenotype.* J Thromb Haemost, 2004. **2**(11): p. 2009-19.

308. Kanda, S., et al., *The nonreceptor protein-tyrosine kinase c-Fes is involved in fibroblast growth factor-2-induced chemotaxis of murine brain capillary endothelial cells.* J Biol Chem, 2000. **275**(14): p. 10105-11.

309. Lin, E.Y., et al., *Colony-stimulating factor 1 promotes progression of mammary tumors to malignancy.* J Exp Med, 2001. **193**(6): p. 727-40.

310. Sica, A. and V. Bronte, *Altered macrophage differentiation and immune dysfunction in tumor development.* J Clin Invest, 2007. **117**(5): p. 1155-66.

311. Leek, R.D., et al., *Association of macrophage infiltration with angiogenesis and prognosis in invasive breast carcinoma.* Cancer Res, 1996. **56**(20): p. 4625-9.

312. Paulus, P., et al., *Colony-stimulating factor-1 antibody reverses chemoresistance in human MCF-7 breast cancer xenografts.* Cancer Res, 2006. **66**(8): p. 4349-56.

313. Aharinejad, S., et al., *Colony-stimulating factor-1 antisense treatment suppresses growth of human tumor xenografts in mice.* Cancer Res, 2002. **62**(18): p. 5317-24.

314. Aharinejad, S., et al., *Colony-stimulating factor-1 blockade by antisense oligonucleotides and small interfering RNAs suppresses growth of human mammary tumor xenografts in mice.* Cancer Res, 2004. **64**(15): p. 5378-84.

315. Hernandez, L., et al., *The EGF/CSF-1 paracrine invasion loop can be triggered by heregulin beta1 and CXCL12.* Cancer Res, 2009. **69**(7): p. 3221-7.

316. Wyckoff, J., et al., *A paracrine loop between tumor cells and macrophages is required for tumor cell migration in mammary tumors.* Cancer Res, 2004. **64**(19): p. 7022-9.

317. Kanda, S., H. Kanetake, and Y. Miyata, *Downregulation of Fes inhibits VEGF-A-induced chemotaxis and capillary-like morphogenesis by cultured endothelial cells.* J Cell Mol Med, 2007. **11**(3): p. 495-501.

318. Kanda, S., A. Naba, and Y. Miyata, *Inhibition of endothelial cell chemotaxis toward FGF-2 by gefitinib associates with downregulation of Fes activity.* Int J Oncol, 2009. **35**(6): p. 1305-12.

319. Sangrar, W., et al., *Vascular defects in gain-of-function fps/fes transgenic mice correlate with PDGF- and VEGF-induced activation of mutant Fps/Fes kinase in endothelial cells.* J Thromb Haemost, 2004. **2**(5): p. 820-32.

320. Senis, Y.A., et al., *Fps/Fes and Fer non-receptor protein-tyrosine kinases regulate collagen- and ADP-induced platelet aggregation.* J Thromb Haemost, 2003. **1**(5): p. 1062-70.

321. Craig, A.W. and P.A. Greer, *Fer kinase is required for sustained p38 kinase activation and maximal chemotaxis of activated mast cells.* Mol Cell Biol, 2002. **22**(18): p. 6363-74.

322. Smithgall, T.E., G. Yu, and R.I. Glazer, *Identification of the differentiation-associated p93 tyrosine protein kinase of HL-60 leukemia cells as the product of the human c-fes locus and its expression in myelomonocytic cells.* J Biol Chem, 1988. **263**(29): p. 15050-5.

323. Condeelis, J. and J.W. Pollard, *Macrophages: obligate partners for tumor cell migration, invasion, and metastasis.* Cell, 2006. **124**(2): p. 263-6.

324. Robinson, B.D., et al., *Tumor microenvironment of metastasis in human breast carcinoma: a potential prognostic marker linked to hematogenous dissemination.* Clin Cancer Res, 2009. **15**(7): p. 2433-41.

325. Patsialou, A., et al., *Invasion of human breast cancer cells in vivo requires both paracrine and autocrine loops involving the colony-stimulating factor-1 receptor.* Cancer Res, 2009. **69**(24): p. 9498-506.

326. Kim, J. and R.A. Feldman, *Activated Fes protein tyrosine kinase induces terminal macrophage differentiation of myeloid progenitors (U937 cells) and activation of the transcription factor PU.1.* Mol Cell Biol, 2002. **22**(6): p. 1903-18.

327. Kim, J., Y. Ogata, and R.A. Feldman, *Fes tyrosine kinase promotes survival and terminal granulocyte differentiation of factor-dependent myeloid progenitors (32D) and activates lineage-specific transcription factors.* J Biol Chem, 2003. **278**(17): p. 14978-84.

328. Parsons, S.A., et al., *The Fps/Fes kinase regulates leucocyte recruitment and extravasation during inflammation.* Immunology, 2007. **122**(4): p. 542-50.

329. Sangrar, W., et al., *Fer-deficiency correlates with enhanced EGFR internalization rates, Lapatinib sensitivity and Erk signaling strength, but reduced mitogenic sensitivity and delayed HER2 tumor onset in vivo: A*

systems dynamic analysis. Submitted.

330. McInnes, A. and D.M. Rennick, *Interleukin 4 induces cultured monocytes/macrophages to form giant multinucleated cells.* J Exp Med, 1988. **167**(2): p. 598-611.

331. McNally, A.K. and J.M. Anderson, *Interleukin-4 induces foreign body giant cells from human monocytes/macrophages. Differential lymphokine regulation of macrophage fusion leads to morphological variants of multinucleated giant cells.* Am J Pathol, 1995. **147**(5): p. 1487-99.

332. Moreno, J.L., et al., *IL-4 promotes the formation of multinucleated giant cells from macrophage precursors by a STAT6-dependent, homotypic mechanism: contribution of E-cadherin.* J Leukoc Biol, 2007. **82**(6): p. 1542-53.

333. Rhee, I., et al., *Macrophage fusion is controlled by the cytoplasmic protein tyrosine phosphatase PTP-PEST/PTPN12.* Mol Cell Biol, 2013. **33**(12): p. 2458-69.

334. Kovacsovics-Bankowski, M. and K.L. Rock, *A phagosome-to-cytosol pathway for exogenous antigens presented on MHC class I molecules.* Science, 1995. **267**(5195): p. 243-6.

335. Mantovani, A., et al., *The chemokine system in diverse forms of macrophage activation and polarization.* Trends Immunol, 2004. **25**(12): p. 677-86.

336. Mantovani, A., et al., *Macrophage polarization: tumor-associated macrophages as a paradigm for polarized M2 mononuclear phagocytes.* Trends Immunol, 2002. **23**(11): p. 549-55.

337. Grivennikov, S.I., F.R. Greten, and M. Karin, *Immunity, inflammation, and cancer.* Cell, 2010. **140**(6): p. 883-99.

338. Balkwill, F. and L.M. Coussens, *Cancer: an inflammatory link.* Nature, 2004. **431**(7007): p. 405-6.

339. Clevers, H., *At the crossroads of inflammation and cancer.* Cell, 2004. **118**(6): p. 671-4.

340. Dobrovolskaia, M.A. and S.V. Kozlov, *Inflammation and cancer: when NF-kappaB amalgamates the perilous partnership.* Curr Cancer Drug Targets, 2005. **5**(5): p. 325-44.

341. Elliott, B.E., et al., *Karyotypic evolution of a murine mammary adenocarcinoma in vitro and during progression from primary to metastatic growth in vivo.* Genes Chromosomes Cancer, 1992. **4**(4): p. 281-9.

342. Greer, P.A., S. Kanda, and T.E. Smithgall, *The contrasting oncogenic and tumor suppressor roles of FES.* Front Biosci (Schol Ed). **4**: p. 489-501.

343. Dankort, D., et al., *Multiple ErbB-2/Neu Phosphorylation Sites Mediate Transformation through Distinct Effector Proteins.* J Biol Chem, 2001. **276**(42): p. 38921-8.

344. Zhang, J., P.L. Yang, and N.S. Gray, *Targeting cancer with small molecule kinase inhibitors.* Nat Rev Cancer, 2009. **9**(1): p. 28-39.

345. Kanda, S. and Y. Miyata, *The c-Fes protein tyrosine kinase as a potential anti-angiogenic target in cancer.* Front Biosci (Landmark Ed), 2011. **16**: p. 1024-35.

346. Hellwig, S., et al., *Small-molecule inhibitors of the c-Fes protein-tyrosine kinase.* Chem Biol, 2012. **19**(4): p. 529-40.

347. Galkin, A.V., et al., *Identification of NVP-TAE684, a potent, selective, and efficacious inhibitor of NPM-ALK.* Proc Natl Acad Sci U S A, 2007. **104**(1): p. 270-5.

348. Hemmila, M.R. and A.E. Chang, *Clinical implications of the new biology in the development of melanoma vaccines.* J Surg Oncol, 1999. **70**(4): p. 263-74.

349. Jager, E., D. Jager, and A. Knuth, *Clinical cancer vaccine trials.* Curr Opin Immunol, 2002. **14**(2): p. 178-82.

350. Moingeon, P., *Cancer vaccines.* Vaccine, 2001. **19**(11-12): p. 1305-26.

351. Yannelli, J.R. and J.M. Wroblewski, *On the road to a tumor cell vaccine: 20 years of cellular immunotherapy.* Vaccine, 2004. **23**(1): p. 97-113.

352. Rosenberg, S.A., *Gene therapy for cancer.* JAMA, 1992. **268**(17): p. 2416-9.

353. Nelson, W.G., et al., *Cancer cells engineered to secrete granulocyte-macrophage colony-stimulating factor using ex vivo gene transfer as vaccines for the treatment of genitourinary malignancies.* Cancer Chemother Pharmacol, 2000. **46 Suppl**: p. S67-72.

354. Tani, K., et al., *Progress reports on immune gene therapy for stage IV renal cell cancer using lethally irradiated granulocyte-macrophage colony-stimulating factor-transduced autologous renal cancer cells.* Cancer Chemother Pharmacol, 2000. **46 Suppl**: p. S73-6.

355. Qian, H.N., et al., *The experimental study of ovarian carcinoma vaccine modified by human B7-1 and IFN-gamma genes.* Int J Gynecol Cancer, 2002. **12**(1): p. 80-5.

356. O'Rourke, M.G., et al., *Immunotherapy, including gene therapy, for metastatic melanoma.* Aust N Z J Surg, 1997. **67**(12): p. 834-41.

357. Schadendorf, D., A. Paschen, and Y. Sun, *Autologous, allogeneic tumor cells or genetically engineered cells as cancer vaccine against melanoma.* Immunol

Lett, 2000. **74**(1): p. 67-74.

358. Antonia, S.J., et al., *Phase I trial of a B7-1 (CD80) gene modified autologous tumor cell vaccine in combination with systemic interleukin-2 in patients with metastatic renal cell carcinoma.* J Urol, 2002. **167**(5): p. 1995-2000.

359. Ellem, K.A., et al., *A case report: immune responses and clinical course of the first human use of granulocyte/macrophage-colony-stimulating-factor-transduced autologous melanoma cells for immunotherapy.* Cancer Immunol Immunother, 1997. **44**(1): p. 10-20.

360. Dranoff, G., et al., *A phase I study of vaccination with autologous, irradiated melanoma cells engineered to secrete human granulocyte-macrophage colony stimulating factor.* Hum Gene Ther, 1997. **8**(1): p. 111-23.

361. Soiffer, R., et al., *Vaccination with irradiated autologous melanoma cells engineered to secrete human granulocyte-macrophage colony-stimulating factor generates potent antitumor immunity in patients with metastatic melanoma.* Proc Natl Acad Sci U S A, 1998. **95**(22): p. 13141-6.

362. Simons, J.W., et al., *Induction of immunity to prostate cancer antigens: results of a clinical trial of vaccination with irradiated autologous prostate tumor cells engineered to secrete granulocyte-macrophage colony-stimulating factor using ex vivo gene transfer.* Cancer Res, 1999. **59**(20): p. 5160-8.

363. Simons, J.W., *Bioactivity of human GM-CSF gene therapy in metastatic renal cell carcinoma and prostate cancer.* Hinyokika Kiyo, 1997. **43**(11): p. 821-2.

364. Simons, J.W., et al., *Bioactivity of autologous irradiated renal cell carcinoma vaccines generated by ex vivo granulocyte-macrophage colony-stimulating factor gene transfer.* Cancer Res, 1997. **57**(8): p. 1537-46.

365. Xu, S., et al., *Constitutive MHC class I molecules negatively regulate TLR-triggered inflammatory responses via the Fps-SHP-2 pathway.* Nat Immunol, 2012. **13**(6): p. 551-9.

366. Aceto, N., et al., *Tyrosine phosphatase SHP2 promotes breast cancer progression and maintains tumor-initiating cells via activation of key transcription factors and a positive feedback signaling loop.* Nat Med, 2012. **18**(4): p. 529-37.

367. Craig, A.W., et al., *Mice devoid of fer protein-tyrosine kinase activity are viable and fertile but display reduced cortactin phosphorylation.* Mol Cell Biol, 2001. **21**(2): p. 603-13.

Appendix 1: Quantitative RT-PCR primers

Gene	Sequence (5'→3')	Product size (bp)
Arg1	cgcctttctcaaaaggacag (forward)	181
	acagaccgtgggttcttcac (reverse)	
Ym1	actttgatggcctcaacctg (forward)	173
	aatgattcctgctcctgtgg (reverse)	
MMR	atgccaagtgggaaaatctg (forward)	153
	tgtagcagtggcctgcatag (reverse)	
IL-4	tcaacccccagctagttgtc (forward)	184
	tctgtggtgttcttcgttgc (reverse)	
IL-10	ccagggagatcctttgatga (forward)	173
	cattcccagaggaattgcat (reverse)	
IL-12	aggtgcgttcctcgtagaga (forward)	241
	aaagccaaccaagcagaaga (reverse)	
β-actin	agccatgtacgtagccatcc (forward)	228
	ctctcagctgtggtggtgaa (reverse)	

Appendix 1. Primers that were designed to study M1/M2 macrophage polarization by quantitative RT-PCR are shown in the table above. Arg1, arginase 1; MMR, macrophage mannose receptor.

Appendix 2: Inhibition of Fes phosphorylation by Fes kinase inhibitor TAE684 *in vitro*

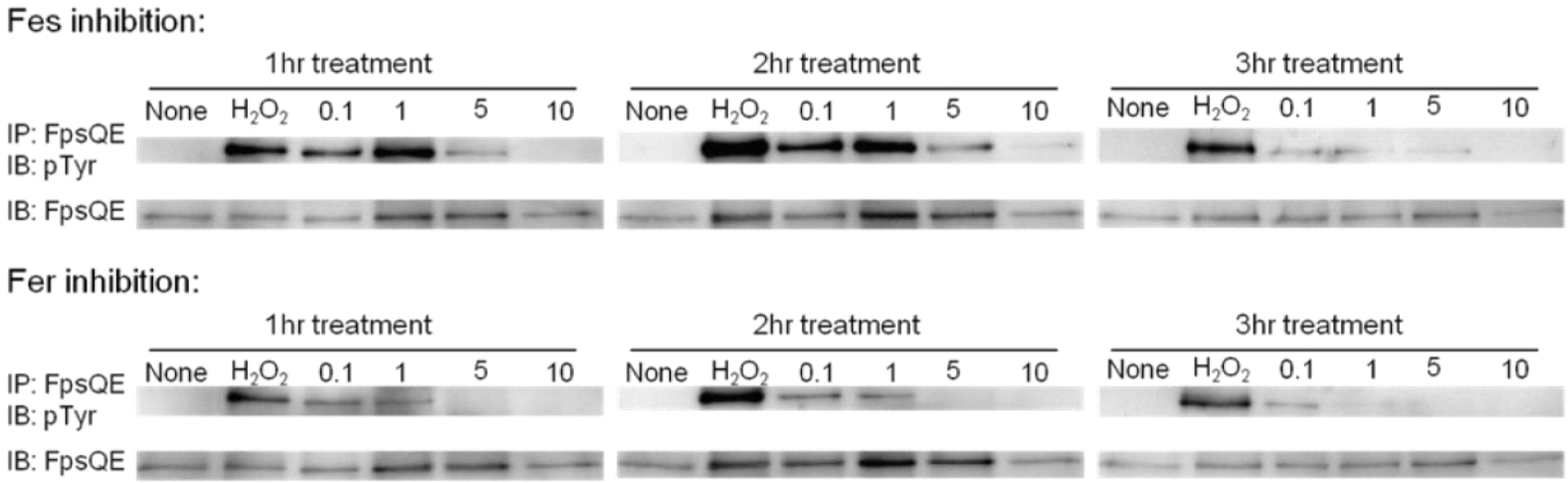

Appendix 2. Parental AC2M2 cells were transduced with retroviruses expressing kinase-activated Fes (MyrFes-AC2M2). Cells were plated on three 6-well plates and allowed to grow to 90-100% confluency. A stock solution of 5mM Fes kinase inhibitor TAE684 [346] was made by dissolving 3mg TAE684 powder in 1ml DMSO. Cell were treated with either DMSO alone or different concentrations (0.1, 1, 5 or 10μM) of TAE684 for 1 hour, 2 hours or 3 hours. After pre-treatment with TAE684 for different lengths of time, cells were stimulated with 9mM H_2O_2 for 10 min. After protein normalization, soluble cell lysates were split into two aliquots. One aliquot was immunoprecipitated with anti-FpsQE antibody which recognizes both Fes and Fer, and immunoblotted with anti-phospho-tyrosine (pTyr) antibody to detect Fes and Fer phosphorylation levels. Or, soluble cell lysates were run on SDS-PAGE and immunoblotted with anti-FpsQE antibody to detect the total Fes and Fer protein levels.

A

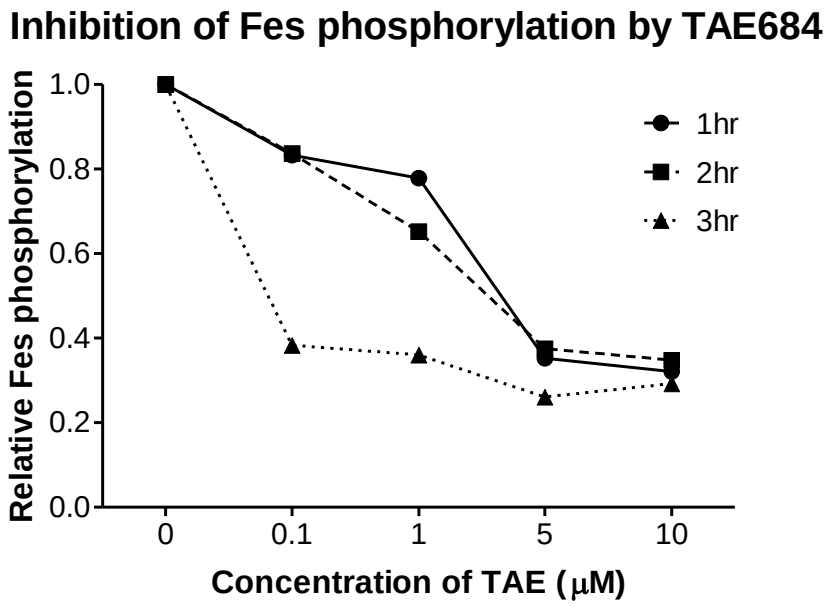

B

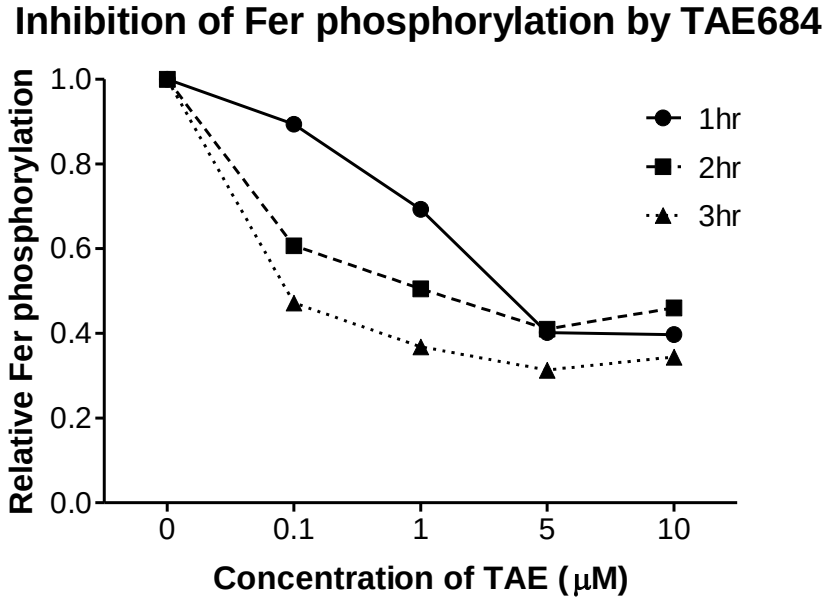

Appendix 2. Protein levels were determined by densitometry using Image Pro software. A) Similar inhibitory effects were observed with either 1 hr or 2 hr TAE684 pre-treatment—5μM TAE684 was able to inhibit Fes phosphorylation by 50%. However, as low as 0.1μM TAE684 achieved 60% inhibition of Fes phosphorylation when cells were pretreated for 3hrs. B) 0.1μM TAE684 inhibited Fer phosphorylation by 40% after a 2 hr pre-treatment. Overall, TAE684 seems show a better inhibitory effect on Fer phosphorylation as compared to Fes phosphorylation.

Appendix 3: Fes and Fer deficiency delayed tumor onset in MMTV-Neu transgenic mice in an additive manner

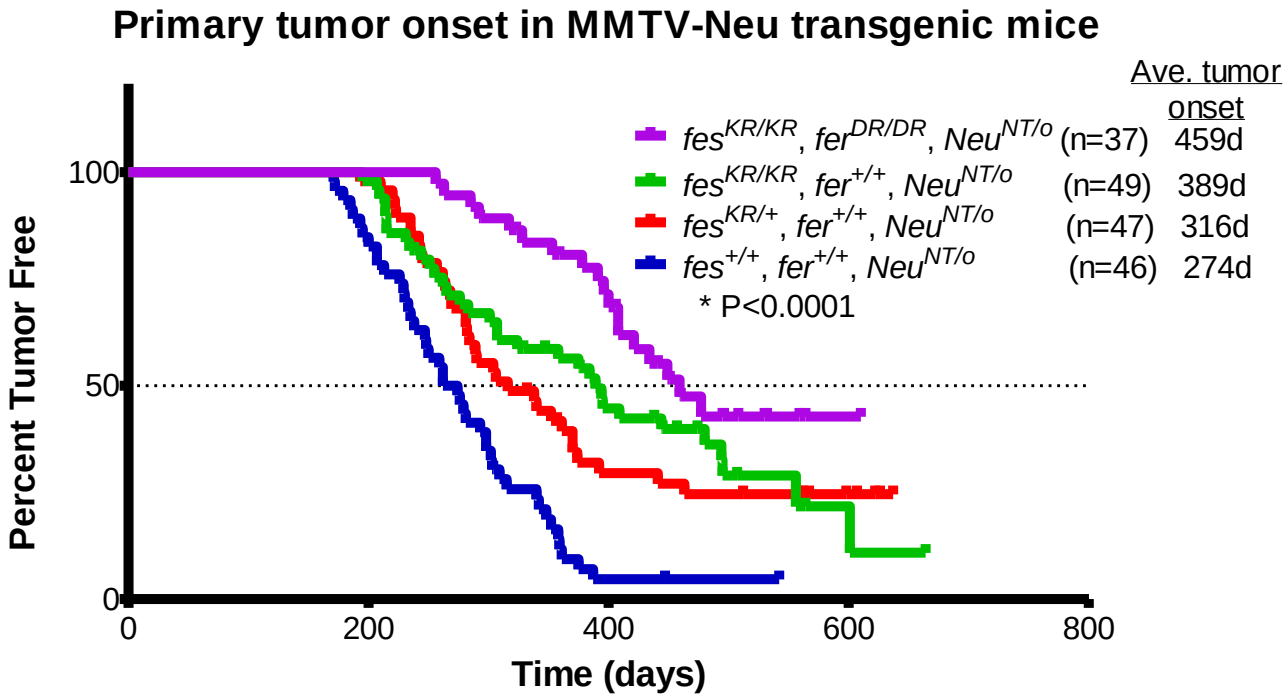

Appendix 3. Mice targeted with mutations in *fes* (*fes*$^{KR/KR}$) [163]or *fer* (*fer*$^{DR/DR}$) [367]were crossed with MMTV-Neu (*Neu*$^{NT/o}$) transgenic mice [105] to produce wild-type (*fes*$^{+/+}$, *fer*$^{+/+}$, *Neu*$^{NT/o}$), heterozygous (*fes*$^{KR/+}$, *fer*$^{+/+}$, *Neu*$^{NT/o}$), homozygous (*fes*$^{KR/KR}$, *fer*$^{+/+}$, *Neu*$^{NT/o}$) and double-knockout (*fes*$^{KR/KR}$, *fer*$^{DR/DR}$, *Neu*$^{NT/o}$) mice. Primary tumor onsets of these mice were monitored by physical palpation weekly. On average, wild-type (*fes*$^{+/+}$, *Neu*$^{NT/o}$) MMTV-Neu transgenic mice developed spontaneous tumors at 274 days of age. However, in homozygous *fes*-deficient (*fes*$^{KR/KR}$, *Neu*$^{NT/o}$) mice, the average tumor onset was delayed for over 100 days (389 days). Mice with both Fes and Fer kinase-inactivated (*fes*$^{KR/KR}$, *fer*$^{DR/DR}$, *Neu*$^{NT/o}$) showed an even longer tumor latency of 459 days (P< 0.0001; n= 46 for *fes*$^{+/+}$, *fer*$^{+/+}$, *Neu*$^{NT/o}$; n= 47 for *fes*$^{KR/+}$, *fer*$^{+/+}$, *Neu*$^{NT/o}$; n= 49 for *fes*$^{KR/KR}$, *fer*$^{+/+}$, *Neu*$^{NT/o}$ and n= 37 for *fes*$^{KR/KR}$, *fer*$^{DR/DR}$, *Neu*$^{NT/o}$).